5-2014

Labyrinth Weirs: A Look into Geometric Variation and Its Effect on Efficiency and Design Method Predictions

Tyler Robert Seamons
Utah State University

LABYRINTH WEIRS: A LOOK INTO GEOMETRIC VARIATION AND ITS EFFECT ON EFFICIENCY AND DESIGN METHOD PREDICTIONS

by

Tyler Robert Seamons

A thesis submitted in partial fulfillment
of the requirements for the degree

of

MASTER OF SCIENCE

in

Civil and Environmental Engineering

Approved:

_____	_____
Blake P. Tullis Major Professor	Brian M. Crookston Committee Member
_____	_____
Joseph A. Caliendo Committee Member	Mark R. McLellan Vice President for Research and Dean of the School of Graduate Studies

UTAH STATE UNIVERSITY
Logan, Utah

2014

ABSTRACT

Labyrinth Weirs: A Look into Geometric Variation and Its Effect on Efficiency and Design Method Predictions

by

Tyler Robert Seamons, Master of Science

Utah State University, 2014

Major Professor: Dr. Blake P. Tullis
Department: Civil and Environmental Engineering

The rehabilitation of dams often requires spillway capacity upgrades. Replacing a less hydraulically efficient linear weir with a labyrinth weir can be an effective way to increase discharge efficiency (discharge at a given upstream head) for a fixed-width channel. Labyrinth weirs are linear weirs folded in plan view to increase total spillway crest length (which in turn increases discharge efficiency within a channel). Labyrinth weirs potentially have limitless geometric configurations. This study was performed to analyze the effects of varying certain geometric parameters on discharge efficiency and design method predictions.

Due to limited cross-sectional flow area near the upstream apex, labyrinth weirs experience nappe collision and local submergence that potentially reduce discharge efficiency. The increase of upstream apex width may be a feasible method to decrease the negative effects of nappe interference, which in turn may increase discharge efficiency.

This was analyzed in this study by testing a series of eight laboratory scaled labyrinth weirs (with sidewall angles of 12°), with various upstream apex widths. Upstream apex width tests were performed in a fixed and varied channel width setting.

The design method developed by Crookston and Tullis is based on laboratory scaled physical models. This method is very useful in the estimation of performance for geometrically similar prototype labyrinth weirs. However, due to difficulty in obtaining data on completed prototype weirs, design method predictions are rarely verified. To help validate Froude scaling and design method predictions of prototype weirs, a series of physical model tests (with sidewall angles of 15°) were performed with varying scale sizes (0.5 to 3.0 compared to the size of weir used in the design method).

To expand the applicability of the design method to common geometric variations, tests were performed on weirs of varying weir height and cycle width (with sidewall angles of 15°). These variations were applied independently and analyzed to determine their effects on discharge efficiency and design method predictions. A correction factor is then presented to be used in conjunction with Crookston and Tullis's design method for these geometric variations. All conclusions are presented in this thesis.

(104 pages)

PUBLIC ABSTRACT

Labyrinth Weirs: A Look into Geometric Variation and Its Effect on Efficiency and Design Method Predictions

by

Tyler Robert Seamons, Master of Science

Utah State University, 2014

Major Professor: Dr. Blake P. Tullis
Department: Civil and Environmental Engineering

The rehabilitation of dams often requires spillway capacity upgrades. Replacing a less hydraulically efficient linear weir with a labyrinth weir can be an effective way to increase discharge efficiency (discharge at a given upstream head) for a fixed-width channel. Labyrinth weirs are linear weirs folded in plan view to increase total spillway crest length (which in turn increases discharge efficiency within a channel). Labyrinth weirs potentially have limitless geometric configurations. This study was performed to analyze the effects of varying certain geometric parameters on discharge efficiency and design method predictions.

Due to limited cross-sectional flow area near the upstream apex, labyrinth weirs experience nappe collision and local submergence that potentially reduce discharge efficiency. The increase of upstream apex width may be a feasible method to decrease the negative effects of nappe interference, which in turn may increase discharge efficiency.

This was analyzed in this study by testing a series of eight laboratory scaled labyrinth weirs (with sidewall angles of 12°), with various upstream apex widths. Upstream apex width tests were performed in a fixed and varied channel width setting.

The design method developed by Crookston and Tullis is based on laboratory scaled physical models. This method is very useful in the estimation of performance for geometrically similar prototype labyrinth weirs. However, due to difficulty in obtaining data on completed prototype weirs, design method predictions are rarely verified. To help validate Froude scaling and design method predictions of prototype weirs, a series of physical model tests (with sidewall angles of 15°) were performed with varying scale sizes (0.5 to 3.0 compared to the size of weir used in the design method).

To expand the applicability of the design method to common geometric variations, tests were performed on weirs of varying weir height and cycle width (with sidewall angles of 15°). These variations were applied independently and analyzed to determine their effects on discharge efficiency and design method predictions. A correction factor is then presented to be used in conjunction with Crookston and Tullis's design method for these geometric variations. All conclusions are presented in this thesis.

-Tyler Robert Seamons

ACKNOWLEDGMENTS

The time working on this project has been a very positive educational experience for me. I have learned many valuable skills that I will be able to apply throughout my life. There are many people that have helped me throughout this process that deserve recognition. I'd like to thank Dr. Blake Tullis (my major professor and mentor) for all of his guidance and advice. He has helped me grow a lot as a student and I feel that he has prepared me well to enter into the professional world. I would also like to thank my other committee members, Dr. Brian Crookston and Dr. Joe Caliendo, for all of their time and effort they have put forth in giving me helpful guidance and suggestions.

Others that have helped building and installing the weirs that I'd like to also thank are Aaron Anderson, Mitch Dabling, and Riley Bradshaw. Thanks to the shop crew down in the lab for all of their support. I really appreciate all of my fellow students and shop crew's help. Thanks to Carlie Christensen for her help in proof reading and allowing me to practice my thesis defense with her. I want to especially thank my family for their encouragement and support, for the way my parents raised me, and for their unconditional love. I give thanks to God for giving me the will and strength to pursue and finish this project.

I have enjoyed this project and have learned a lot. I really appreciate everybody's help and I couldn't have done it without them. Thanks!

-Tyler Robert Seamons

CONTENTS

Page

LIST OF TABLES

LIST OF FIGURES

NOMENCLATURE

A	Inside upstream apex width
A/w	Apex Ratio
A_c	Apex center-line width
A_c/l_c	Crest ratio
α	Sidewall angle
B	Labyrinth depth, the length of labyrinth weir in flow direction
B_d	Length of labyrinth weir (in flow direction) affected by nappe interference. Calculated from L_d developed by Indlekofer and Rouvé (1975)
B_{int}	Measured length of labyrinth weirs (in flow direction) affected by nappe interference as described by Crookston (2010)
C_d	Discharge coefficient
C_m	Mean discharge coefficient in the zone of disturbance
$C_{d(90°)}$	Discharge coefficient for linear weirs
ε'	Cycle efficiency, $\varepsilon' = C_d L_{c\text{-}cycle} / w$
g	Acceleration due to gravity
h	Depth of flow over the weir crest
h_m	The head upstream of the weir that consists of a specific upstream depth and two velocity components as defined by Indlekofer and Rouvé (1975)
HR	Half-round crest shape

H_T	Total upstream head on weir
H_T/P	Headwater ratio
L	Characteristic weir length
L_c	Total centerline length of weir, $L_c = 2N\ (l_c + A_c)$
l_c	Centerline length of sidewall
L_{de}	A theoretical effective disturbance length where Q and $C_d = 0$ (Indlekofer and Rouvé 1975)
L_d	A theoretical disturbance length where the flow is affected by nappe interference (Indlekofer and Rouvé 1975)
L_d/l_c	Disturbance length ratio
L_e	Total effective length of labyrinth weir
N	Number of cycles
P	Weir height
P/t_w	Relative thickness ratio
Q	Discharge over weir
QR	Quarter-round crest shape
R_{crest}	Weir crest radius
t_w	Thickness of weir wall
V	Average upstream cross-sectional velocity
vw	Varied width channel [refers to models tested in a narrower (45in.) channel used in this study]
W	Width of channel

w	Width of a single labyrinth weir cycle
w/P	Cycle width ratio
ω_Q	Uncertainty interval for flow rate
ω_{Lc}	Uncertainty interval for centerline crest length
ω_W	Uncertainty interval for channel width
ω_{Ptgage}	Uncertainty interval for point gage reading
ω_{Yref}	Uncertainty interval for crest reference
ω_{mA}	Uncertainty interval for pressure transducer
ω_{Yramp}	Uncertainty interval for ramp height
$\omega_{Yplatform}$	Uncertainty interval for platform height

CHAPTER I

INTRODUCTION

Weirs are widely used in many different forms to regulate and measure the flow of water. The parameter that contributes the most to a weir's discharge efficiency (discharge at a given upstream total head) is its crest length (Falvey 2003). A labyrinth weir is a linear weir folded in plan-view to increase its overall crest length (L_c), for a given channel width. The increase in crest length, in most instances, will increase discharge efficiency (Crookston 2010). This makes labyrinth weirs an effective alternative for use in spillway rehabilitation projects. The longer weir length, and subsequent increased discharge efficiency, means that for a given upstream pool elevation, the labyrinth weir will produce a larger discharge relative to a linear weir. This means that the amount of freeboard required for flood storage can also be reduced.

A trapezoidal labyrinth weir cycle is most common; however, triangular and rectangular cycle shapes are also possible (Fig. 1). Within the trapezoidal labyrinth weir

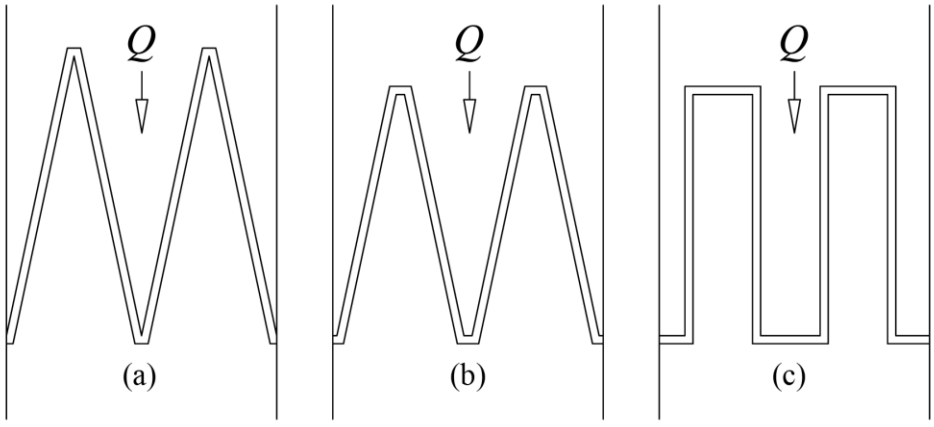

Fig. 1. Geometric classifications of labyrinth weirs;
Triangular (a), Trapezoidal (b), and Rectangular (c)

geometric classification, there are countless geometric design possibilities. This study evaluated four different geometric variations that could be applied to labyrinth weir design, which include (Fig. 2 for trapezoidal labyrinth weir variable definition):

- variations in A with corresponding shortening of l_c to maintain a constant W
- upstream apex width (A) variations with fixed sidewall (l_c) and downstream apex lengths [the channel/weir width (W) is variable]
- evaluation of the use of Froude scaling and size-scale effects
- evaluation of the influence of the cycle width ratio (w/P) [cycle width (w) and weir height (P) were varied independently] on discharge characteristics.

In an effort to reduce nappe interference and increase discharge efficiency for trapezoidal labyrinth weirs, various upstream apex widths were analyzed and compared. By increasing the upstream apex width, local submergence is reduced and the discharge coefficient (C_d) approaches that of a linear weir. With a fixed channel width and sidewall angle, increasing the apex width will decrease the overall crest length. The weirs with wider upstream apexes may be more efficient per unit length, but the overall length of the

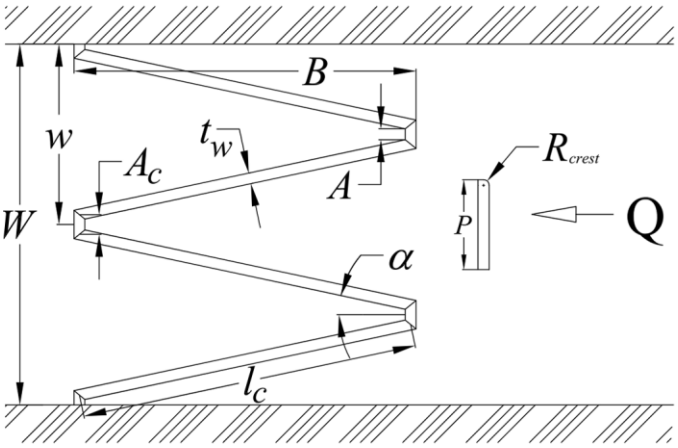

Fig. 2. Trapezoidal Labyrinth weir variables defined

weir will be decreased (shorter L_c, see Fig. 3). Thus, there is a tradeoff between L_c and A that will be evaluated. Three different upstream apex widths were tested at one common sidewall angle (α=12°) to determine and compare flow efficiencies of each design.

It is common that geometric boundaries, such as a spillway on top of an existing dam, determine the geometry of a weir. In such cases, W may be restricted and a full or half cycle (N) of a designed labyrinth weir may not fit within the given apron width. In order to utilize the full possible apron width, maintaining α and either a full or half cycle number, one has the option to increase the weirs width by either increasing A or increasing l_c (Fig. 4). By increasing A, nappe interference should decrease and increase discharge efficiency locally. However, by maintaining A constant and increasing l_c, overall crest length (L_c) will increase more (which increases discharge efficiency). Comparisons were made to determine the highest increase in flow efficiency when varying channel width (W) by either increasing A or l_c.

In the case where the labyrinth weir length (B) is limited, it may be beneficial to

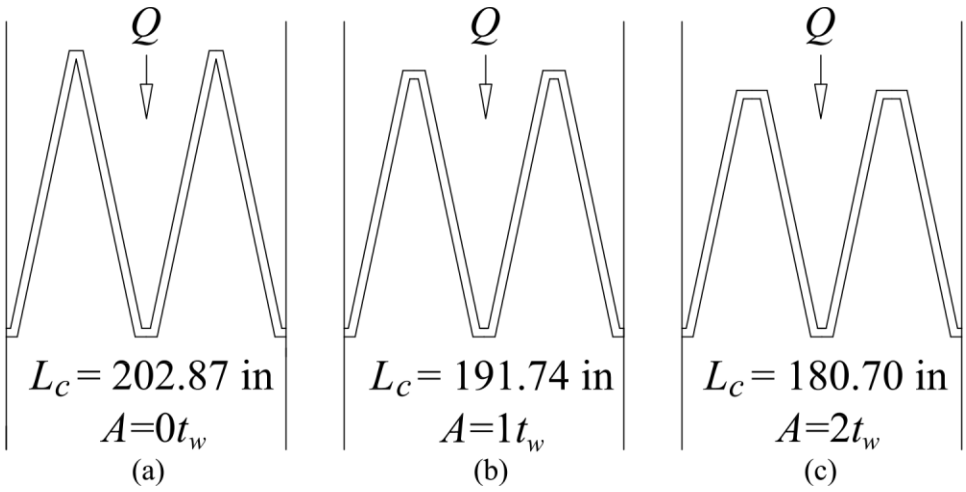

Fig. 3. Variation of A [in terms of sidewall thickness (t_w)] and its effect on L_c

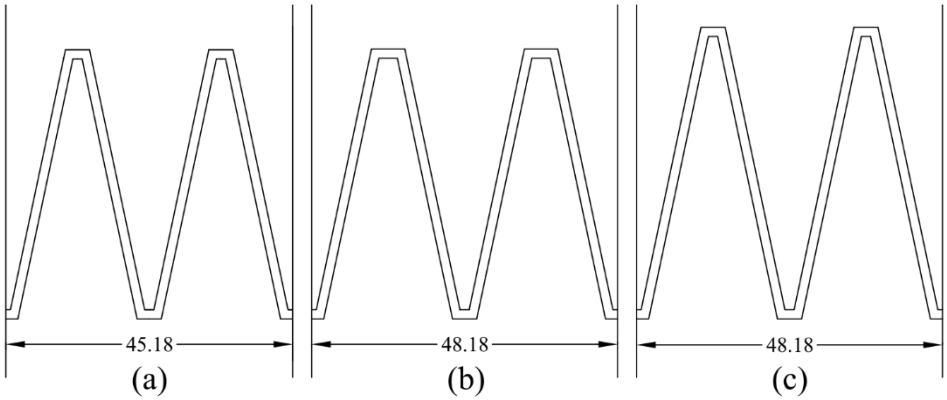

Fig. 4. Small *W* (a), enlarged *W* by increasing *A* (b), enlarged *W* by increasing l_c (c)

increase the number of cycles (*N*), while maintaining α, weir height (*P*), wall thickness (t_w), and centerline apex width (A_c) constant. However, these influences on head-discharge characteristics are unknown. As *N* increases per given channel width, while maintaining the aforementioned variables constant, cycle width (*w)* decreases and may cause the cycle width ratio (*w*/*P*) to be outside of the experimental data range tested. The labyrinth weir design method presented by Crookston and Tullis (2013a) uses design curves formulated from physical models of weirs with *w*/*P*=2. Thus, as *w*/*P* differs from the physical models tested, the accuracy of the design method may vary. Accuracy of design method predictions and weir discharge performance were analyzed to more fully understand the effects of varying *w*/*P* by changing *w*.

Applying design methods to specific case studies, such as Dog River Dam (Savage et al. 2004), where *P* of the existing labyrinth weir walls was increased can be very beneficial. By changing *P* only and leaving all other parameters the same may move *w*/*P* away from the 2.0 ratio tested by Crookston and Tullis (2013a), but may still be a feasible design. The headwater ratio (H_T/*P*) is also affected for a given total head (H_T).

The design method of Crookston and Tullis (2013a) was developed with a rating curve dependent on H_T/P. When P is varied, this ratio along with the design method predictions will change. However one would suspect that flow efficiencies would be similar for smaller discharges, since both weirs have identical plan views and crest geometries. Model studies evaluated the effect of varying P on design predictions and weir performance. Adjusted C_d values are given for labyrinth weirs with w/P ratios differing from the design method due to changes in w and P.

The use of Froude scaling has been widely used in the construction of physical models to test prototype spillway designs. Physical models are used to confirm prototype design and test different spillway configurations. There is some uncertainty involved when using physical models due to size-scale effects (surface tension, air entrainment, etc.) that may not be reasonably accounted for when using Froude scaling. An analysis was made using three different geometric scales to investigate the effects of Froude scaling.

Contributions to the labyrinth weir knowledge base have been made by Taylor (1968), Hay and Taylor (1970), Indlekofer and Rouvé (1975), Houston (1982), Hinchliff and Houston (1984), Lux (1984; 1989), Cassidy et al. (1985), Lux and Hinchliff (1985), Tullis et al. (1995), Falvey (2003), Savage et at. (2004), Tullis et al. (2007), Crookston and Tullis (2012a, b, c; 2013a, b), and Dabling et al. (2013). Conclusions made through this study will help extend this knowledge base of labyrinth weir design methods and applications.

CHAPTER II

BACKGROUND LITERATURE

Nappe Interference and Local Submergence

A head-discharge relationship for labyrinth weirs is commonly performed using a general form of the weir equation, Eq. (1).

$$Q = \frac{2}{3} C_d L_c \sqrt{2g} H_T^{3/2} \quad (1)$$

where C_d is the dimensionless discharge coefficient, L_c is the total weir length, g is the acceleration due to gravity, and H_T is the total upstream head which can be written as $H_T = V^2/2g + h$ (V and h are the average cross-sectional velocity and piezometric head upstream of the weir relative to the weir crest elevation, respectively, both measured at a cross section upstream from the weir). An accurate head-discharge relationship [Eq. (1)] requires accurate C_d data. For labyrinth weirs, C_d values are typically determined experimentally at the laboratory scale and are a function of H_T, α, wall thickness (t_w), weir wall height (P), crest shape, approach flow conditions, nappe aeration behavior (clinging, aerated, partially aerated, and drowned nappe flow), and A (Crookston and Tullis 2012c).

Due to their geometry, labyrinth weirs produce unique flow conditions. One of these conditions, nappe interference, occurs near the upstream apex where nappe flow from the adjacent sidewalls and apex interact. Local submergence occurs because of nappe collisions and the limited cross-sectional flow area near the upstream apexes. This is when tailwater conditions locally exceed the weir crest elevation. Local submergence differs from traditional weir submergence in that local submergence does not necessarily

encompass the entire labyrinth weir (it begins at the upstream apexes and extends downstream with increasing discharge) and it is not caused by a downstream tailwater control. Nappe collisions and local submergence effects that are significant enough to reduce the discharge efficiency are referred to as nappe interference (Crookston and Tullis 2012c). Efforts have been made to account for this decrease in discharge efficiency by using an "effective" weir length (L_e) in Eq. (1) rather than the actual weir length (Tullis et al. 1995). Inherently, the C_d value accounts for any losses associated with nappe interference. However, developing a better understanding of the influence on nappe interference on discharge capacity would provide useful information to practitioners.

Taylor (1968) performed several experimental model tests on different configurations of labyrinth weirs in order to develop a design method. As part of his research, he studied the effects of nappe interference on labyrinth weir performance. He used the vertical aspect ratio (w/P) to predict the effects of nappe interference. He tested weirs of different w and concluded that when w/P is large, the effects of nappe interference can be effectively eliminated. However when w/P is small, nappe interference becomes a determining factor in labyrinth weir performance. In order to avoid the negative effects of nappe interference on discharge efficiency, he states that w/P should be as large as possible and greater than 2 at a minimum.

Indlekofer and Rouvé (1975) evaluated a corner weir, which is similar to a single-cycle triangular labyrinth weir with a reservoir approach flow condition (i.e., the flow approached each weir sidewall perpendicularly). Relative to the corner weir, they evaluated nappe interference by categorizing two regions of weir flow. The first region, called the zone of disturbance, includes the weir length [disturbance length (L_d)]

corresponding to nappe collisions and local submergence. The second weir flow region corresponds to linear weir flow conditions (i.e., all streamlines are perpendicular to the weir and free of nappe collisions). They reported that L_d increases linearly with increased H_T. If an equivalent corner weir discharge were passed over a linear weir at a common upstream head, the difference between the required linear weir length and the actual corner weir length was defined as the effective disturbance length (L_{de}). L_{de} [see Eq. (2)] represents an assumed length of corner weir with an effective discharge of zero. The sum of the weir lengths and discharges over the assumed linear weir and L_{de} corner weir segments sum to the actual values for the corner weir.

$$L_{de} = (1 - C_m)L_d = 2l_c - \frac{3Q}{2C_{d\_90}\sqrt{2g}h_m^{3/2}} \qquad (2)$$

In Eq. (2), C_m is the mean discharge coefficient in the zone of disturbance, l_c is one sidewall crest length, h_m is the head upstream of the weir as defined by Indlekofer and Rouvé (1975), and C_{d_90} is the discharge coefficient for a linear weir. This relationship is based on the following assumptions: the weir is sharp crested, which provides a fully aerated and stable nappe; nappe interference is the sole contributor to decrease in overall weir discharge efficiency relative to a linear weir; and the disturbance length and effective disturbance length increase linearly with total head (Indlekofer and Rouvé 1975). The disturbance length ratio, L_{de}/l_c, compares the effective disturbance length to the sidewall length of a labyrinth weir. This was developed to determine the extent of nappe interference on a given weir, with the assumption that overall labyrinth weir performance declined with increasing values of L_{de}/l_c.

Cassidy et al. (1985) performed a detailed study on the Boardman labyrinth spillway and found that the calculated discharge coefficients determined from extrapolated results from Hay and Taylor (1970) were not consistent with their model study. They found differences in discharge capacity between 20-25% at high heads.

Falvey (2003) noted that for a labyrinth weir, the approach flow streamlines were only perpendicular to the crest at low discharges. At higher discharges, the streamlines were not perpendicular to the crest even beyond the nappe disturbance region. Despite the differences in flow characteristics between corner and labyrinth weirs, based on comparing the Indlekofer and Rouvé relationship to data from several labyrinth weir model studies, Falvey tried to develop L_{de} empirical relationships for labyrinth weirs [see Eqs. (3) and (4)].

$$\frac{L_{de}}{H_T} = 6.1 * e^{-0.052\alpha} \qquad \alpha \geq 10° \qquad (3)$$

$$\frac{L_{de}}{l_c} = C_1 \ln\left(\frac{H_T}{P}\right) + C_2 \qquad \alpha \leq 20° \text{ and } H_T/P \geq 0.1 \qquad (4)$$

In Eqs (4) and (5), C_1 =0.224 ± 0.053 and C_2 = 0.599 ± 0.104. The coefficient C_2 can be approximated by using $C_2 = 0.94 - 0.03\alpha$ in which α is the sidewall angle in degrees. It should be noted that the total head, H_T, is being used in Eq. (3) instead of the piezometric head and that L_{de} does not have a linear relationship with H_T/P for weirs with $\alpha < 20°$ as previously presented by Indlekofer and Rouvé.

Crookston and Tullis (2012c) analyzed the accuracy of Eq. (3) and (4) and the appropriateness of using the corner weir nappe interference method presented by Indlekofer and Rouvé (1975) on labyrinth weirs. Based on the results of 21 laboratory-scale labyrinth weir models featuring quarter- and half-round crest shapes and $6° \leq \alpha \leq$

35°, they recognized several problems with applying the Indlekofer and Rouvé method to labyrinth weirs, including: non-perpendicular labyrinth weir approach flow streamlines with the exception of small H_T values; crest shapes can influence the nature of nappe interference regions substantially; stability and aeration of the nappe vary with H_T; L_d and L_{de} do not vary linearly with H_T; and the efficiency of labyrinth weirs are affected by upstream flow conditions, local submergence, and weir geometry. They do note that L_d and L_{de} nearly have a linear relationship when $\alpha > 35°$. Indlekofer and Rouvé used corner weirs with $\alpha > 23°$. Crookston and Tullis (2012c) found very limited correlation between Eqs. (3) and (4) and their experimental data.

Since L_d and L_{de} are not physically measurable and in the absence of a reliable method for predicting their value for labyrinth weirs, Crookston and Tullis (2012c) introduced an alternative, physically measurable, nappe interference parameter, B_{int}. B_{int} is measured from the downstream face of the upstream apex wall to the point where the nappe flow crosses the weir crest elevation and is related to L_d by [$L_d \approx B_{int}\cos(\alpha)$] (see

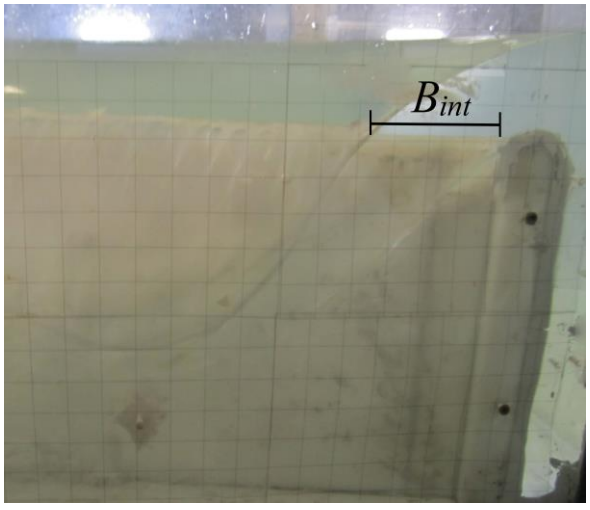

Fig. 5. B_{int}; α=12°, A=1t_w, and H_T/P = 0.325

Fig. 5). They concluded that Eq. (2) accurately described the discharge efficiency and weir length differences between linear weirs and labyrinth weirs at equivalent heads but does not accurately represent nappe interference. An effective method for correlating the value of B_{int}, nappe interference, and a reduction in discharge capacity has yet to be determined.

Apex Width Variation

Lux and Hinchliff (1985) suggests that nappe interference is a function of A_c/w and t_w/P. Later Lux (1989) recommends A_c/w should be as low as possible to increase weir performance. For trapezoidal weirs, he suggested that $A_c/w \leq 0.0765$ can be used without suffering large decreases in performance due to nappe interference.

Tullis et al. (1995) also recommended that the apex width should be as small as possible to increase weir capacity, but due to constructability limits, apex widths usually range between 1- to 2-t_w. Crookston states that A_c is commonly determined by minimum workspace requirements for construction (Brian Crookston, personal communication, May 15, 2013). However, it is still beneficial to determine, through model studies, the effects of A_c on discharge efficiency to determine if larger apexes are hydraulically more efficient.

One of the purposes of this study is to provide new data and information to support a conclusion on the optimal upstream apex width (A) to maximize discharge efficiency for half- and quarter-round crested labyrinth weirs with a sidewall angle of α=12°. Other design parameters such as P and t_w were dimensionally consistent with the weirs used by Crookston and Tullis (2013a). An analysis was performed by testing and

comparing overall discharge efficiencies and unit discharges of labyrinth weirs with varying upstream apex widths (A) of $A=0t_w$, $A=1t_w$, and $A=2t_w$ as shown in Fig. 2.

Effects of Varying *w* on Design Method Predictions

Waldron (1994), among other tests, evaluated four geometrically dissimilar α = 12° labyrinth weirs with varying N (2.5, 3, 3.34, and 4). Each weir was tested in a 3-ft wide flume and with $A_c=1t_w$. He found that the discharge coefficient is mostly independent of the number of cycles (Fig. 6). From further examination of his data, the 3.34 cycle weir has consistently lower discharge coefficients over the entire range of H_T/P and the 4-cycle weir has slightly lower discharge coefficients compared to N = 2.5 and 3 weirs. Compared to the 2.5-cycle labyrinth weir (Fig. 7), the 3.34-cycle weir shows a

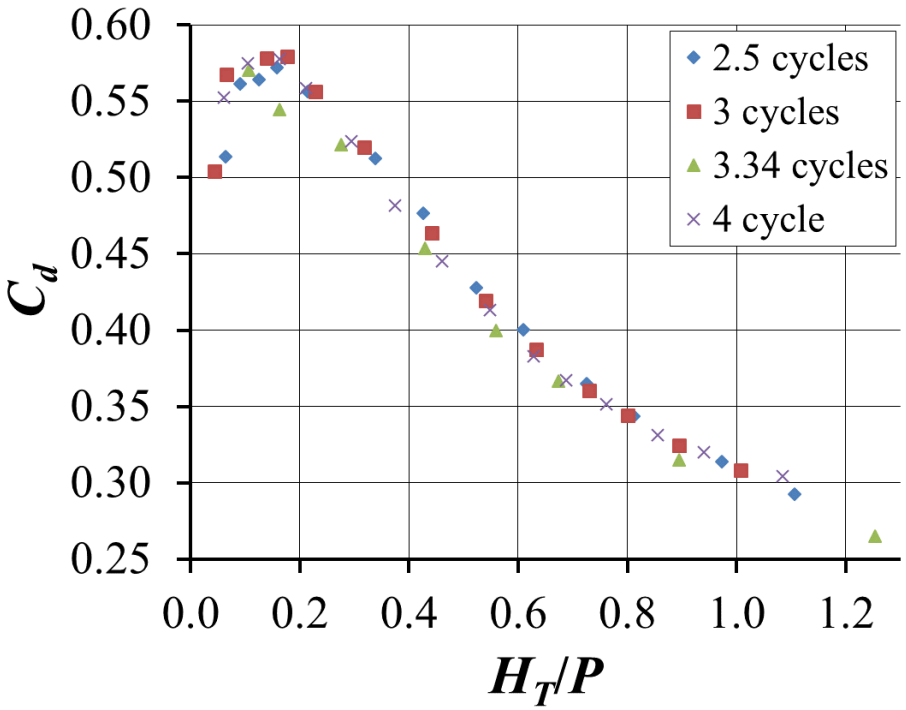

Fig. 6. C_d vs H_T/P data of labyrinth weirs (α=12°) with varying N (Waldron 1994)

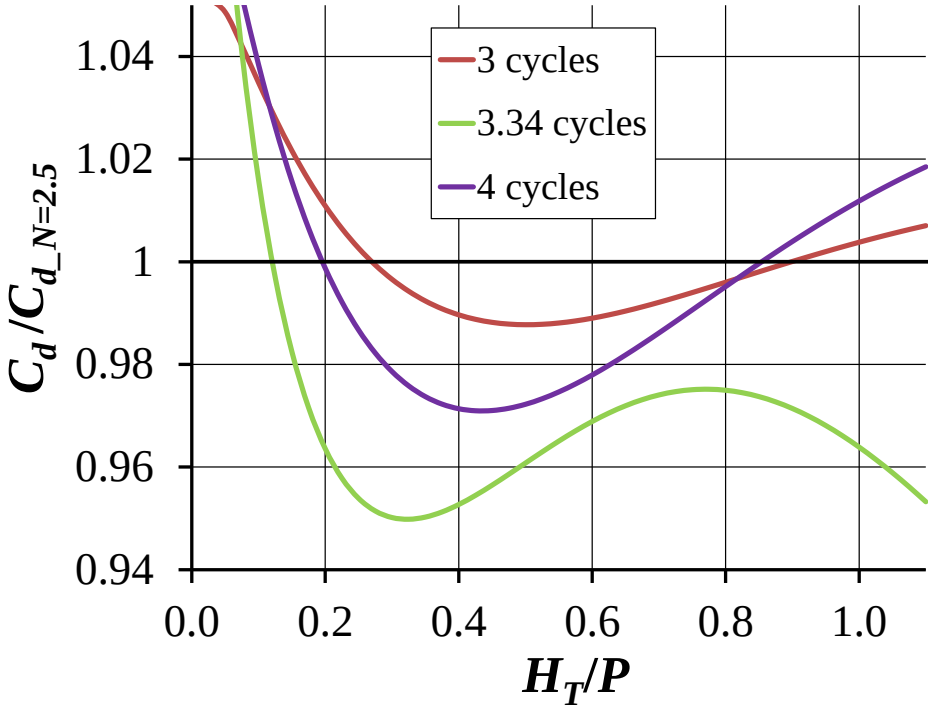

Fig. 7. Cycle number variation - C_d comparison to 2.5 cycle weir (Waldron 1994)

C_d percent decrease of up to ~5%, ~3% for the 4-cycle weir, and ~1% for the 3-cycle weir. It should be noted that P of the N = 3.34 weir is about half of that of the other weirs, which may have also influenced the C_d values.

Crookston et al. (2012) tested a total of six $\alpha = 15°$ trapezoidal labyrinth weirs. Three of these weir designs maintained constant P, t_w, A_c, and α values and varied N, w, and l_c. They found that as A_c / l_c increases, cycle efficiency decreases significantly. Since the apex contributes the least to the overall discharge efficiency, as it becomes a larger portion of the overall cycle length and sidewall length decreases, overall discharge efficiency decreases. Also, as N increases (in a given channel width), the total crest length is decreased. This also negatively affects discharge efficiency. Crookston's data shows that, for a given channel width, when the weir is scaled down, the weir's discharge

efficiency is not significantly affected. However, if *N* is increased while maintaining *A*, t_w, *P*, and α constant, then discharge capacity decreases and approaches that of a linear weir with a crest length equal to the channel width. This is due largely to the increase in A_c / l_c (larger portion of weir is apex) and decrease in l_c. The decrease of l_c with the increase of *N* can be seen in Fig. 8.

As *N* changes, while maintaining *A*, t_w, *P*, and α constant, the *w*/*P* ratio also changes (since *w* is directly related to *N*) and may fall outside the design method limits. No publications have been found that present a design method to predict discharge efficiencies for dissimilar labyrinth weirs of varying *N* with similar *A*, t_w, *P*, and α.

Effects of Varying *P* on Design Method Predictions

A numerical study conducted by Savage et al. (2004) and compared to physical models performed by the Bureau of Reclamation found that current design methods (Lux and Hinchliff 1985; Tullis et al. 1995) were not complete for weirs with varying *P* values. As *P* was increased, the hydraulic performance data fell outside of the bounds of the

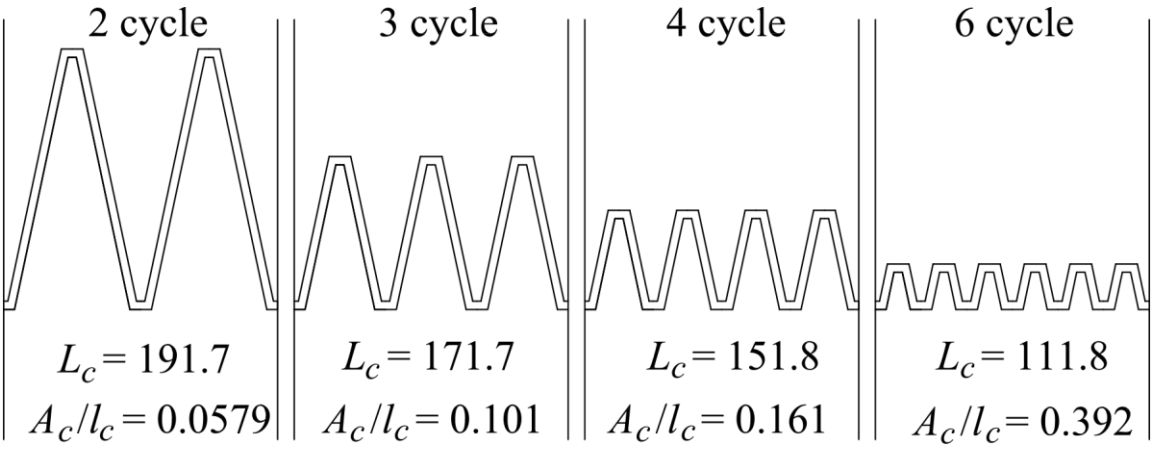

Fig. 8. Effects of *N* on cycle length and *w/P* for weirs of similar *A*, t_w, *P*, and α

experimental data used to develop the design methods. The applicability of these design methods is limited to the dimensions specified. Savage et al. (2004) found that when *P* was increased by 66.7%, the design method predications were within ± 25% of the physical model results. This is in part due to the fact that the rating curve for the design methods of Tullis et al. (1995) and Lux and Hinchliff (1985) are dependent upon H_T/P, which is affected by the change of *P*. Savage et al. (2004) noted that physical models have been the standard for discharge verification and suggests the use of computation fluid dynamics (CFD) modeling as a cost effective alternative, which showed relatively good correspondence (within ~10%) to the physical model.

Crookston et al. (2012) tested 3 physical models of labyrinth weirs to determine the effects of varying the *w/P* ratio on discharge efficiency. They stated that the width ratio (*w/P*) does not completely describe the effects of nappe interference on the head-discharge characteristics but can provide useful guidelines for determining the accuracy of design method predictions. They found that when *P* was decreased by 50%, *Q* was decreased by approximately 20%. When *P* was increased by 100%, *Q* was increased by approximately 6%. They also noted that similar cycle geometries are possible with different *w/P* ratios, thus all labyrinth weir geometries must be examined closely. The ability of current design methods to predict flows of weirs with similar plan view dimensions but varying weir heights is not accurate and more research is needed in this area.

Froude Scaling and Size-Scale Effects

Hay and Taylor (1970) concluded that for geometrically similar labyrinth weirs, scaling the weir does not have a significant effect on performance. However, after some investigation into the data presented, the two trapezoidal weirs (N = 2 ½ and 3), had similar performances at low H_T/P (≤ 0.25) but had noticeable differences in performance at higher H_T/P values ($H_T/P > 0.25$). Data presented for the N = 2.5 weir do not exceed $H_T/P \approx 0.33$. Therefore, due to the lack of data at higher heads, no conclusions can be made about size-scale effects at higher heads. It can be seen from this study that for small changes in scale, there are practically no performance difference at lower heads. It would be of interest to see the effects of large changes in scale through a larger $H_T/$P range.

Research Objectives

This study focuses on various geometric deviations, from current labyrinth weir design methods, and their effects on discharge efficiencies. The results are limited to the geometric configurations of the models tested (specified below) and within a range of $0.1 > H_T/P > 0.8$. The main objectives of this study are to:

- Provide rating curves for $A=1t_w$, $A=2t_w$, and $A=0t_w$ labyrinth weirs with quarter and half-rounded crests and α=12° (test matrix is shown in Table 1).
- Provide apex width design criteria for quarter and half-round labyrinth weirs that optimize discharge efficiency (for weirs with α=12°).
- Provide data to support a conclusion on whether discharge efficiency is increased more for a fixed and varied channel width by increasing upstream apex width (A) or crest length (l_c) (for weirs with α=12°).

- Determine if the effective length parameter presented by Tullis et al. (1995) is an effective way of quantifying the effects of nappe interference.
- Determine the effects from varying w/P ($0.69 > w/P > 2.01$) by changing w, while maintaining P, t_w, A_c, and α constant, on discharge efficiency and the effectiveness of current design methods to predict these flows. Develop a method to accurately predict discharge efficiencies for this type of variation (for weirs with α=15°).
- Determine the effects of varying w/P ($1.02 > w/P > 4.02$) by changing P, while maintaining w, t_w, A_c, and α constant on current design method discharge efficiency predictions. Develop a method to accurately predict discharge efficiencies for this type of variation (for weirs with α=15°).
- Determine the effects of using Froude scaling to scale model data. Size-scale effects, such as surface tension, will be analyzed and quantified for geometrically similar weirs scaled to 0.5 and 3.0 times that of the weirs (α=15°) used in the design method of Crookston and Tullis (2013a).

CHAPTER III

EXPERIMENTAL SETUP

Test Facilities and Instrumentation

Research was performed at the Utah Water Research Laboratory (UWRL), located on the Utah State University Campus in Logan Utah. All models were tested in a tilting rectangular flume, 4-ft wide x 48-ft long x 3-ft deep (1.2-m wide x 14.6-m long x 0.9-m deep). The flume's frame is constructed out of steel and the floors and walls are 3/4 in (1.9 cm) acrylic sheeting (Fig. 9). A rolling cage with a sliding point gage mounted on it was used for B_{int} measurements and determining accurate crest references. The slope of the flume floor is adjustable by four mechanical jacks. For all tests, the slope of the flume floor was set to 0° (horizontal). Water is gravity fed to the UWRL from First dam (a nearby reservoir along the Logan River). Flow into the flume is provided by a 20-in (50.8-cm) or 8-in (20.3-cm) diameter supply pipelines, each controlled by separate butterfly valves (Fig. 9). Flows to the flume enter the bottom of the headbox. To help ensure uniform flow, a baffle structure and wave suppressor board were installed at the upstream end of the flume (Fig. 10). Piezometric head was measured 39.5 in (1.00 m) upstream of the platform with a vernier scale point gage [readable to ± 0.0005 ft. (0.15 mm)] that measures the water height in a cylindrical stilling basin (Fig. 11). Care was taken to always wet the tip of the point gage before each measurement, to ensure an accurate and consistent reading.

The flow rates of each supply line were measured using calibrated orifice plates and measuring the differential pressure. The differential pressure was measured with a

pressure transducer connected to a data logger. Upstream pressure taps are located 21 in (53.3 cm) for the 20 in (50.8 cm) pipe and 12.5 in (31.8 cm) for the 8 in (20.3 cm) pipe from the orifice plate, while downstream pressure taps are located 11 in (27.9 cm) for the 20 in (50.8 cm) pipe and 4 in (10.2 cm) for the 8 in (20.3 cm) pipe from the orifice plate (Fig. 10). A Hart communicator was connected to the pressure transducer to zero it out and set appropriate ranges to accurately measure the desired flow rate.

(a) (b)

Fig. 9. Four foot flume (a) and control valves (b)

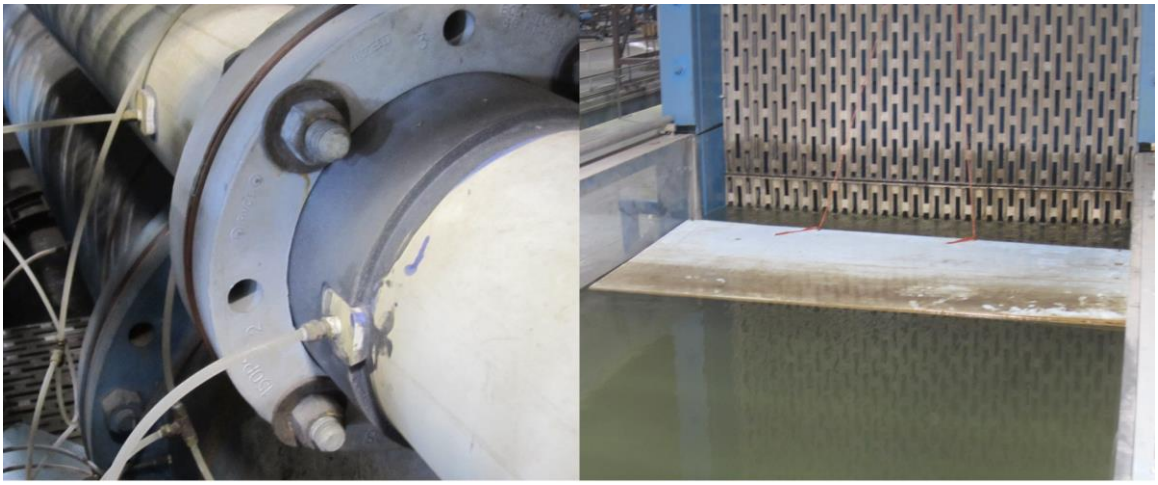

(a) (b)

Fig. 10. Pressure taps on 8-inch supply line (a) and aluminum grate and plywood board to help ensure uniform flow (b)

Fig. 11. Stilling basin with point gage

Assembly and Installation of Labyrinth Weir Models

Tests were performed on a total of 13 laboratory-scaled labyrinth weirs with varying crest shapes, upstream apex widths (A), wall heights (P), channel width (W), and sidewall angles (α). All labyrinth weirs tested consisted of two full cycles (N=2) and had a crest radius of half the wall thickness ($R_{crest} = t_w/2$).

For the variable channel width experiment, models 5, 8, and 9 (Table 1) were used and analyzed. One A=1t_w, α=12° (model 9) weir was modified and tested in a narrower 45-in (114.3 cm) wide channel to be able to test methods of increasing discharge efficiency when additional channel width (W) is available. This weir will be referred to as $A=1t_{w\text{-}vw}$ (varied width). This was accomplished by adding a false wall in the flume. The false wall started 8 ft (2.4 m) upstream of the weir and continues 1 ft (30.5 cm)

downstream of the weir. A 1 ft (30.5 cm) tapered transition was also placed at the start of the false wall that helped ensure uniform flow.

For the apex variation tests, the inverted orientation (Fig. 12) was chosen to be able to test 2 full upstream apexes instead of partial apexes. Eight weirs (models 1-8, Table 1) were built to compare the effects of varying the upstream apex widths (A). They had A equal to 1 wall thickness (A=1t_w), A=2t_w, and A = 0t_w (triangular apex) with quarter- and half-round crests. For the A = 0t_w models, due to difficulty in construction, a blunted triangular weir was tested (see A = 0t_w in Fig. 3).

Four α =15° labyrinth weirs were built to determine the effects of varying P on discharge capacity and design method effectiveness. Weirs were built out of High Density Polyethylene (HDPE) and PVC sheeting. See Table 1 for all physical models tested in this study. The weirs were built on a 3/4 in (1.9 cm) HDPE sheet and placed on a platform inside of the flume. An 8 ft (2.4 m) HDPE sheet was used as a ramp to create a smooth transition to the base of the platform. A plan view schematic of the flume with

Table 1. Physical Models Test Matrix (Current Study)

Model	***A***	***l_c***	***W***	***w/P***	***α***	***P***	***P/t_w***	**Crest**	**Orientation**
( )	**(in)**	**(in)**	**(in)**	**( )**	**(°)**	**(in)**	**( )**	**( )**	**( )**
1	0	48.8	48.2	2.01	12	12	8	QR	Inverted
2	0	48.8	48.2	2.01	12	12	8	HR	Inverted
3	0	48.8	48.2	2.02	12	12	8	HR	Inverted
4	1.45	45.3	48.2	2.01	12	12	8	QR	Inverted
5	1.45	45.3	48.2	2.01	12	12	8	HR	Inverted
6	1.45	45.3	48.2	2.01	12	12	8	HR	Normal
7	2.90	41.8	48.2	2.01	12	12	8	QR	Inverted
8	2.90	41.8	48.2	2.01	12	12	8	HR	Inverted
9	1.45	41.8	45.2	1.88	12	12	8	HR	Inverted
10	1.45	45.3	48.2	1.34	12	18	12	QR	Normal
11	1.45	36.6	48.2	1.34	15	18	12	QR	Normal
12	1.45	36.6	48.2	1.61	15	15	10	QR	Normal
13	1.45	36.6	48.2	2.01	15	12	8	QR	Normal

the false wall in place can be seen in Fig. 13 and an elevation view schematic of the flume is shown in Fig. 14. All labyrinth weir model drawings and dimensions can be found in Appendix A.

When installing the weir inside of the flume, survey equipment was used to level the weir crest. Metal pieces 1/32 in (0.8 mm) thick were placed underneath the weir until the weir crest was leveled to ± 1/32 in (±0.8 mm).

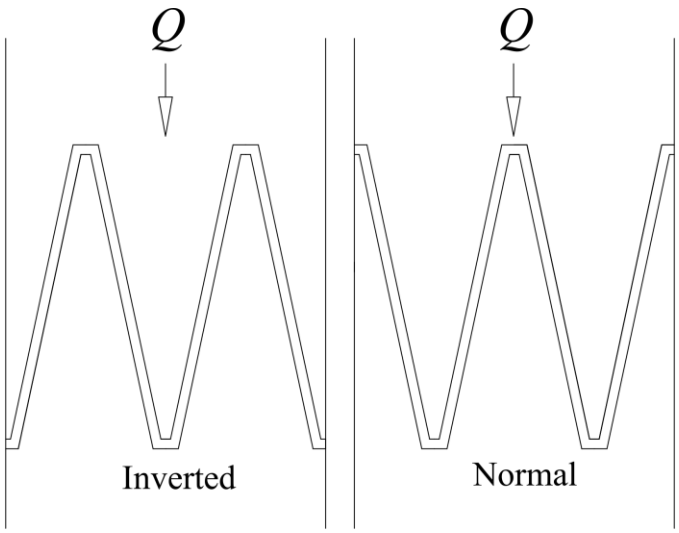

Fig. 12. Normal vs. inverted orientation in channelized flume

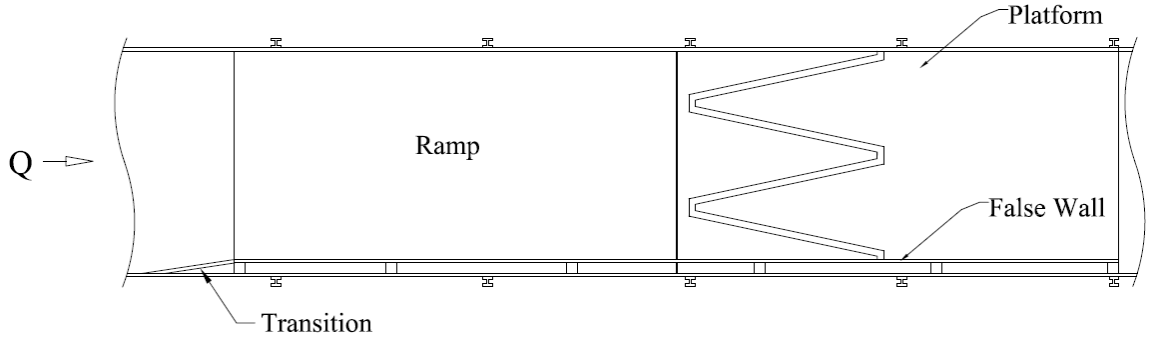

Fig. 13. Plan view of four foot flume with false wall

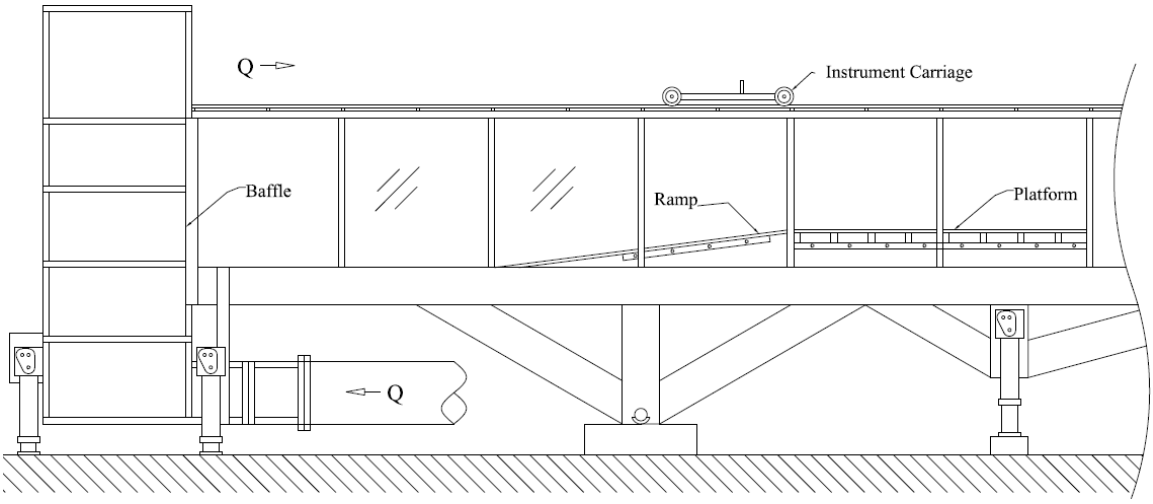

Fig. 14. Elevation view of four foot flume setup

Test Procedure

Thirteen physical model labyrinth weirs were tested in a 4 ft. (1.2 m) flume. Each weir was tested following the same steps to ensure consistency and repeatability. After installation, the flume was filled with water and allowed 30 min before testing to accommodate thermal expansion/contraction. During this time a leak rate was also determined. This was calculated by using the water surface elevation over a period of time and the area of the flume. An accurate crest reference is a critical part of providing an accurate set of data. The crest elevation reference was determined by measuring the crest height at 12 locations distributed along the weir length using the point gauge on the rolling carriage, calculating the corresponding average point gauge crest elevation reference. The upstream water level in the flume was measured using the point gauge on the rolling carriage and the point gauge in the stilling well. The different between the average crest and water surface elevations was added to the stilling well water surface

reading to determine the crest reference elevation in the stilling well. The repeatability associated with multiple crest reference procedures served as an indication of accuracy.

With an accurate crest reference, data were collected over a flow range corresponding to $0.1 < H_T/P < 0.8$. There were approximately 20-30 flow measurements tested for each weir. Data were collected by adjusting the flow rate (Q) and measuring the piezometric head (h). To see each set of collected data and details of the weir being tested, see Appendix B. To ensure steady state conditions, measurements were not taken until a sufficient amount of time had passed (at least 4 min). Once steady state was achieved, Q and h were measured and recorded. These values, along with a description of the nappe behavior, were entered directly into an Excel spreadsheet and logged in a notebook. H_T was calculated by adding the velocity head to the h. Accuracy was ensured by repeating several flow measurements within the data range. Rating curves for each labyrinth weir were established and flow efficiencies were compared. If any irregularities were discovered in the data collection process, data points were recollected and analyzed

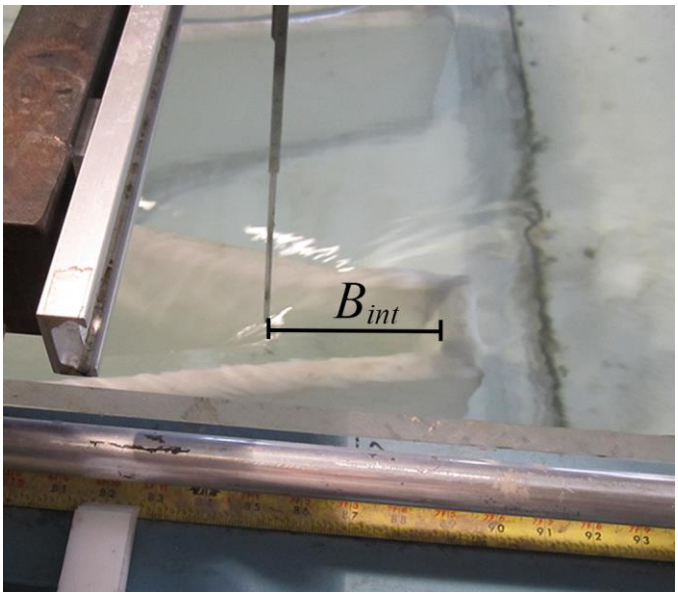

Fig. 15. Measuring B_{int}

to ensure accuracy. In order to quantify nappe interference and local submergence, B_{int} was recorded using the point gage on the rolling carriage (Fig. 15). A measuring tape was attached to the top of the flume wall and the distance from the downstream side of the upstream apex to the point where the nappe fell below the top of the crest of the weir was measured to determine B_{int}. B_{int}, along with videos and pictures, were recorded in increments of 0.1 H_T/P.

CHAPTER IV

EXPERIMENTAL RESULTS

Data comparison

C_d values over a range of $0.1 < H_T/P < 0.8$ were collected and compared to the Crookston (2010) curve fit equation. C_d vs. H_T/P for the 12° half-round (*HR*) and 12° quarter-round (*QR*) weirs are shown in Fig. 16 and 17, respectively. In these figures, the $A=0t_{w\text{-}US\text{-}DS}$ weir represents the weir with upstream and downstream apexes equal to $0t_w$, the $A=0t_w$ weir has upstream apexes equal to $0t_w$ and downstream apexes equal to $1t_w$. The subscript 'Normal' refers to the orientation and the subscript 'Crookston' refers to the curve fitted equation used by Crookston (2010). Trend lines were fit to all data curves (using curve-fit software) using the same curve fit equation that Crookston (2010) used for his labyrinth weir data [see Eq. (6)]. These curve-fit equations matched collected data

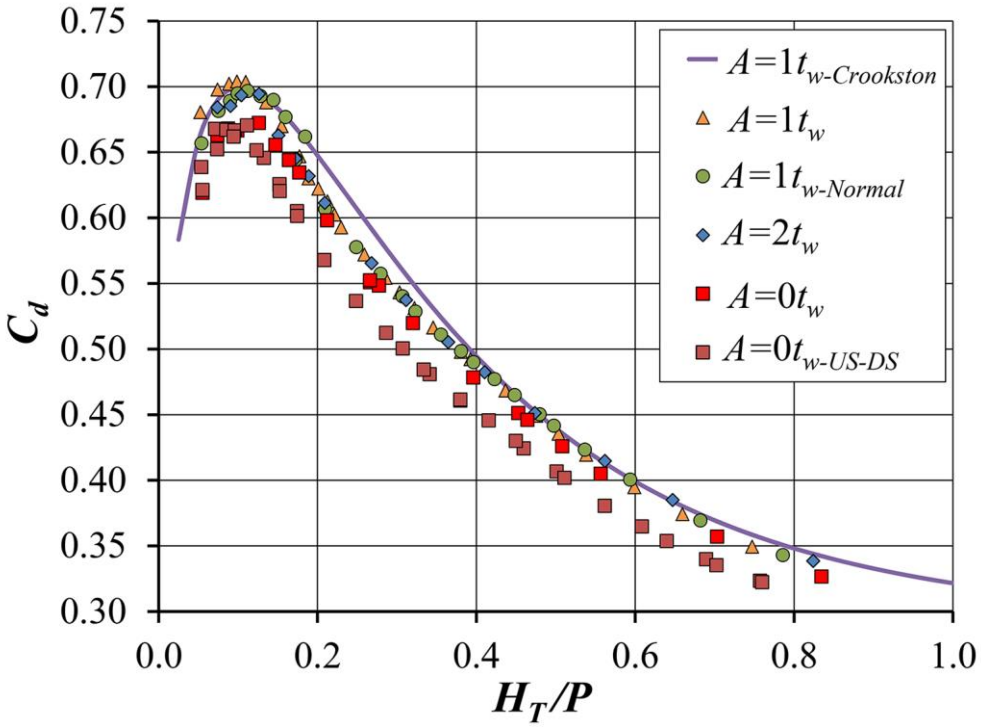

Fig. 16. C_d vs. H_T/P for the α=12°-*HR* weirs (data comparison)

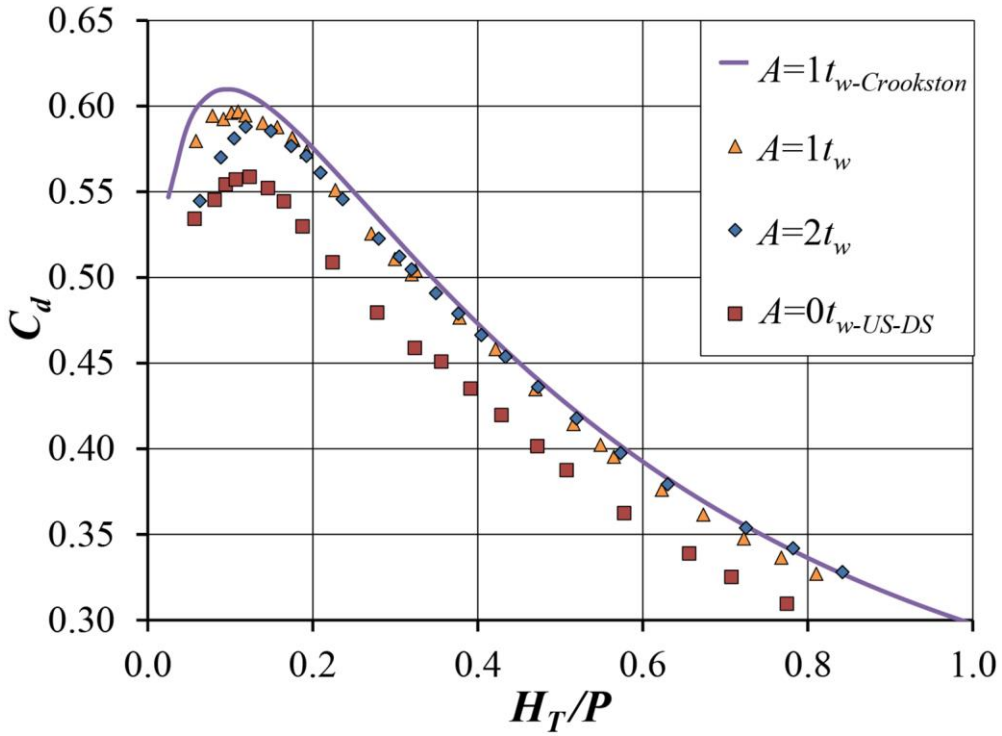

Fig. 17. C_d vs. H_T/P for the α=12°-*QR* weirs (data comparison)

with an average R^2 value of 0.997. Table 2 shows the coefficients for each weir's curve-fit equation.

Using these curve-fit equations to compare collected data, the 12°-*HR*, $A=1t_w$ inverted and normal orientation (Fig. 12 shows the difference between the inverted and normal orientation) data was compared with Crookston's (2010) collected data for the identical physical model tested in the normal orientation. The normal orientated weir compared to the inverted oriented weir (both built and tested by the author) had slightly higher C_d values, this difference is ~1.0%. The inverted oriented weir is within ~ 3.5% of Crookston's normal oriented weir's published results while the normal oriented weir is within ~ 2.5% (Fig. 18). The collected C_d data for the *QR*, $A=1t_w$ inverted oriented weir is ~1-2% lower than Crookston's *QR* normal oriented weir (Fig. 19). For the α=15° $P/t_w = 8$

weir, results were within 1.5% of Crookston's results of the identical weir. The range of data collected in the current study was limited due to water usage restrictions that were in place at the time of testing (Fig. 19). Experimental uncertainties are present in any physical model test, these can originate from several different sources including measurements of length, flow, and head elevations. An uncertainty analysis was performed and average experimental uncertainty ranged between 0.78-1.39% and maximum uncertainties ranged as high as 4.55% (Table 5 and 6). The results of this study and Crookston's (2010) study are within the experimental uncertainty range.

$$C_d = A * \frac{H_T}{P}^{B*\frac{H_T}{P}^C} + D \qquad (6)$$

Table 2. Curve-fit Coefficients for Labyrinth Weirs Tested (12°)

Model	Description	A	B	C	D	R^2
1	*QR*, $A=0t_{w\text{-}US\text{-}DS}$	0.05466	-2.181	0.4444	0.2219	0.998
2	*HR*, $A=0t_{w\text{-}US\text{-}DS}$	0.02607	-3.008	0.4142	0.2739	0.996
3	*HR*, $A=0t_w$	0.02360	-3.275	0.4380	0.2954	0.994
4	*QR*, $A=1t_w$	0.07608	-1.911	0.4369	0.2183	0.998
5	*HR*, $A=1t_w$	0.04151	-2.513	0.3975	0.2766	0.997
6	*HR*, $A=1t_{w\text{-}normal}$	0.02351	-3.273	0.4302	0.3062	0.994
7	*QR*, $A=2t_w$	0.03561	-2.881	0.4920	0.2753	0.999
8	*HR*, $A=2t_w$	0.04341	-2.483	0.4043	0.2759	0.997
9	*HR*, $A=1t_{w\text{-}vw}$	0.03861	-2.712	0.4233	0.2719	0.997

Another observation that should be noted is the sensitivity of the nappe behavior to small differences in weir construction and installation. This was noticed when comparing nappe behavior for the α=12°-*HR*, $A = 1t_w$ weir. Crookston's nappe behavior remained clinging until $H_T/P \sim 0.25$ while the nappe behavior of the weir tested in this study only remained clinging until $H_T/P \sim 0.19$. Since the C_d value is dependent on nappe behavior it is of importance to understand what may have caused the differences in nappe

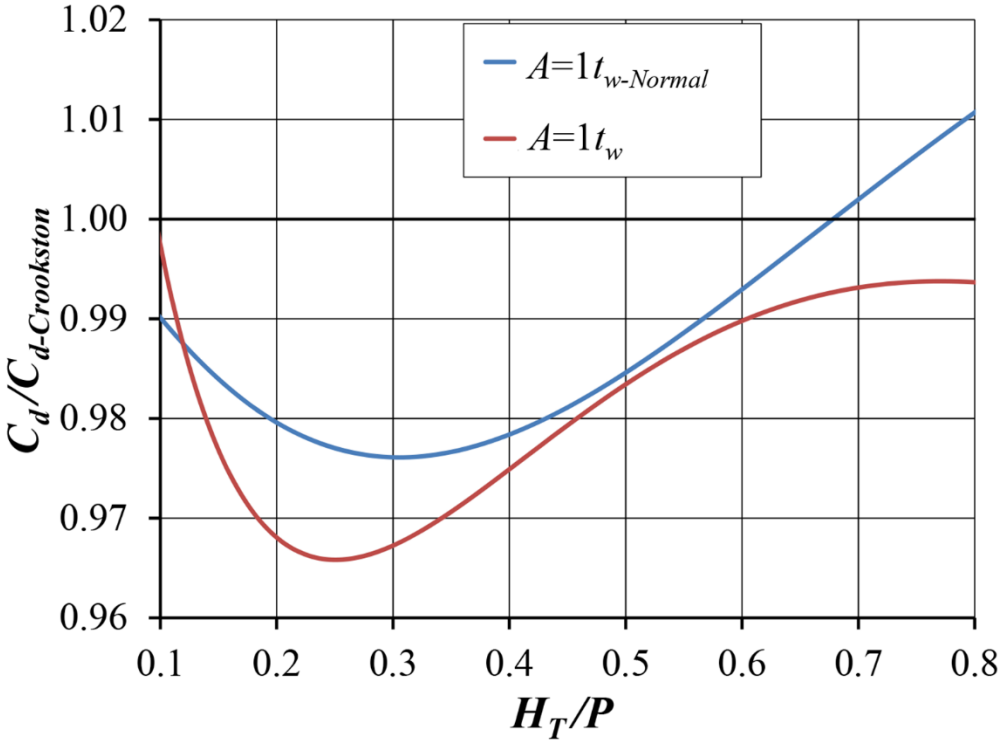

Fig. 18. C_d (curve fit) comparison to Crookston's (2010) normal oriented labyrinth weir (α=12°-*HR*)

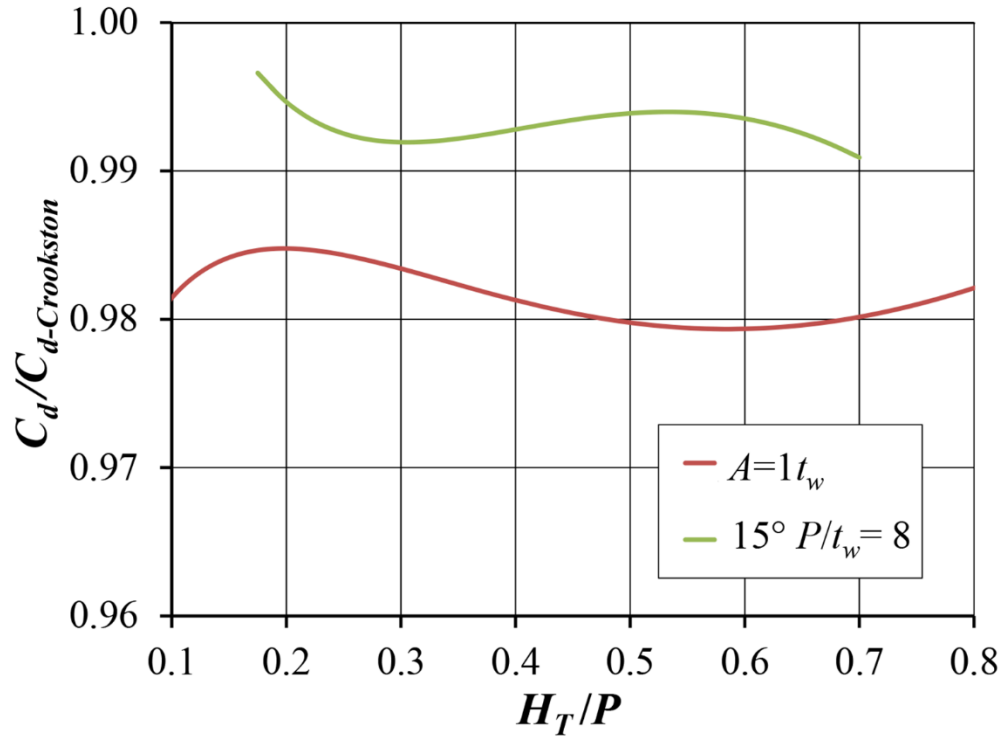

Fig. 19. C_d (curve fit) comparison to Crookston's (2010) normal oriented labyrinth weirs (*QR*)

behavior between this study and Crookston's. Some possible differences include construction methods, finishing quality and methods, and levelness of the weir. Small imperfections can disrupt the nappe and cause aeration to occur sooner which in turn affects the C_d value.

15°-*QR*, N=6, C_d vs. H_T/P data from the current study was also compared with similar data presented by Crookston et al. (2012) (Fig. 20). The discontinuities in the data trends are a direct result of changes in the nappe aeration condition and their effects on discharge efficiency. The data correlate especially well and build confidence that the data collection methods are accurate and repeatable.

Effectiveness of L_e in Describing Effects of Nappe Interference

The effective length (L_e) parameter (Tullis et al. 1995), which subtracts some of the "ineffective" weir crest length associated with apex corners, was calculated for each of the weirs tested and used in Eq. (1) instead of the actual weir centerline length, L_c, to calculate C_d; the goal was to determine if using L_e accurately accounted for the effects of nappe interference. If the effects of nappe interference where completely accounted for in L_e, then the rating curves of the A=0t_w, A=1t_w, and A=2t_w would align. This is however, not the case. As seen in Fig. 21, the rating curves are shifted up, as expected, but the data do not collapse to a single curve. Since the use of L_e does not remove the influence of nappe interference with respect to C_d vs. H_T/P, no adjustment to the weir crest centerline, L_c, is recommended for use in Eq. (1); this recommendation is consistent with that by Crookston and Tullis (2013a).

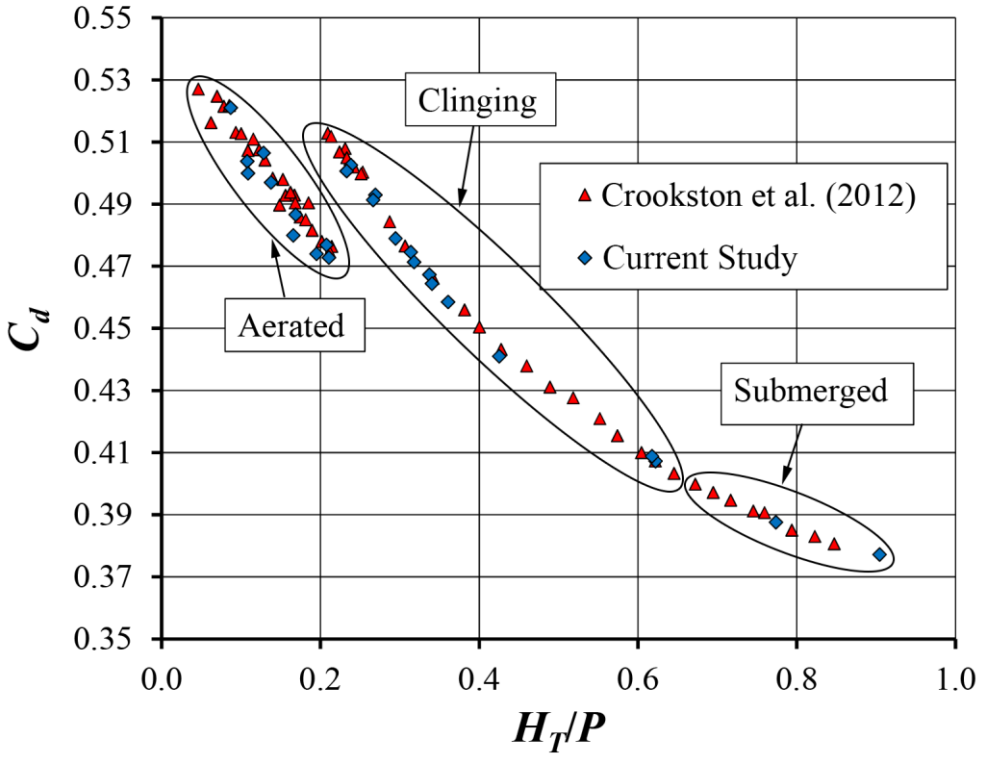

Fig. 20. C_d vs. H_T/P comparison (α=15°-*QR*, N=6)

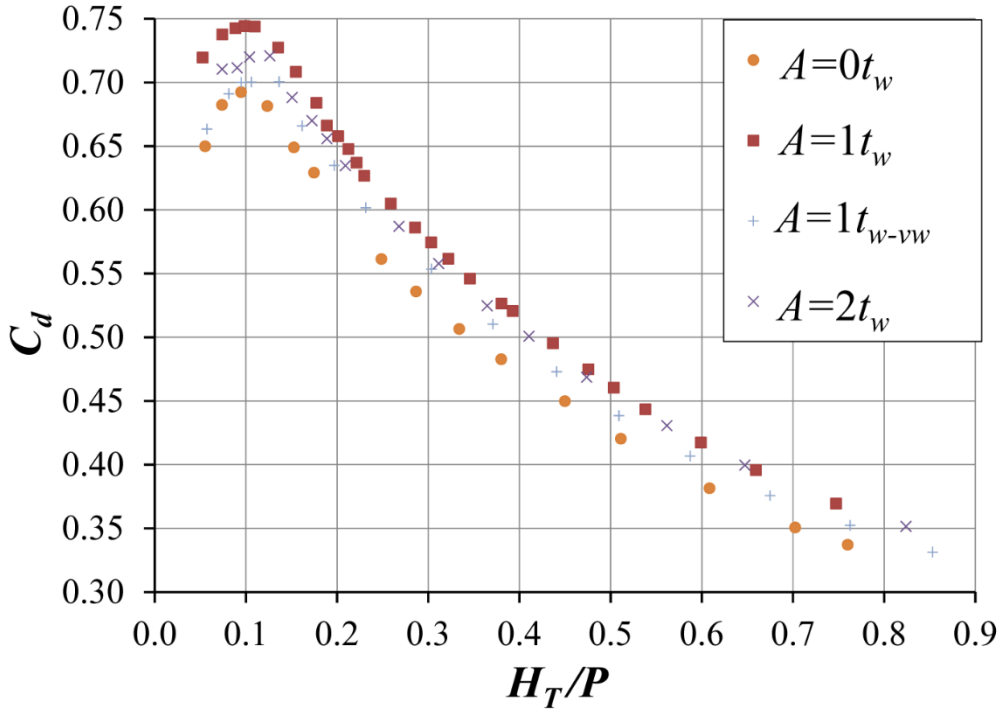

Fig. 21. C_d vs. H_T/P (C_d calculated using experimental data, Eq. (1), and L_e in place of L_c)

Influence of Apex on Discharge Efficiency

Constant Channel Width

Quarter and half round crested (α=12°) labyrinth weirs with upstream apex widths of A=1t_w, A=2t_w, and A=0t_w were studied to determine the effect of increased/decreased upstream apex width on overall discharge efficiency (in terms of channel width). The discharge efficiency of the A=0$t_{w\text{-}US\text{-}DS}$ (blunt triangular apexes for the upstream and downstream apexes) and A=0t_w (blunt triangular apex for the upstream apex, A=1t_w for the downstream apex) weirs were very similar, within ±1% (Fig. 22). These weirs provided the highest discharge efficiency per given channel width, however this came at a cost. Total centerline crest length (L_c) for the A=0$t_{w\text{-}US\text{-}DS}$ weir was increased by

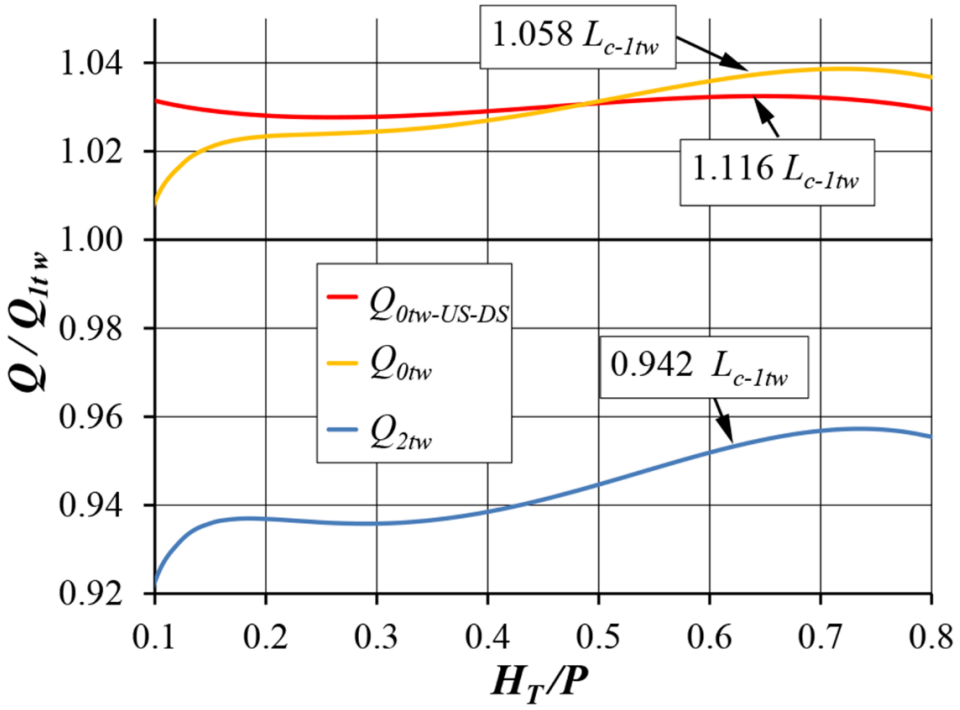

Fig. 22. Q and L_c comparison for α=12°-*HR* labyrinth weirs as a function of H_T/P and normalized by Q (A=1t_w)

~11.5%, relative to the $A=1t_w$ weir, while the discharge was only increased by ~3%. This means that the C_d for the $A=0t_w$ is less than the $A=1t_w$, but the overall weir discharge increased due to the increase in total weir length. In Fig. 22 and 23, discharge efficiency (Q vs H_T/P) and overall crest length (L_c) is compared to the discharge efficiency and L_c of the $\alpha=12°$, $A=1t_w$ weir and the tradeoff between increased crest length and increase in discharge efficiency can be seen.

The $A=0t_w$ weir increased flow efficiency by ~3% with only a 5.8% increase in L_c. The $A=0t_w$ weir produced the same increase in discharge capacity, relative to the $A=0t_{w\text{-}US\text{-}DS}$, with significantly less weir length. This suggests that upstream triangular apexes have a more significant effect on discharge efficiency than downstream triangular apexes. If maximizing labyrinth weir discharge is a priority, using the $A=0t_w$ configuration over

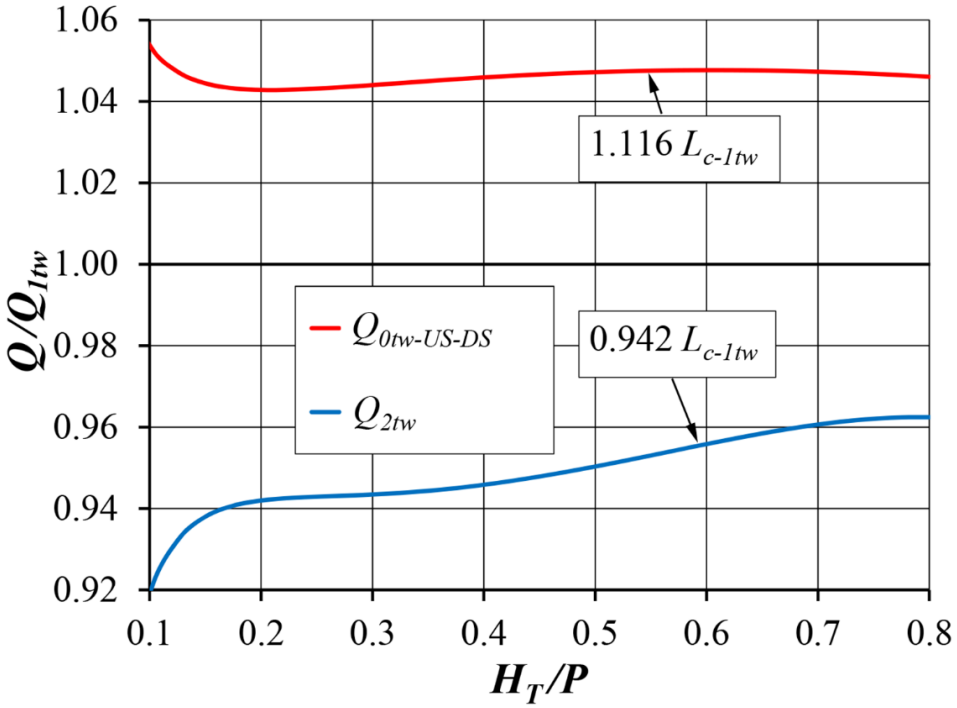

Fig. 23. Q and L_c comparison for $\alpha=12°$-*QR* labyrinth weirs (apex variation for constant channel width)

the $A=0t_{w\text{-}US\text{-}DS}$ or $A=1t_w$ configurations is recommended (construction costs should also be considered in the analysis). However, in practice, a completely triangular apex is difficult to build because it does not provide the minimum required workspace for construction. Therefore, a complete analysis of multiple parameters (discharge efficiency, constructability, costs... etc.) must be considered when determining an appropriate labyrinth weir apex width.

The $A=2t_w$ weir provided the lowest channel width discharge efficiency out of the three configurations tested. However, unlike the $A=0t_w$ weir, the percent decrease in L_c and decrease in Q were proportional for lower heads and Q actually showed a lower percent decrease compared to the percent change in L_c for $H_T/P > 0.4$ (see Fig. 22 and 23). This can be attributed to decreased nappe interference and local submergence at higher heads for the $A=2t_w$ weir compared to the $A=1t_w$ weir. This can be confirmed by the B_{int} data collected (Fig. 24 and 25). When analyzing the B_{int} data, a standing wave was observed downstream of the upstream apexes for the $A=0t_w$ and $1t_w$ weirs for heads between $0.1 < H_T/P < 0.4$, see Fig. 26 (standing waves were more prevalent for the *QR* weirs). This occurred due to the nappe collisions of the adjacent sidewall near the upstream apex. Since the flow elevation was above the crest elevation, B_{int} was measured near the end of this standing wave where it fell below the crest elevation. At larger flows, this behavior was not observed.

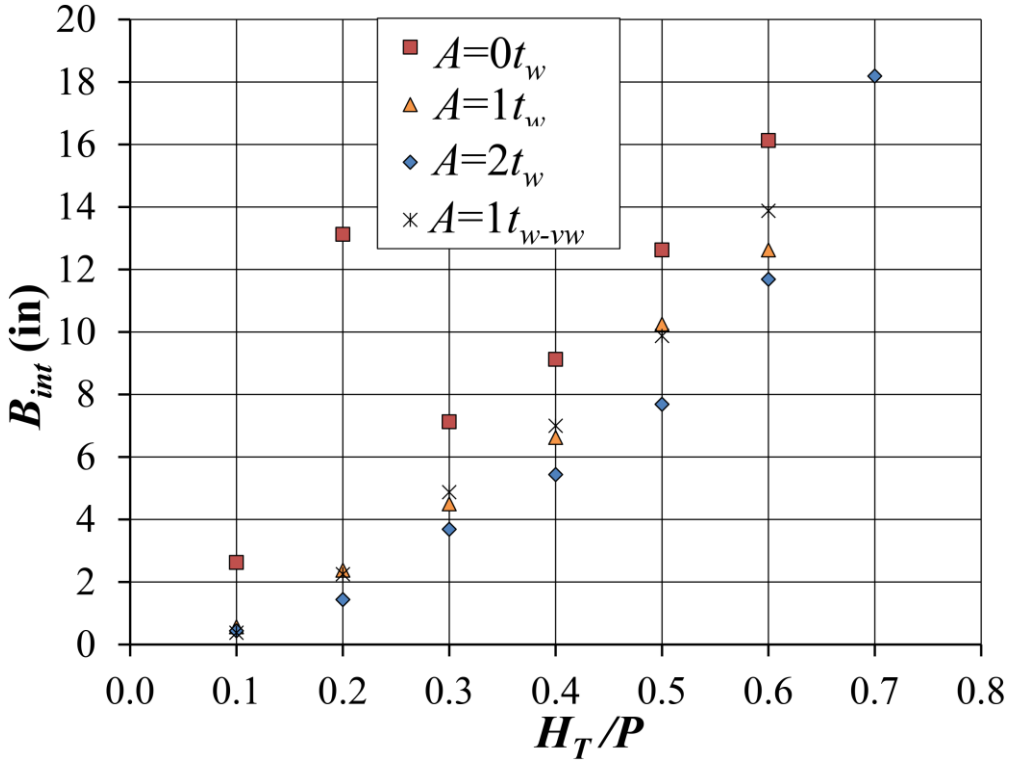

Fig. 24. Nappe Interference, B_{int} vs. H_T/P for α=12°-*HR* weirs (apex variation)

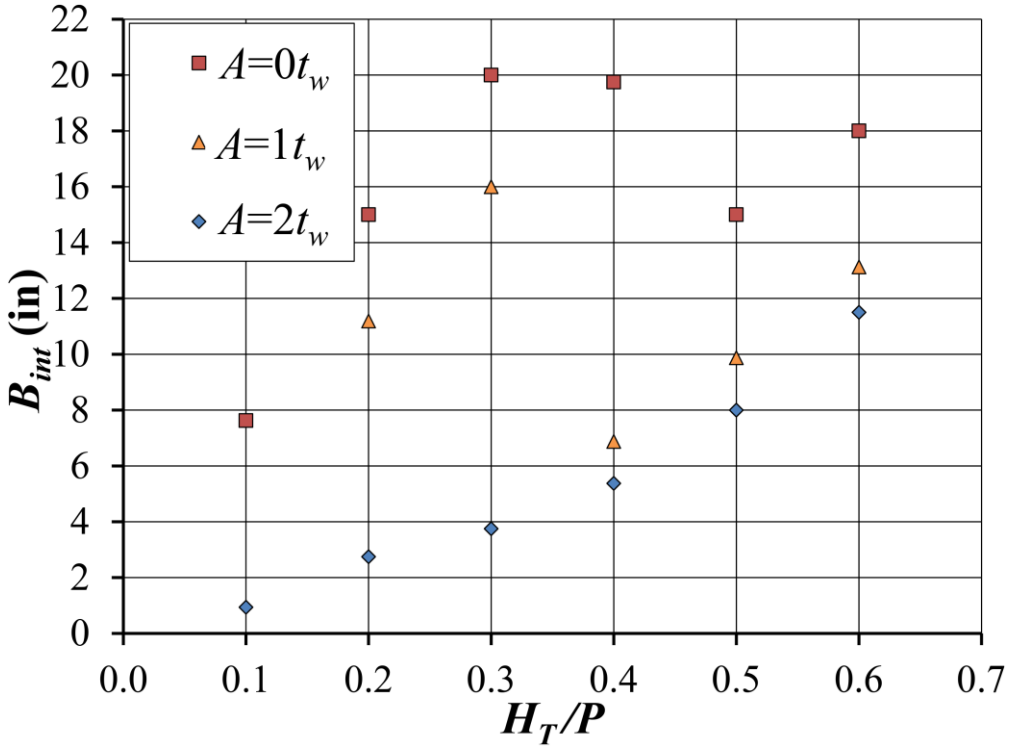

Fig. 25. Nappe interference, B_{int} vs. H_T/P for α=12°-*QR* weirs (apex variation)

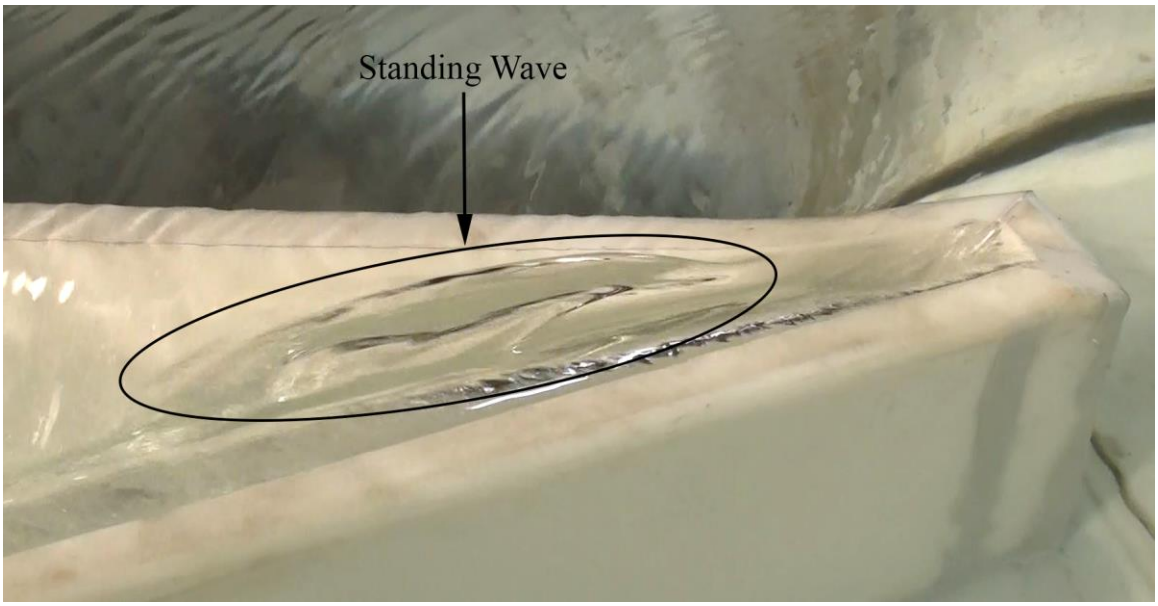

Fig. 26. Standing wave near the upstream apex of the α=12°-*QR* A=1t_w weir

For a constant W weir design, increasing A requires a reduction in l_c (if all other geometric parameters are held constant). Since l_c comprises the largest portion of the crest length in a labyrinth cycle, a reduction to accommodate an increase in A results in an overall decrease in discharge capacity for the channel width despite the reduced effects of nappe interference and local submergence. Consequently, to maximize trapezoidal labyrinth weir discharge capacity, A should be as small as possible while still maintaining the minimal space needed for construction (sidewall angle of α=12° was tested). The A=1t_w weir likely represents a practical design for labyrinth weirs in that the discharge capacity is just slightly less than the A=0t_w (see Fig. 22 and 23) with less total weir length. Relative to the A=0t_w weir, the A=1t_w weir is likely cheaper to construct and provides better accessibility for construction.

Variable Channel Width

Increasing *A* should reduce the nappe interference and local submergence effects on the head-discharge relationship for labyrinth weirs. *A* can be increased while maintaining constant l_c if the channel width, *W*, is not constrained. Table 3 shows the three weirs used to test the apex width contribution in a variable channel width (denoted with the subscript *vw*) scenario. Model 1* (12°-*HR*-*A*=$1t_{w\_vw}$) was selected as the standard for comparisons. This weir has upstream and downstream apexes equal to $1t_w$ and was built within a channel of 45 in. width. For a plan section view of the false wall used to narrow the channel see Fig. 13. Models 2* (12°-*HR*-*A*=$1t_w$) and 3* (12°-*HR*-*A*=$2t_w$) maintain α, *P*, t_w, and downstream apex width consistent with model 1* while increasing *W* (by either changing *A* or l_c). *W* was increased by increasing l_c for Model 2* and *A* for model 3* (Fig. 4). By comparing the discharge efficiencies of Model 2* and 3* to that of Model 1* we were able to draw conclusions on the effectiveness of increasing *W* by either the increase of either *A* or l_c.

Results are shown in Fig. 27. The discharge of model 2*, when compared to model 1*, was increased by ~8-9% while the discharge of model 3* was only increased by 1-4% (depending on upstream head). *W* was increased for both weirs by ~6.6% compared

Table 3. Variable Channel Width Weirs Tested

Weir ( )	Model ( )	*W* (in)	*A* (in)	l_c (in)
12°-*HR*-*A*=$1t_{w\text{-}vw}$	1*	45.2	1.45	41.8
12°-*HR*-*A*=$1t_w$	2*	48.2	1.45	45.3
12°-*HR*-*A*=$2t_w$	3*	48.2	2.90	41.3

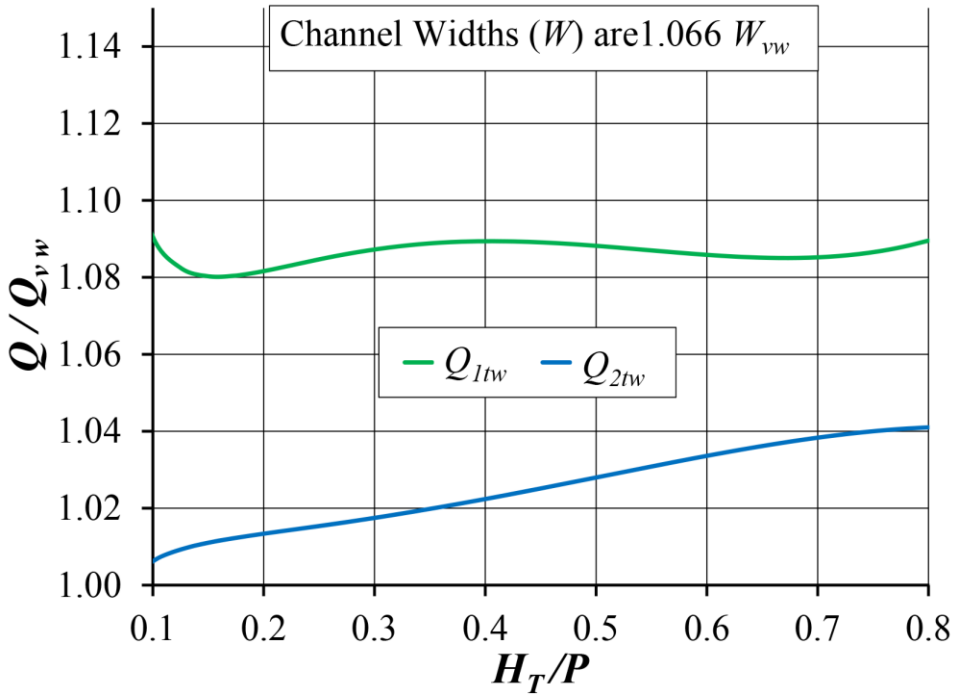

Fig. 27. Varied channel width flow comparison (α=12°-*HR* weir)

to W_{vw} (the channel width of model 1*). Therefore, when additional channel width is available, it is most beneficial to the overall discharge efficiency to increase l_c rather than *A*. Decreased nappe interference (achieved by increasing *A*) does not outweigh the benefits of increased l_c, for total discharge efficiency on a given channel width. This agrees with the conclusion made previously that the weir sidewall makes the largest contribution to the overall flow of a labyrinth weir.

The Effects of *w*/*P* on Discharge Efficiency and Design Method Predictions

Froude Scaling (Constant w/P)

Data collected by Crookston et al. (2012) comparing laboratory-scale labyrinth weirs of different sizes was used to better understand size scale effects when using

Froude scaling. Models 1^a and 2^a (Table 4) are geometrically similar; Model 1^a was half the size of model 2^a. The design method presented by Crookston and Tullis (2013a) used the exact geometries of Model 2^a to develop the α=15° *QR* rating curve. Model 1^a C_d data were compared to design method C_d predictions (acquired from a model similar to Model 2^a). Results from this comparison show that for $H_T/P < 0.1$, size-scale effects were present (difference peaked at ~20%) between the two model size scales. At $H_T/P > 0.1$, C_d values were within ±3% between the two geometrically similar model weirs (Fig. 28). Results where near the experimental uncertainties which ranged between 0.46 – 1.30%.

A larger scaled (*QR* crested and α=15°) weir was built (Model 7^b) and tested by Crookston (2010). This model had a scale 3 times larger than the Model 2^a; Model 7^b and Model 2^a were not exactly geometrically similar to one another but their geometries were very close (i.e., geometrically comparable) due facility limitations of channel width. Model 7^b has a very similar P/t_w ratio as Model 2^a but differs slightly with the w/P ratio (Table 4). When compared to the design method predictions, the weir performed within 3% of the predicted flows [ignoring low heads (H_T/P<0.1)]. See Fig. 28 for the C_d comparison. These results show that for small physical variations from the design method will still produce predictable flow rates for a given head [within ± 3% ($0.1 < H_T/P < 1.0$) for the scales tested in this study]. At low heads, $H_T/P < 0.1$, the actual C_d values were ~15% higher than the calculated predicted values. This data was within the experimental uncertainty range of 0.86 – 4.3%.

For $H_T/P > 0.1$, the influence of size-scale effects, on discharge efficiency (other characteristics where not analyzed, i.e. aerations and nappe behavior), appears to be relatively small (within experimental uncertainty) for the geometrically similar and

geometric comparable labyrinth weirs tested. Size-scale effects produce noticeable differences at relatively low heads ($H_T/P < 0.1$) but these differences diminish as the head increases. This may be due to the fact that the surface tension effects play a larger role at low heads and smaller scales. Also, as the scale size increases, these size scale effects diminish (size-scale effects are more pronounced at smaller scales).

Table 4. Physical Model Test Matrix (Crookston et al. 2012 and Crookston 2010)

Model	***α***	***P***	***t_w***	***P/t_w***	***w***	***$L_{c\text{-}cycle}$***	***$L_{c\text{-}cycle}/w$***	***w/P***	***N***
( )	**(°)**	**(ft)**	**(in)**	**( )**	**(in)**	**(ft)**	**( )**	**( )**	**( )**
1[a]	15	0.5	0.75	8	12.1	3.267	3.254	2.01	4
2[a]	15	1.0	1.5	8	24.2	6.533	3.254	2.01	2
3[a]	15	1.0	1.5	8	12.1	2.655	2.645	1.03	4
4[a]	15	1.0	1.5	8	8.07	1.362	2.036	0.69	6
5[a]	15	0.5	1.5	4	24.2	6.533	3.254	4.02	2
6[a]	15	1.0	0.75	16	12.1	3.267	3.254	1.02	4
7[b]	15	3.02	4.49	8.07	96	26.13	3.255	2.66	1

[a]Crookston et al. (2012)
[b]Crookston (2010)

Effects of Changing w/P by Varying P

The accuracy of the Crookston and Tullis (2013a) labyrinth weir hydraulic design data (C_d vs. H_T/P) is based upon the geometries tested. Predictive accuracy may decrease for geometric designs that significantly deviate from the models tested. Crookston and Tullis recommend that the results be verified with modeling. Crookston and Tullis presented all of their C_d data in terms of the upstream total head, H_T, normalized by the weir height P. Knowing the possibilities of distortion, this was still chosen as the best

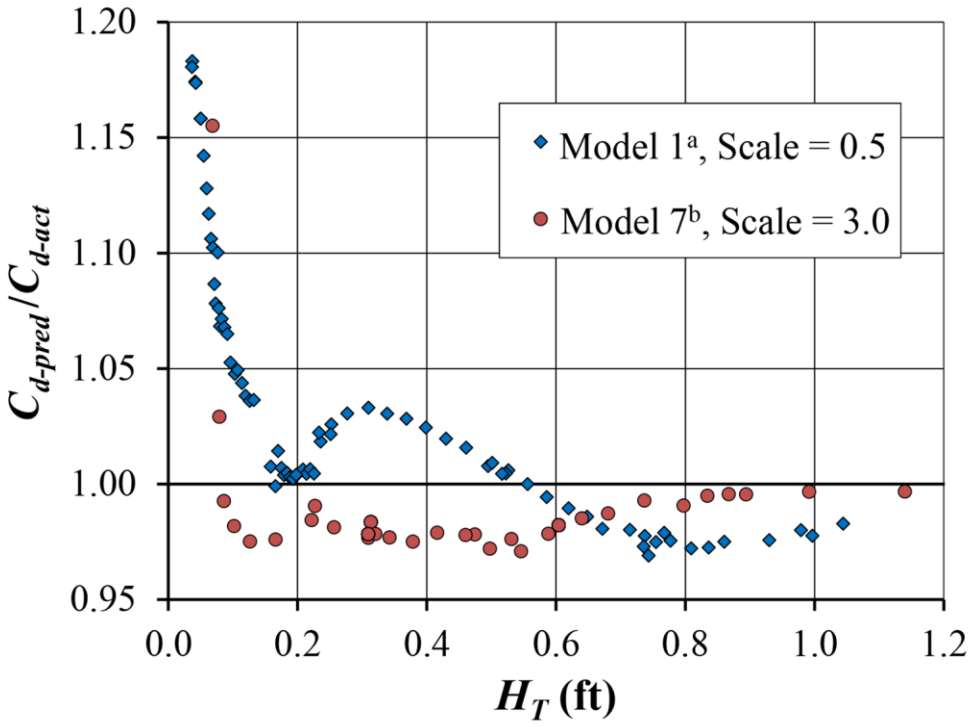

Fig. 28. Size-scale effects on C_d values (α=15°-*QR*)

option in normalizing H_T. All weirs whose data were included in the Crookston and Tullis (2013a) design method had a common *P* (12 inches). This raises the question of what type of discharge performance variations might result from maintaining all labyrinth weir dimensions (w, t_w, α, A, and l_c) consistent with the Crookston and Tullis (2013a) weir geometries but adjusting the weir height.

To look into the effects of varying *P*, data from the α=15° - *QR* crested labyrinth weir model tests were used from Crookston et al. (2012) and tests performed in the current study (Models 2[a], 5[a], and 6[a] from Table 4 and the current study models 11, 12, and 13 in Table 1). Model 2[a] represents the exact geometric weir used in the Crookston and Tullis design method. Model 5[a] has the same geometries as Model 2[a] except for *P*, which is only half the weir height of Model 2[a]. Due to the limited depth of the test flume,

doubling the size of P was not possible, therefore Model 6^a was scaled to ½ of Model 2^a and then doubled P. The collected data was then scaled (Froude scaling) up (2 times) to replicate a P twice the size of the P in Model 2^a. Model 11 and 12 had a P of 1.5 and 1.25 times the height of Model 2^a respectively.

When $P/t_w = 4$ (P is half the size of the design P), the weir performed within ±13% of predicted C_d values. When $P/t_w = 16$ (P is twice the size of the design P), the design method over predicted C_d by ~20% at H_T >0.4 ft (this difference can be attributed to the distortion in H_T/P that is not accounted for explicitly). The two α=15° -QR labyrinth weirs that were tested in the current study with $P/t_w = 12$ and 10 (P is 1.5 and 1.25 times the size of the design P, respectively) yielded similar trends. The design method over predicted the $P/t_w = 12$ weir discharge by ~13% at H_T >0.65 ft and by ~5% for the $P/t_w = 10$ weir at H_T >0.5 ft. The design method seems to follow a trend of over predicting performance as P/t_w increases above 8 and under predicts performance as P/t_w decreases below 8 (Fig. 29).

It is expected that the design method is limited to geometrically similar weirs due to the fact that the hydraulic characteristics (C_d vs. H_T/P) are based on one labyrinth weir geometry. By having the headwater ratio as the independent variable of the rating curve, variations of P potentially have a large effect on the ability of the design method to accurately predict a weirs performance. In an effort to increase the applicability in which this design method may be used for weirs of different heights, a H_T/P corrected term (H_T/P') was developed to accommodate weirs that are not geometrically similar to the design method weir due to a change in P (Brian Crookston, personal communication, July 2, 2013). This corrected headwater ratio was determined by evaluating the design

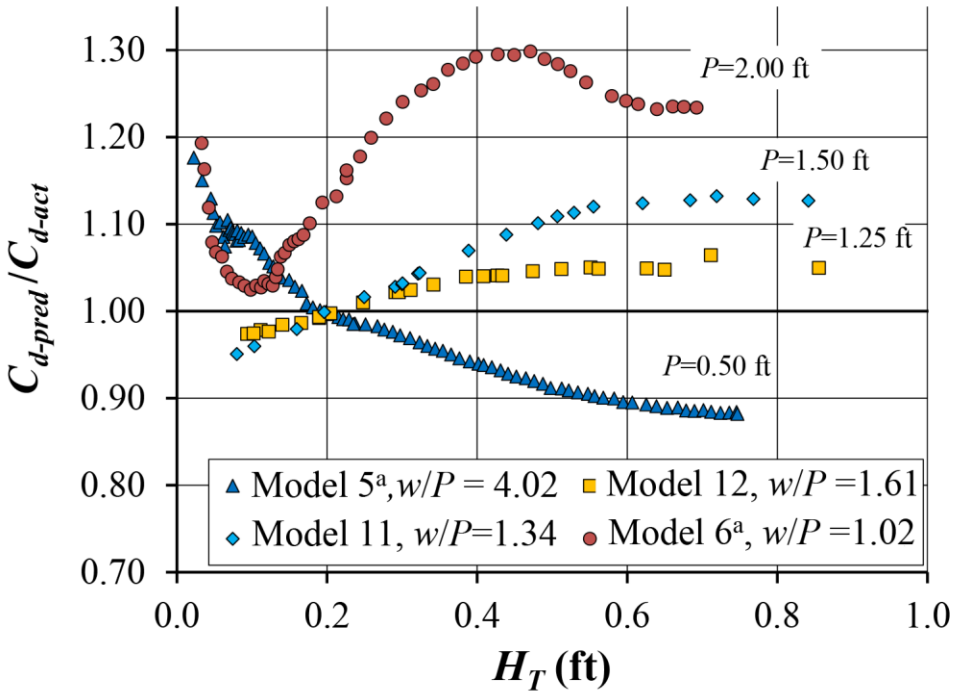

Fig. 29. Effects of varying *P* on design method C_d predictions (α=15°-*QR*)

methods ability to predict the weirs performance and then adjusting H_T/P in such a manner that the design method's rating curve would predict accurately the weirs performance. The new H_T/P value determined through this adjustment is referred to as the corrected headwater ratio (H_T/P'). The H_T/P' curves can be used in conjunction with the design method to predict non-geometrically similar labyrinth weir's performance. To apply this, one would determine the actual headwater ratio of the weir, then use the H_T/P' vs H_T/P relationship for that specific geometry to determine an H_T/P'. Then this corrected headwater ratio (instead of the actual headwater ratio) can be used to estimate accurate C_d values using the existing C_d vs H_T/P relationships within the Crookston and Tullis (2013a) design method. The H_T/P' vs H_T/P relationship can be seen in Fig. 31. For these "varying *P*" curves to apply, all other geometries of the weir (except *P*) must be

geometrically similar to that of the weir used in the design method. The accuracy of this correction method can be seen in Fig. 30. For H_T>0.2, the predictions are within ±2%.

Effects of Changing w/P by Varying w

When w is varied, while maintaining P, t_w, A_c, W, and α constant; N and $L_{c\text{-}cycle}$ must also change. The dimensionless design ratios of A_c/l_c and w/P also change and may not fall within the design method criteria. Crookston et al. (2012) used three physical models, all with *QR* crest and α =15°, to analyze the effects of varying w while maintaining P, t_w, A_c, W, and α constant. All weirs were tested in the 4-ft wide rectangular flume at the UWRL with N = 2, 4, and 6 cycles and w/P = 2.01, 1.03, and 0.69, respectively (Fig. 32)

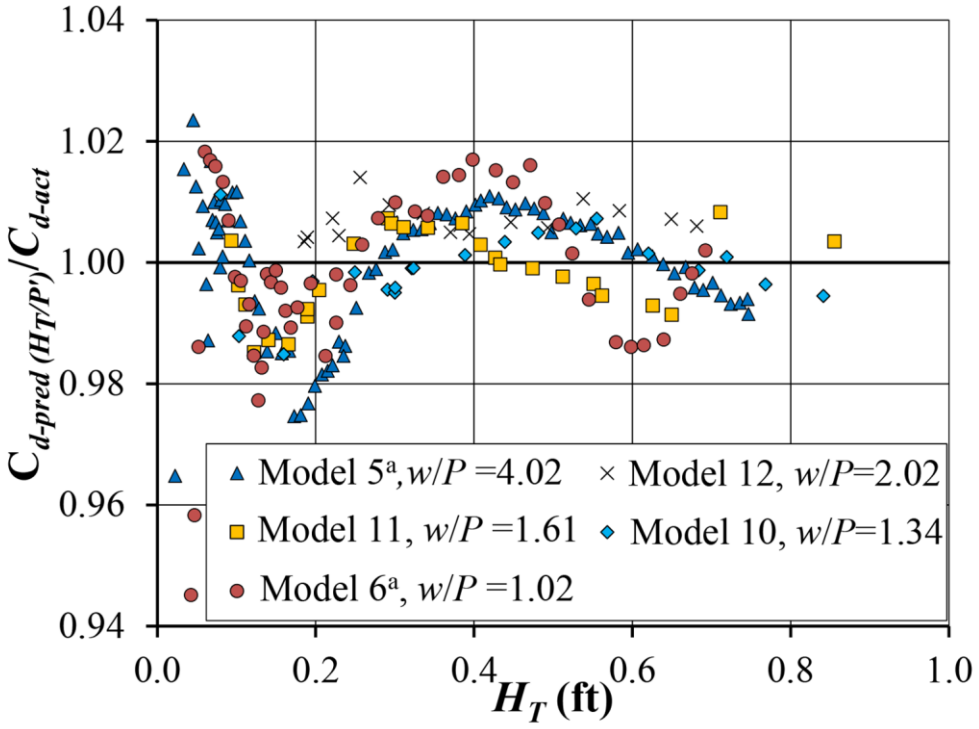

Fig. 30. Predicted C_d values (H_T/P') compared to actual C_d values for weirs of varying P (α=15°-*QR*)

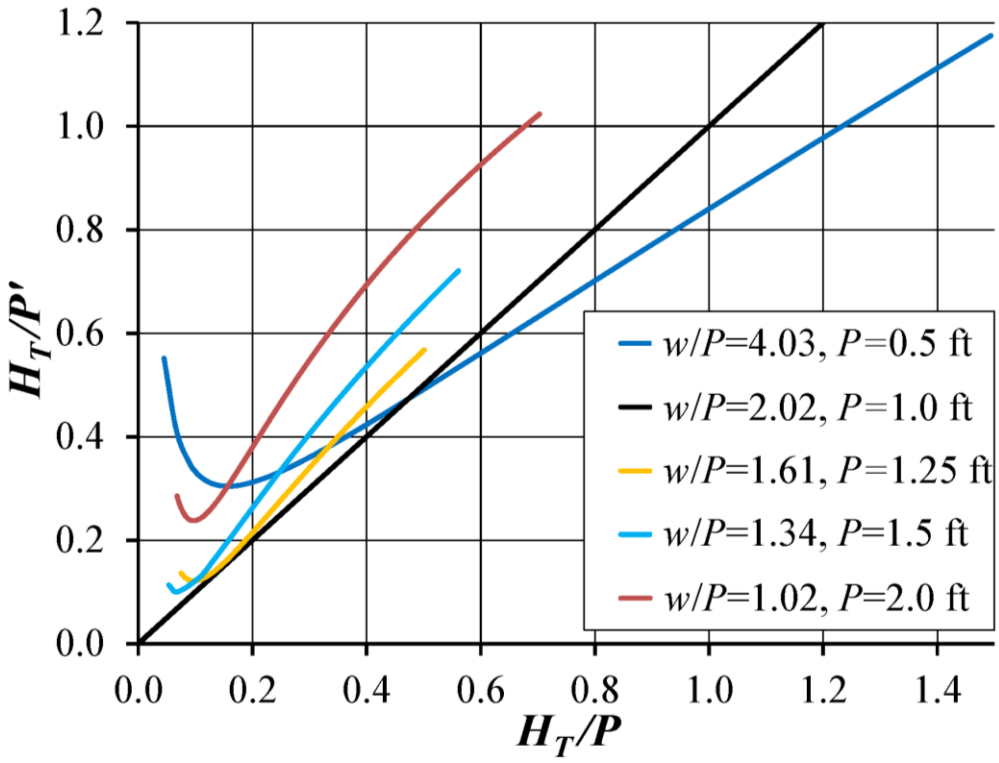

Fig. 31. H_T/P' vs H_T/P for weirs of varying P (α=15°-*QR*)

Crookston et al (2012) found that the accuracy of the Crookston and Tullis (2013a) design method decreased noticeably for $w/P < 2$. When $w/P = 0.69$ the design method over predicted C_d by ~18% at H_T/P=0.3 and under predicted C_d ~5% at H_T/P=0.9, as shown in Fig. 27. For the $w/P = 1.03$ weir, the design method over predicted C_d by ~20% at H_T/P=0.4 (Fig. 32).

A noticeable discontinuity of the points plotted in Fig. 27 caused by non-typical variation in the nappe aeration behavior. During low flows (H_T <0.2), the weirs experienced aerated conditions while at all higher flows (H_T >0.2) the nappe reverted to clinging. Typical nappe behavior usually progresses through clinging, aerated, partially aerated, drowned, and submerged with increasing H_T (Crookston and Tullis 2013b). Another observation that can be made is that discharge efficiency is reduced by 36.6%

and 26.0% for the w/P = 0.69 and 1.03 weirs respectively at ~H_T/P=0.8 when compared to the design method weir of w/P=2.01 (Fig. 33). This can be attributed in part with the increased percentage of the total weir crest length associated with apexes and the reduction in l_c (Fig. 3). When w/P is below the current design method constraints ($2<w/P<4$), the design method does not accurately predict discharges. Further research is required to access the applicability of the design method for weirs of higher w/P ratios outside of the design method constraints.

Following the same method used in the previous section to develop a relationship between H_T/P' and H_T/P, Fig. 34 was developed. For flows between $0.2< H_T/P<0.4$, the uncertainty of the corrected head water ratio is the largest due to the discontinuity in the rating curve of the 2 weirs tested. However, the overall corrected predictions of the C_d

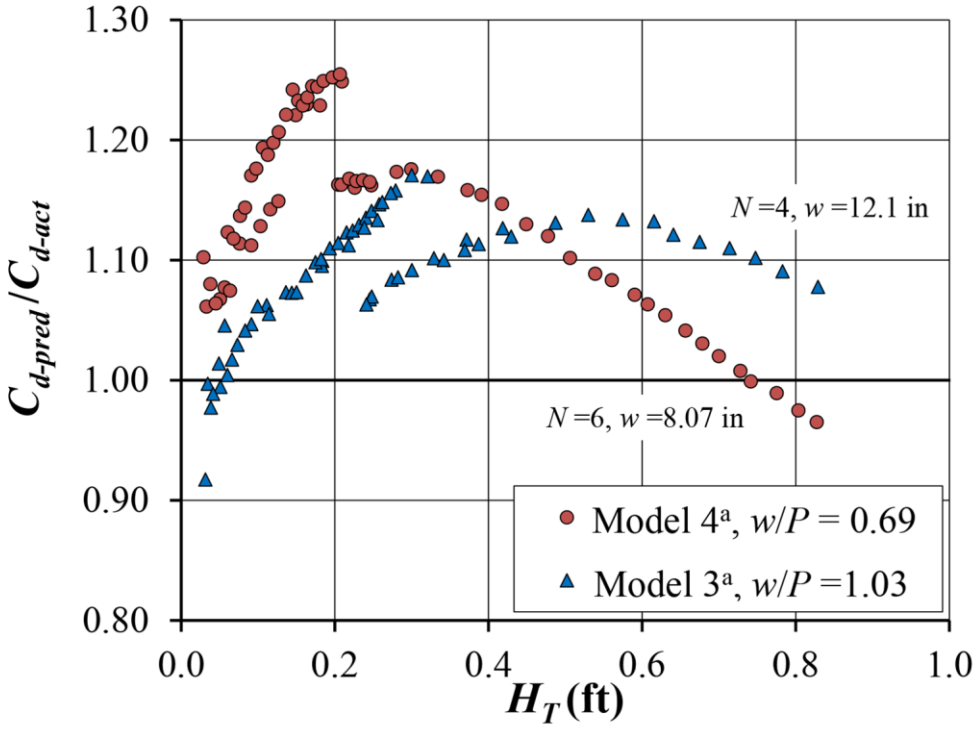

Fig. 32. Effects of varying w on design method C_d predictions (α=15°-QR)

value are within ±5% of the actual values measured (Fig. 35). These results are limited to the α=15°-*QR* crested labyrinth weirs.

Uncertainty Analysis

To quantify the uncertainty involved in this study, the method of Kline and McClintock (1953) for single-sample experiments was used. Uncertainties of physical measurements were determined and an uncertainty for each measured data point was calculated through a partial derivative. These calculations were carried out in VBA, and the code is found in Appendix C. Error ranges are shown in Table 5. Percent uncertainties for each model tested are found in Table 6. Uncertainties in this study can be attributed to flow measurement inaccuracies, human error, difficulty in leveling weir, and accuracies of crest references. Throughout this study a sensitivity analysis was performed and the

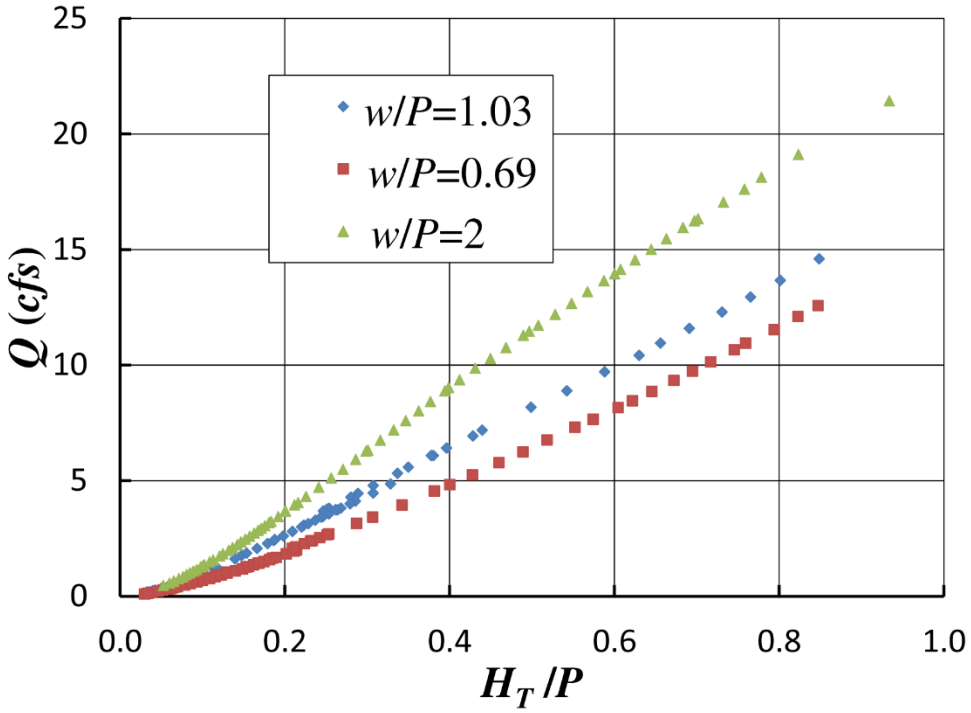

Fig. 33. *Q* vs H_T/P for α=15°-*QR* weirs with varying *w*/*P* (Crookston et al. 2012)

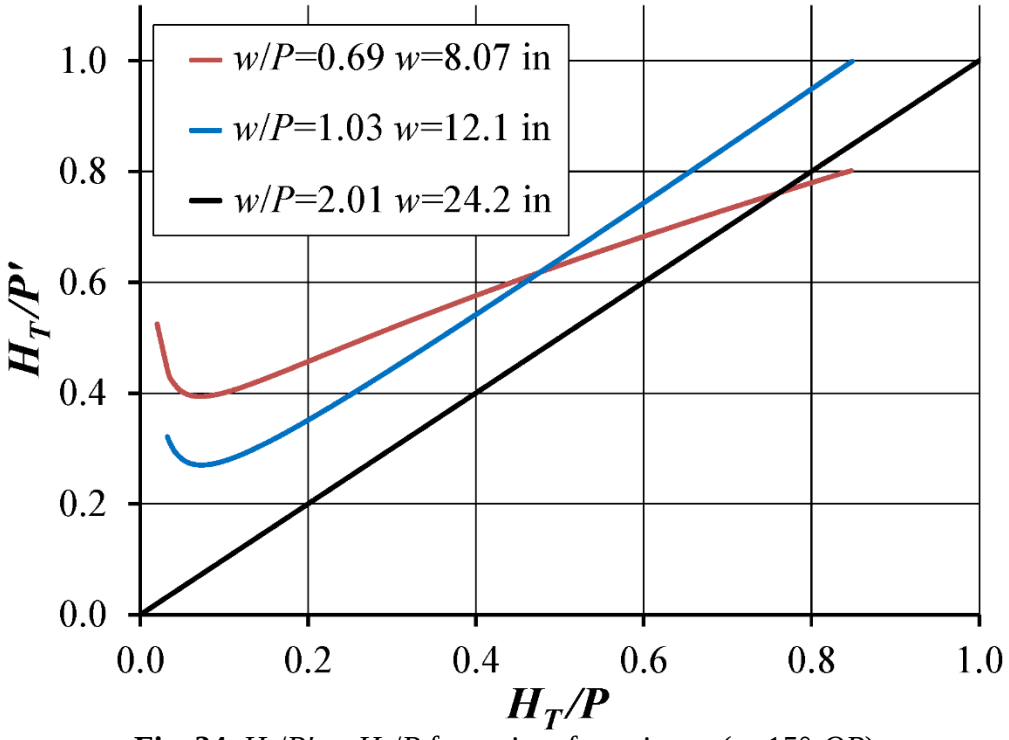

Fig. 34. H_T/P' vs H_T/P for weirs of varying w (α=15°-QR)

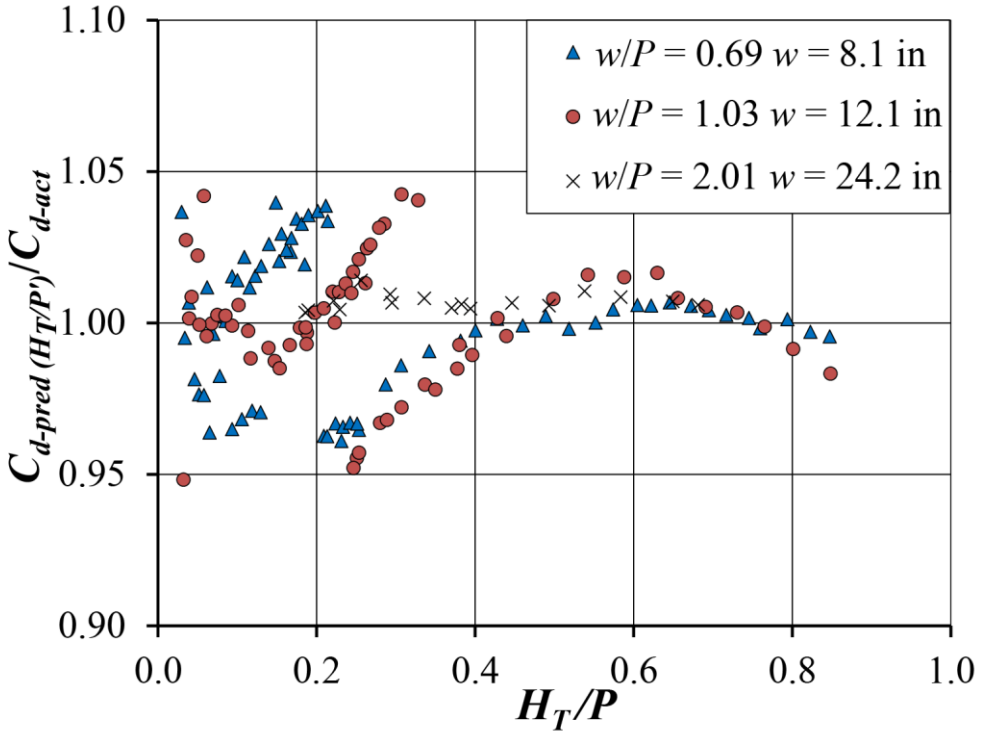

Fig. 35. Predicted C_d values (H_T/P') compared to actual C_d values for weirs of varying w (α=15°-QR)

crest reference was by far the parameter that affected individual rating curves the most. To ensure accurate crest references, multiple measurements were taken until a consistent crest reference was reached.

Table 5. Physical Measurement Uncertainty Ranges

Uncertainty interval	Error Range
ω_Q	±0.25%
ω_{Lc}	±1/64 in.
ω_W	±1/32 in.
ω_{Ptgage}	±0.005 ft.
ω_{Yref}	±0.005 ft.
ω_{mA}	±0.01 mA
ω_{Yramp}	±1/64 in.
$\omega_{Yplatform}$	±1/64 in.

Table 6. Uncertainties for Single Sample Experiments of Tested Labyrinth Weirs

Model	Description	Min (%)	Avg (%)	Max (%)
1	*QR*, A=0t_w	0.44	1.28	4.15
2	*HR*, A=0$t_{w\text{-}US\text{-}DS}$	0.45	1.39	4.44
3	*HR*, A=0t_w	0.46	1.37	4.31
4	*QR*, A=1t_w	0.42	1.38	4.09
5	*HR*, A=1t_w	0.44	1.28	4.55
6	*HR*, A=1$t_{w\text{-}normal}$	0.44	1.28	4.42
7	*QR*, A=2t_w	0.41	1.12	3.79
8	*HR*, A=2t_w	0.42	1.28	3.23
9	*HR*, A=1$t_{w\text{-}vw}$	0.42	1.14	4.17
10	*QR*, α=12°, P=1.5	0.43	1.15	3.81
11	*QR*, α=15°, P=1.5	0.40	0.89	3.00
12	*QR*, α=15°, P=1.25	0.41	1.02	2.56
13	*QR*, α=15°, P=1.0	0.46	0.78	1.30

CHAPTER V

SUMMARY AND CONCLUSIONS

The purpose this study was to determine the effects of varying certain labyrinth weir geometric design parameters to determine the effects on discharge efficiency and ability of the Crookston and Tullis (2013a) design method to accurately predict discharges. Thirteen laboratory scaled labyrinth weir models (α = 12° and 15°) were tested in a 4-ft. wide flume with discharge conditions ranging from $0.1 < H_T/P < 0.8$. Rating curves were formulated and compared for accuracy to Crookston's 12° and 15° labyrinth weir models (Crookston 2010). Efforts were made to confirm the effectiveness of the L_e parameter as described by Tullis et al. (1995) in describing the effects of nappe interference on the head-discharge relationship. Data were analyzed and conclusions made about the effectiveness of increasing upstream A in order to reduce the effects of local submergence and increase discharge efficiency (weirs with A=0t_w, A=1t_w, and A=2t_w were tested). Analysis was also made to determine the effectiveness of increasing A or l_c when changes to the total channel width (W, can be made. Physical model tests performed by Crookston et al. (2012), Crookston (2010), and the current study were used to analyze size-scale effects (associated with Froude scaling) and effects on the accuracy of discharge predictions made by the Crookston and Tullis (2013a) design method for geometrically dissimilar weirs (variation of w and P while maintaining α, A_c, t_w, and W constant). Based upon the findings of this study, the following conclusions are made:

1) Data collected in this study are very comparable with the data of Crookston's (2010) α =12° and 15° labyrinth weirs. C_d data of weirs with identical geometries from the current study and Crookston (2010) are within ~2%. These differences in performance are most likely attributed, in part, to differences in nappe behavior, which may be affected by differences in the weir material surface finish, construction, levelness of the weir, and the accuracy of the crest elevation reference. Weirs placed in the inverted orientation slightly underperform weirs in the normal orientation (peaks at ~2% at H_T/P=0.8 for the *HR* weir). This may be due to the added friction losses associated with the flume walls.

2) The Tullis et al. (1995) effective length parameter (L_e) does not completely account for all nappe interference efficiency losses. This parameter seems to account for some losses but not all. The total crest length (L_c) is recommended for use in design.

3) For a fixed channel width, the discharge capacity of the labyrinth weir increases as *A* is minimized. This is due to the fact that as *A* reduces, the labyrinth weir sidewall length (l_c) increases; l_c represents the more hydraulically efficient portion of the labyrinth weir. Out of the weirs tested, apex width A=1t_w is the most feasible design to maximize discharge efficiency. The increase of upstream apex width does not yield an increase in overall discharge efficiency. Even though nappe interference is decreased with wider apexes, the decrease of l_c is substantial enough to decrease the weirs performance. The weir with A=0t_w (triangular) yielded the highest discharge capacity, but due to the triangular nature of the apex, construction is difficult and it

produced a modest 3% increase in discharge with an 5.8% increase in total weir crest length. If the channel width (W), and longitudinal apron length (B) can be increased, maximum discharge is achieved by reducing the cycle number (N), adding more sidewall length (l_c), and minimizing the apex width. However, if B is limited, the increase of A (e.g., $A=2t_w$) will increase discharge approximately proportional to the increase in weir crest length.

4) Froude scaling was shown to produce favorable results when used to predict flows at larger scales. A model (α=15°-*QR*) 3 times the scale (Crookston 2010) and geometrically comparable to the model used by Crookston and Tullis (2013a) in developing their labyrinth weir design method was compared to the Crookston and Tullis (2013a) weir. The design method predicted flows within 3% of actual flows (excluding flows $H_T/P<0.1$). When compared to a weir that was scaled to half the size of the design method, the design method predicted flows within ±3% (excluding flows $H_T/P<0.1$). It was evident that size scale effects are amplified at smaller heads. This may be attributed to the increased effect that surface tension has on flow at lower heads and the inability of Froude scaling to represent this phenomena.

5) The intended use and proven effectiveness of the design method presented by Crookston and Tullis (2013a) is for geometrically similar weirs to those tested within their study. In an effort to expand the applicability of this design method, non-geometrically similar weirs were tested and compared to design method predictions. A common geometric variation from the design method is varying P.

Analysis of Crookston's data (Crookston et al. 2012) shows that when P is halved (w/P=4) the design method predicts actual flows within ±12% (depending on H_T/P). When P is doubled (w/P=1), the design method over predicts actual flows by ~20%. This is due to the fact that as P increases, H_T/P decreases and a higher C_d value is predicted, when in reality the C_d value remains practically the same. In the case where a weir is geometrically similar to the design method weir (w/P, P/t_w, and other dimensionless ratios are all similar), then P is changed, the design method will not accurately predict flows. A corrected H_T/P value (H_T/P'), for P=0.5, 1.25, 1.5, and 2.0 times that of the design method weir P, was presented to accommodate the design of weirs with this variation.

6) Another common deviation is to vary w (N), while maintaining P, t_w, A_c, W, and α constant. Data collected by Crookston et al. (2012) was used to compare weirs of w/P=0.69, 1.0, and 2.0. The weir that was used in Crookston and Tullis's (2013a) design method was the weir with w/P=2.0. The other two weirs maintained all other parameters and varied w. As w was varied, the design method's ability to predict accurate C_d values decreased significantly. For the weir with w/P=0.69 the difference between predicted and actual peaked at ~ 18%. For the w/P = 1.03 weir, the maximum difference peaked at ~20%. Corrected H_T/P values (H_T/P') were presented for these two weir configurations and can increase the design methods ability to accurately predict C_d values to within ±5%. Discharge efficiency was also noticed to decrease significantly as w was decreased. However, labyrinth weirs with w/P< 2 should not be discounted solely due to this reason. In certain situations this

may be a feasible option. This data is intended to be used in such scenarios with Crookston and Tullis's design method to more accurately predict discharge efficiencies.

This study presents data for only a limited number of geometric variations for labyrinth weirs. Additional studies are still needed to further expand the labyrinth weir knowledge base and more fully understand the best applications of this unique type of weir. Due to the unique hydraulic behaviors of labyrinth weirs, performing model studies still remain a viable and recommended option when verifying a labyrinth weirs performance.

REFERENCES

Cassidy, J., Gardner, C., and Peacock, R. (1985) “Boardman labyrinth – crest spillway” *J. Hydraul. Eng*., 111(3), 398-416.

Crookston, B. M. (2010). "Labyrinth weirs." Ph.D. dissertation, Utah State Univ., Logan, UT.

Crookston, B. M., Paxson, G. S., and Savage, B. M. (2012). “It can be done! Labyrinth weir design guidance for high headwater and low cycle width ratios.” *Proc., Dam Safety 2012*, ASDSO, Denver, CO.

Crookston, B. M., and Tullis, B. P. (2012a). ”Arced labyrinth weirs.” *J. Hydraul. Eng.*, 138(6), 555–562.

Crookston, B. M., and Tullis, B. P. (2012b). ”Discharge efficiency of reservoir-application-specific labyrinth weirs.” *J. Irrig. Drain Eng.* 138(6), 564–568.

Crookston, B. M., and Tullis, B. P. (2012c). ”Labyrinth weirs: Nappe interference and local submergence.” *J. Irrig. Drain Eng.*, 138(8), 757–765.

Crookston, B. M., and Tullis, B. P. (2013a). “Hydraulic design and analysis of labyrinth weirs. I: Discharge relationships.” *J. Irrig. Drain Eng*., 139(5), 363-370.

Crookston, B. M., and Tullis, B. P. (2013b). ”Hydraulic design and analysis of labyrinth weirs. II: Nappe aeration, instability, and vibration.” *J. Irrig. Drain Eng.*, 139(5), 371–377.

Dabling, M. R., Tullis, B. P., and Crookston, B.M. (2013). “Staged labyrinth weir hydraulics.” *J. Irrig. Drain. Eng*., ASCE, 139(11), 955-960.

Falvey, H. (2003). *Hydraulic design of labyrinth weirs*, ASCE, Reston, VA.

Hay, N., and Taylor, G. (1970). “Performance and design of labyrinth weirs.” *J. Hydraul. Eng.*, 96(11), 2337-2357.

Hinchliff, D., and Houston, K. (1984). “Hydraulic design and application of labyrinth spillways.” *Proc., 4th Annual USCOLD Lecture*, Dam Safety and Rehabilitation, Bureau of Reclamation, U.S. Dept. of the Interior, Washington, DC.

Houston, K. (1982). "Hydraulic model study of Ute Dam labyrinth spillway.*" Rep. No. GR-82-7,* U.S. Bureau of Reclamations, Denver.

Indlekofer, H., and Rouvé, G. (1975). "Discharge over polygonal weirs." *J. Hydr. Div.*, 101(3), 385–401.

Kline, S., and McClintock, F. (1953). "Describing uncertainties in single-sample experiments." *Am. Soc. Mech. Eng.* 75(1), 3-8.

Lux, F. (1984). "Discharge characteristics of labyrinth weirs." *Proc., of Conf. on Water for Resources Development*, ASCE, Cour d'Alene, Idaho.

Lux, F. (1989). "Design and application of labyrinth weirs." *Design of hydraulic structures 89*, M. Alberson and R. Kia, eds., Balkema/Rotterdam, Netherlands, 205-215.

Lux , F. and Hinchliff, D. (1985). "Design and construction of labyrinth spillways." *15th Congress ICOLD, Vol. IV, Q59-R15,* ICOLD, Paris, 249-274.

Savage, B., Frizell, K., and Crowder, J. (2004). Brains versus brawn: The changing world of hydraulic model studies. *Proc. of the ASDSO Annual Conference*, Phoenix, Ariz., CD-ROM.

Taylor, G. (1968). "The performance of labyrinth weirs." Ph.D. thesis, Univ. of Nottingham, Nottingham, England.

Tullis, B. P., Young, J., and Chandler, M. (2007). "Head-discharge relationships for submerged labyrinth weirs." *J. Hydr. Eng.*, 133(3), 248-254.

Tullis, P., Amanian, N., and Waldron, D. (1995). "Design of labyrinth spillways." *J. Hydraul. Eng.*, 121(3), 247–255.

Waldron, D. (1994). "Design of labyrinth spillways." M.S. thesis, Utah State Univ., Logan, UT.

APPENDICES

APPENDIX A

Photographs and Drawings of Weirs Tested

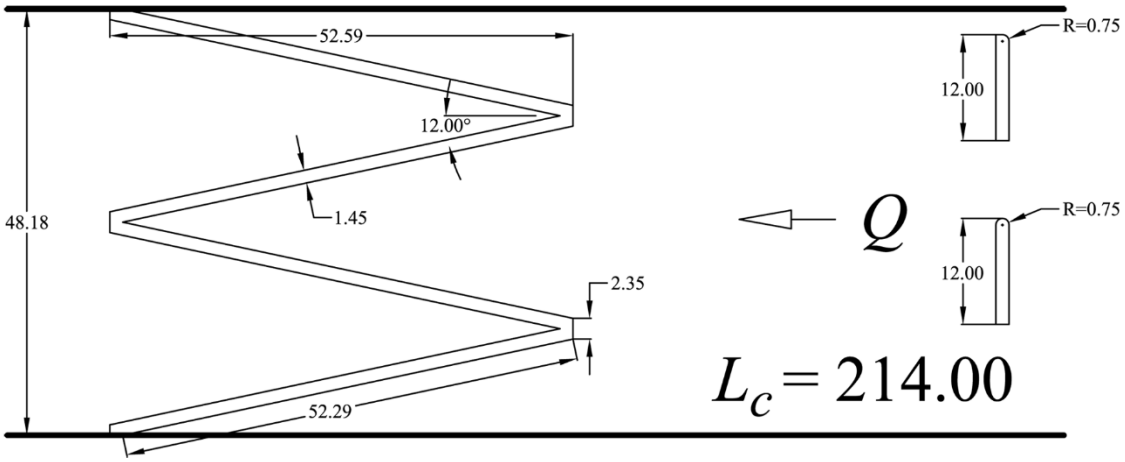

Fig. A-1. α = 12°, *HR* and *QR*, A=0$t_{w\text{-}US\text{-}DS}$, inverted orientation, schematic

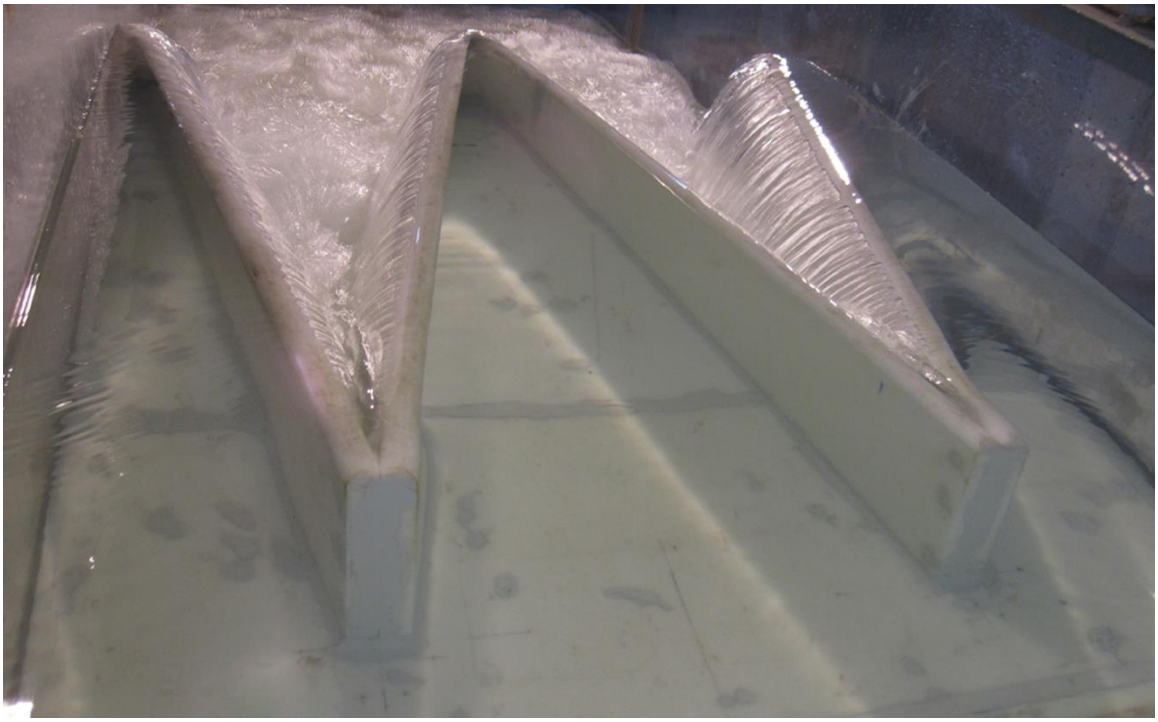

Fig. A-2. α = 12°, *HR*, A=0$t_{w\text{-}US\text{-}DS}$, inverted orientation, H_T/P = 0.175, photograph

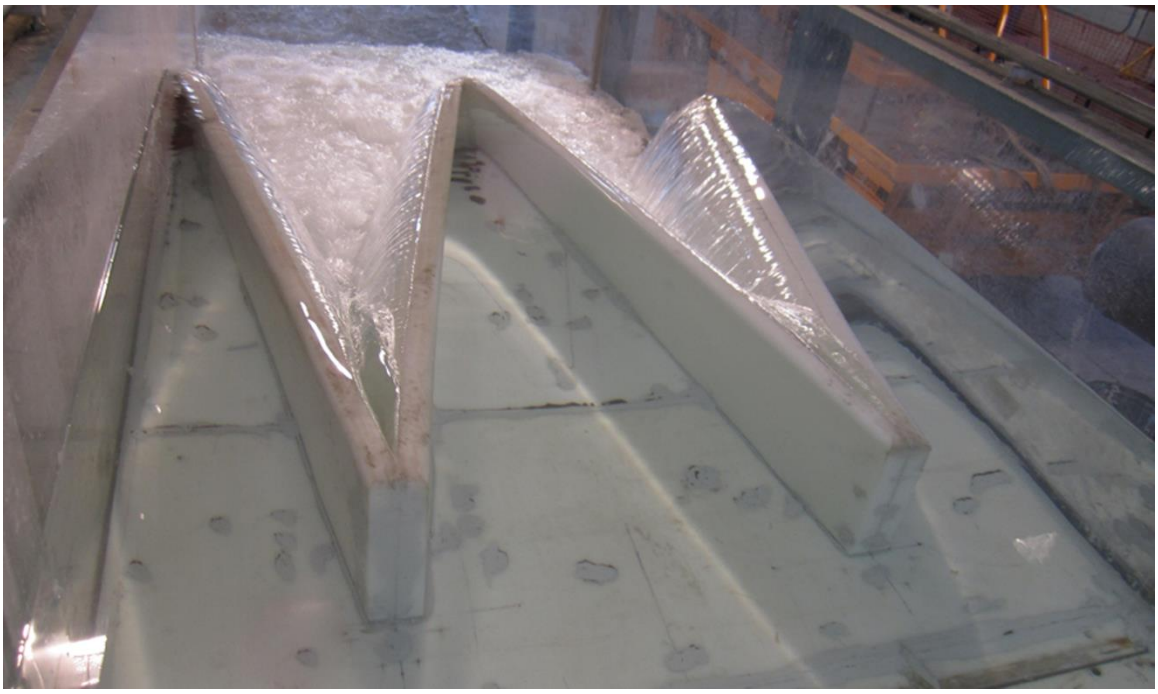

Fig. A-3. α = 12°, *QR*, $A=0t_w$, inverted orientation, H_T/P = 0.175, photograph

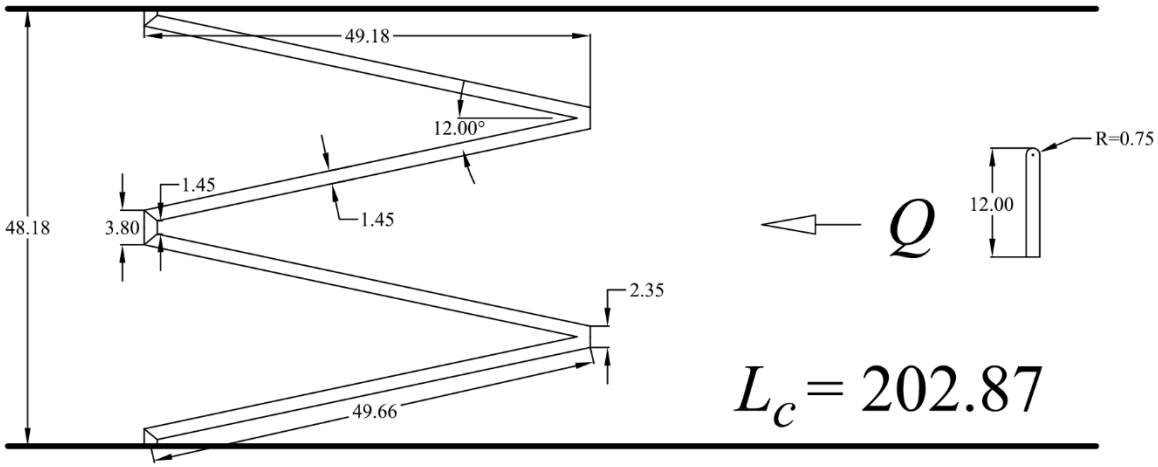

Fig. A-4. α = 12°, *HR* and *QR*, $A=0t_{w\text{-}us}$, inverted orientation, schematic

Fig. A-5. α = 12°, *HR*, A=0$t_{w\text{-}us}$, inverted orientation, H_T/P = 0.147, photograph

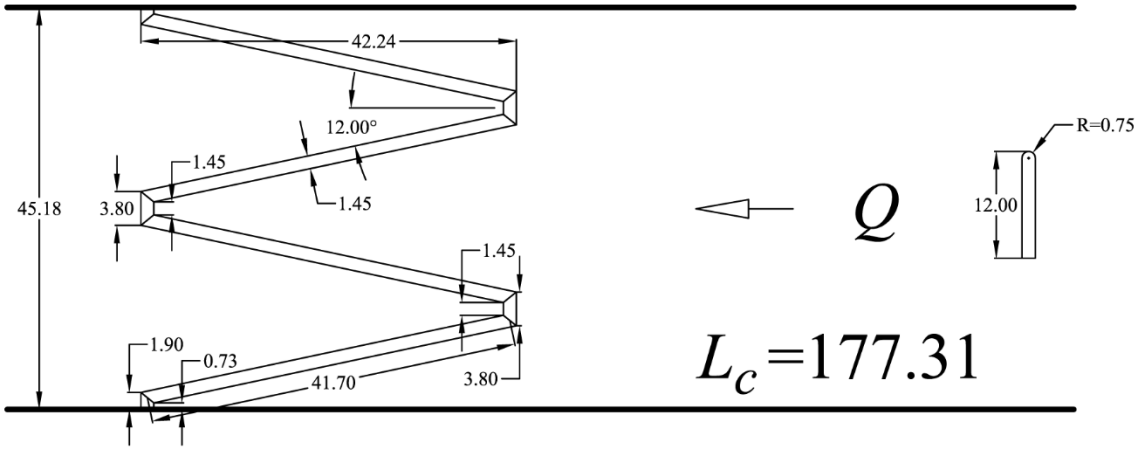

Fig. A-6. α = 12°, *HR*, A=1t_{w_vw}, inverted orientation, false wall, schematic

Fig. A-7. α = 12°, *HR*, *A*=1t_{w_vw}, inverted orientation, false wall, photograph

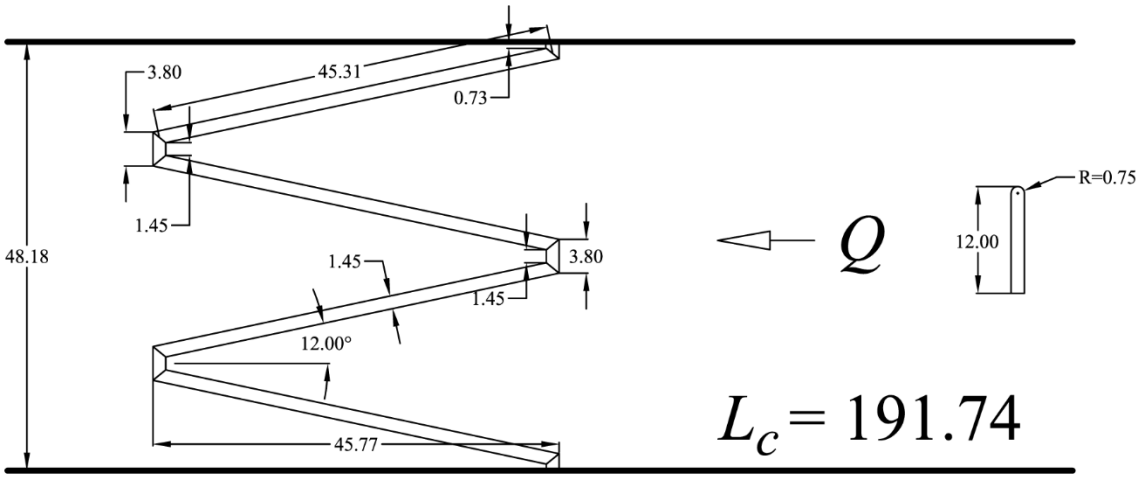

Fig. A-8. α = 12°, *HR*, *A*=1t_w, normal orientation, schematic

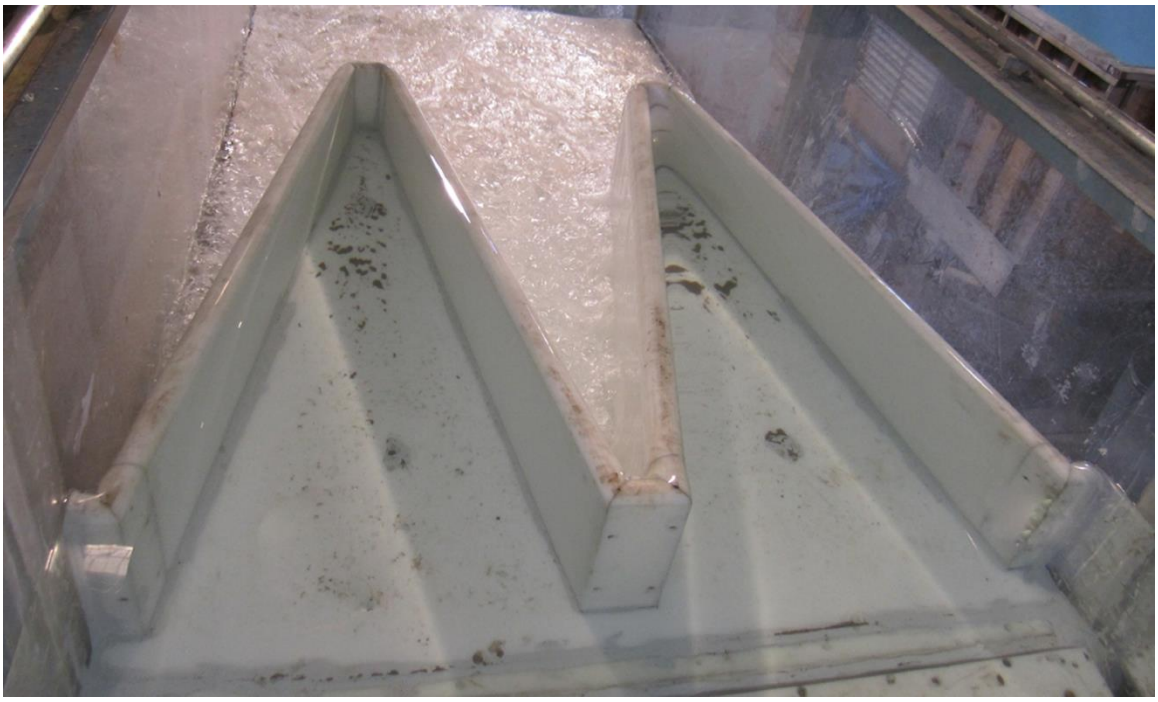

Fig. A-9. α = 12°, *HR*, A=1t_w, normal orientation, H_T/P = 0.1, photograph

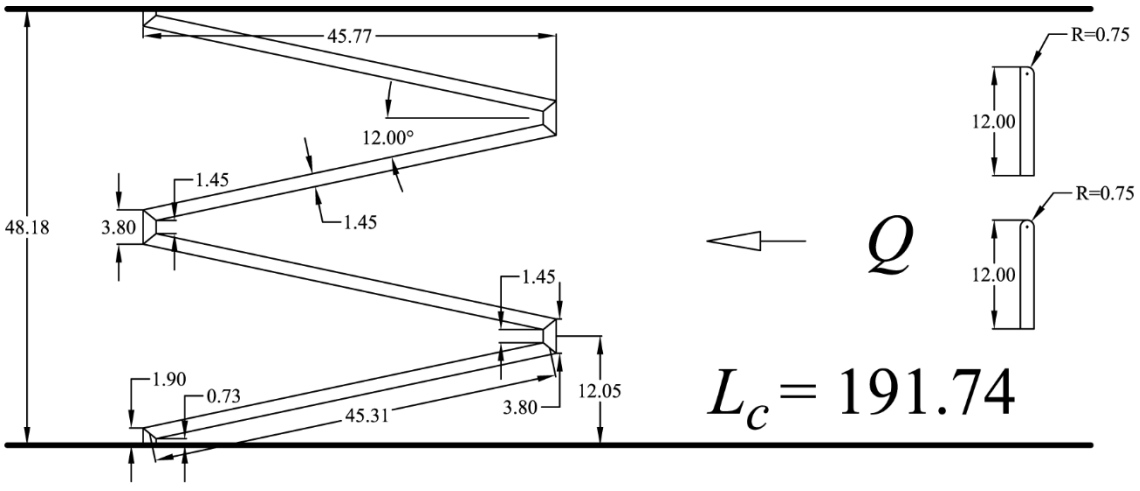

Fig. A-10. α = 12°, *HR* and *QR*, A=1t_w, inverted orientation, schematic

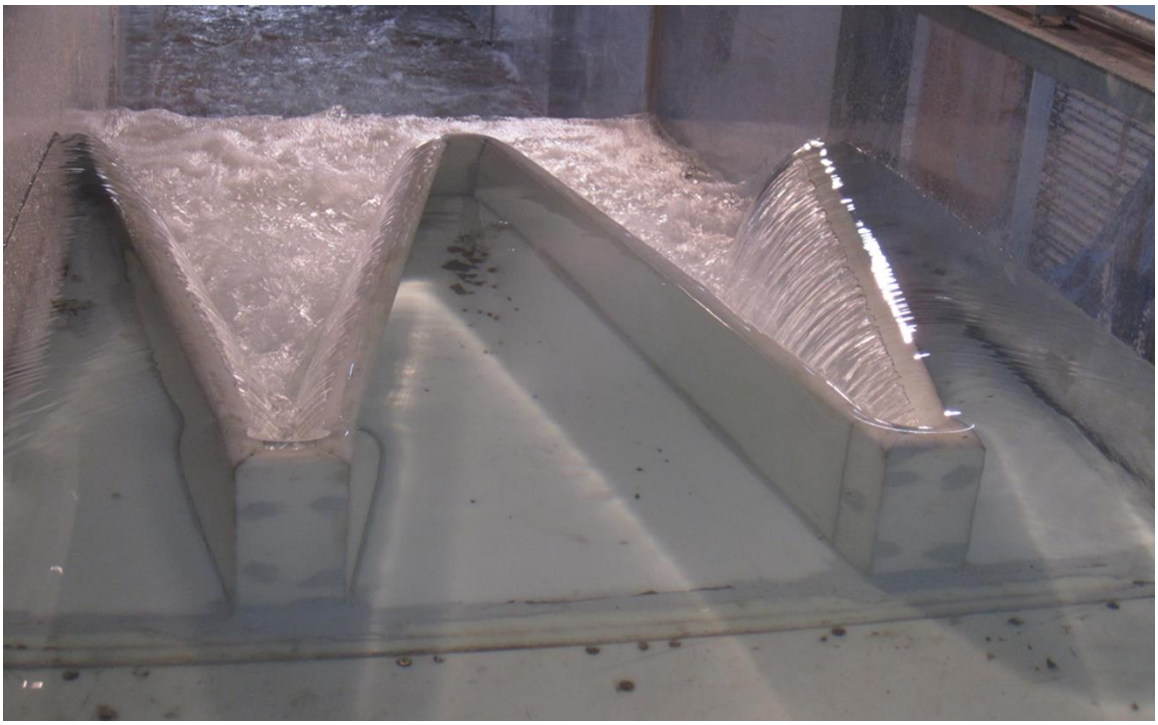

Fig. A-11. α = 12°, *HR*, A=1t_w, inverted orientation, H_T/P = 0.179, photograph

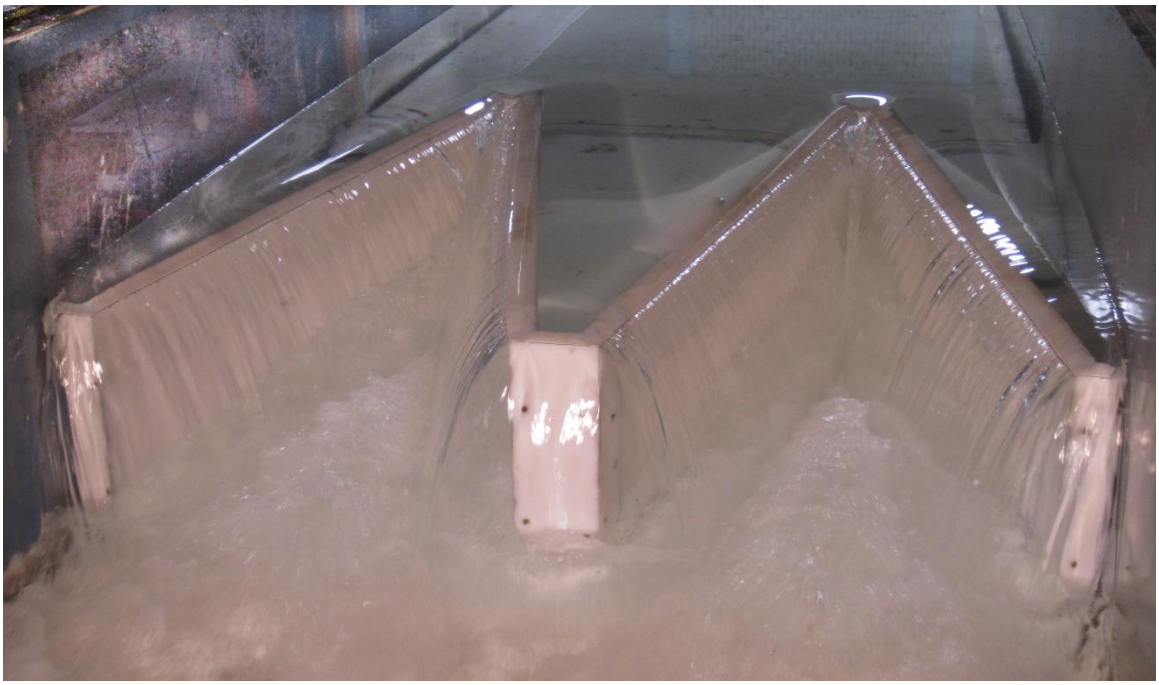

Fig. A-12. α = 12°, *QR*, A=1t_w, inverted orientation, H_T/P = 0.1, photograph

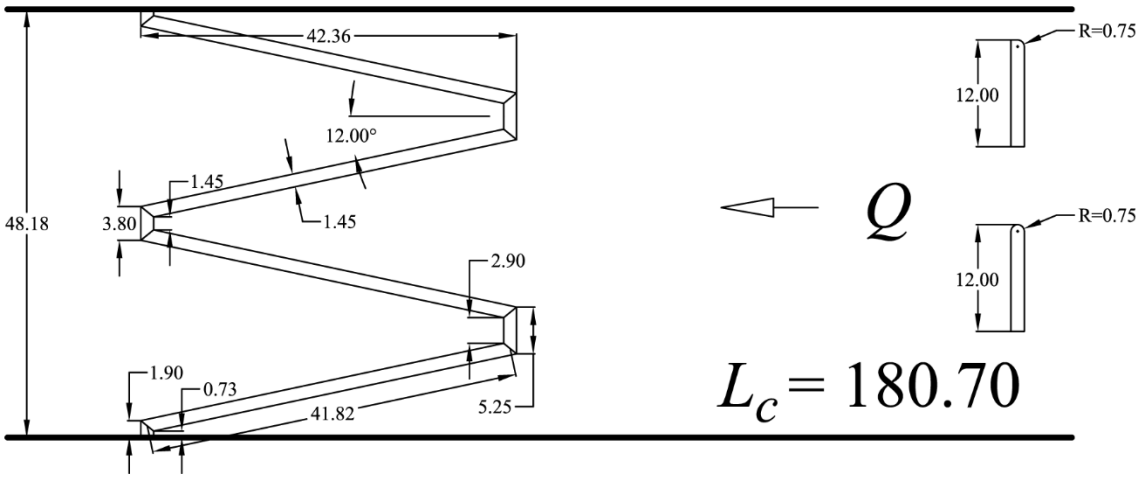

Fig. A-13. α = 12°, *HR* and *QR*, $A=2t_w$, inverted orientation, schematic

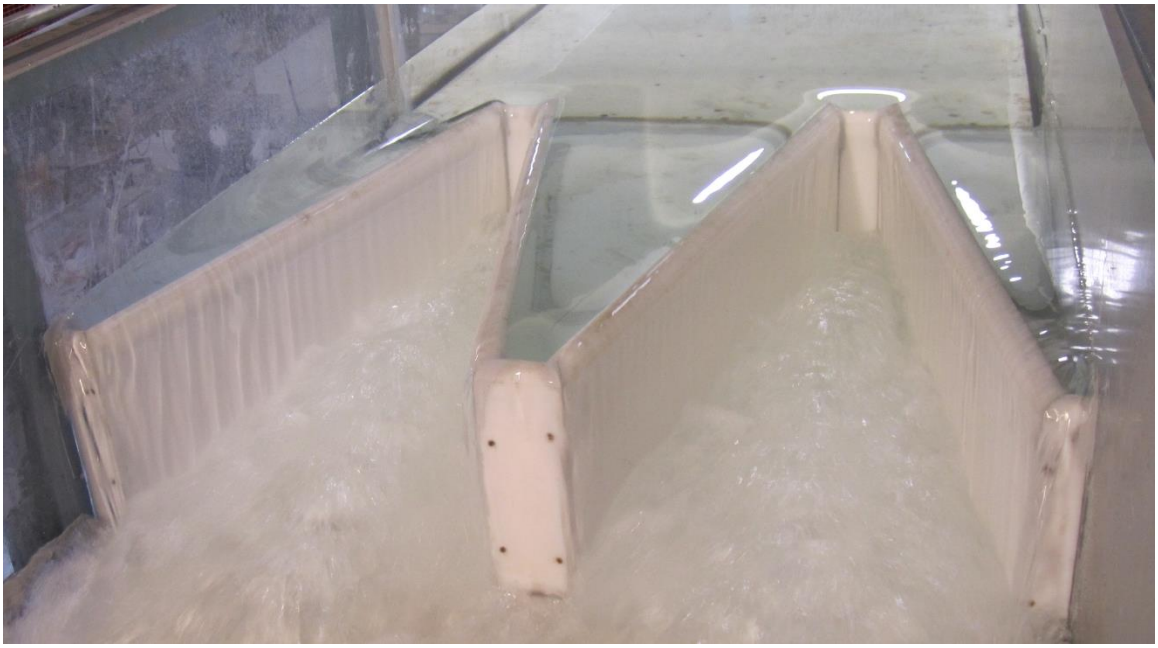

Fig. A-14. α = 12°, *HR*, $A=2t_w$, inverted orientation, H_T/P = 0.1, photograph

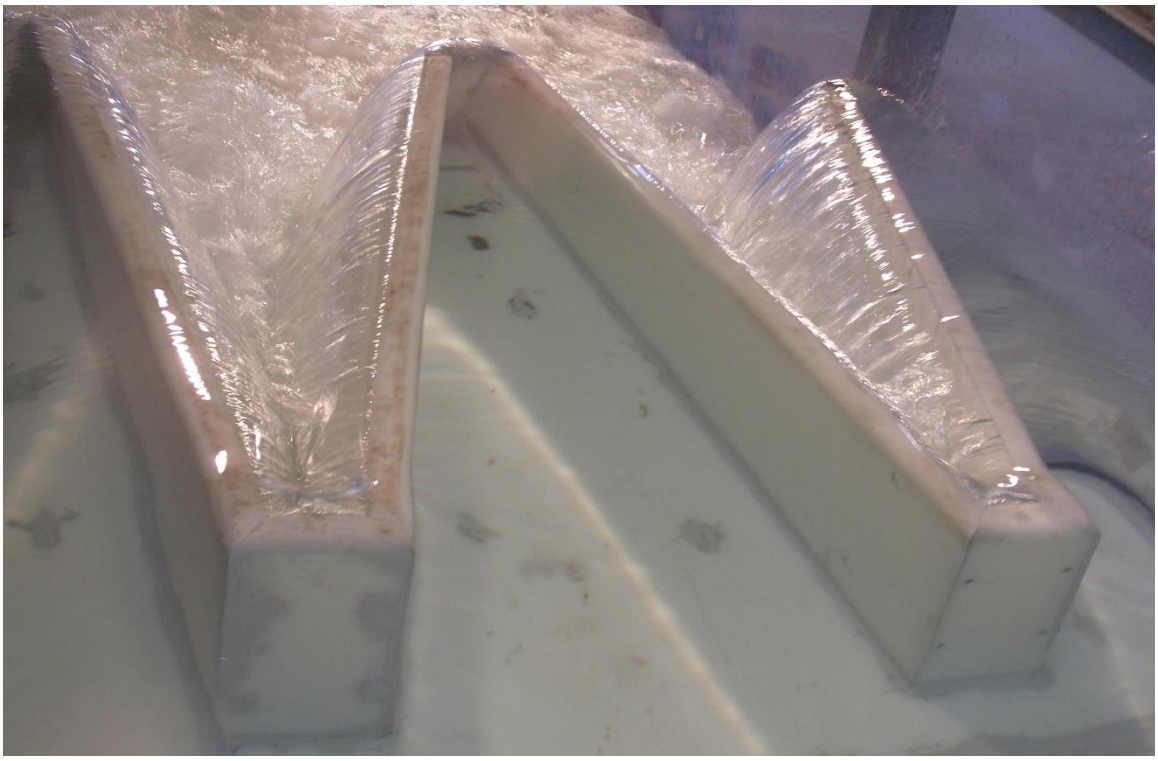

Fig. A-15. α = 12°, *QR*, $A=2t_w$, inverted orientation, H_T/P = 0.175, photograph

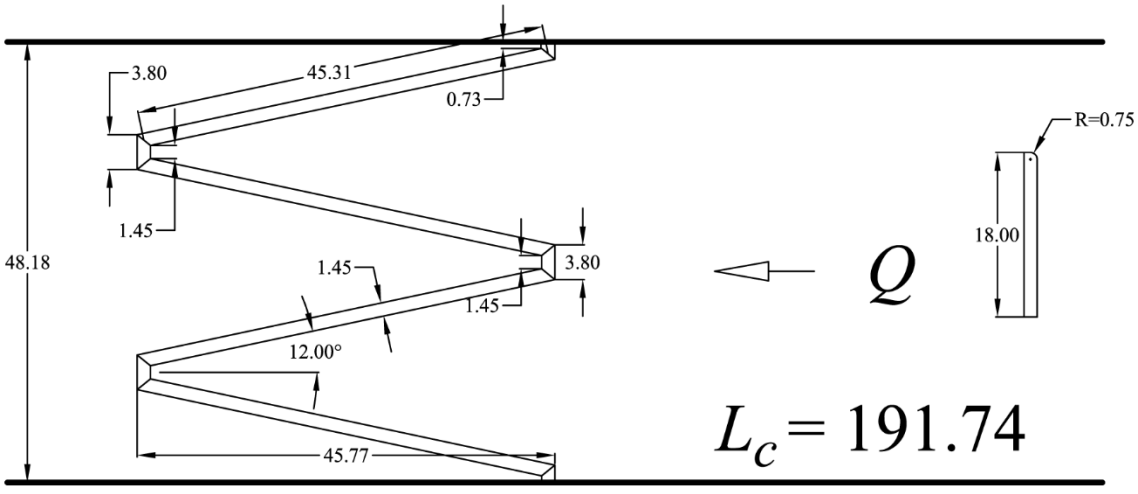

Fig. A-16. α = 12°, *QR*, $A=1t_w$, normal orientation, *P*=18 in, schematic

Fig. A-17. α = 12°, *QR*, *A*=1t_w, normal orientation, *P*=18 in, photograph

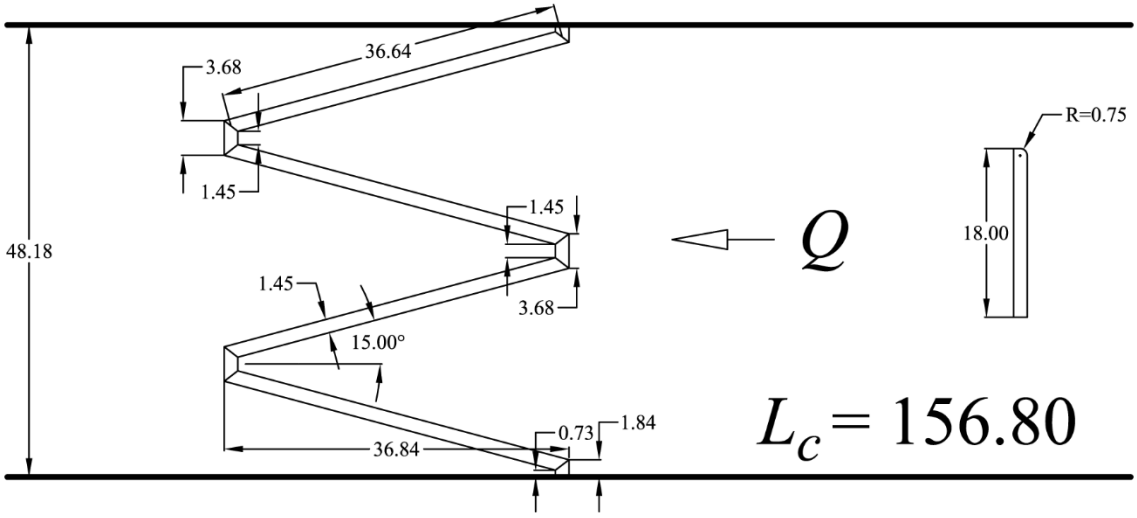

Fig. A-18. α = 15°, *QR*, *A*=1t_w, normal orientation, *P*=18 in, schematic

Fig. A-19. α = 15°, *QR*, *A*=1t_w, normal orientation, H_T/P = 0.1, *P*=18 in, photograph

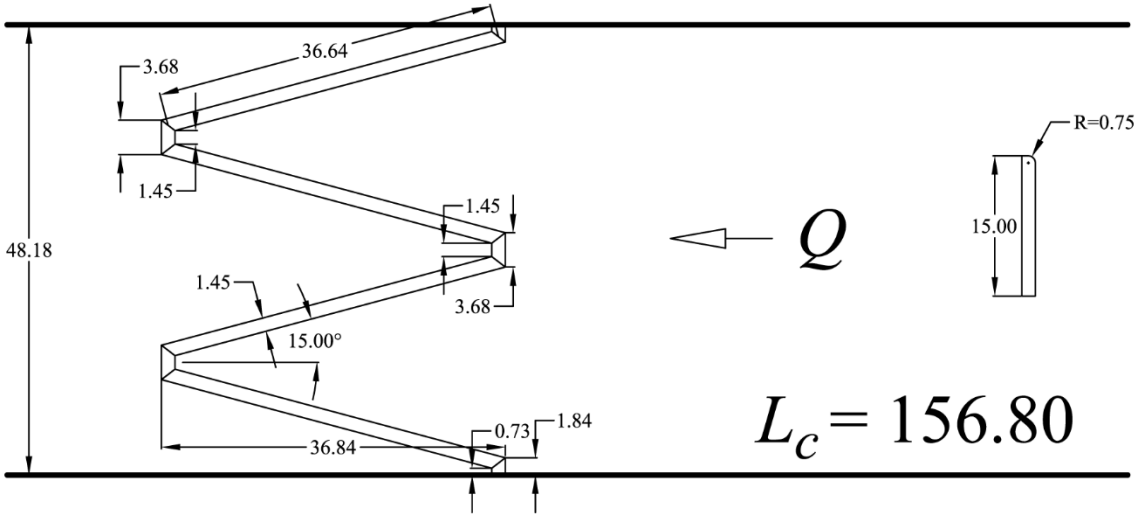

Fig. A-20. α = 15°, *QR*, *A*=1t_w, normal orientation, *P*=15 in, schematic

Fig. A-21. α = 15°, *QR*, *A*=1t_w, normal orientation, H_T/P = 0.1, *P*=15 in, photograph

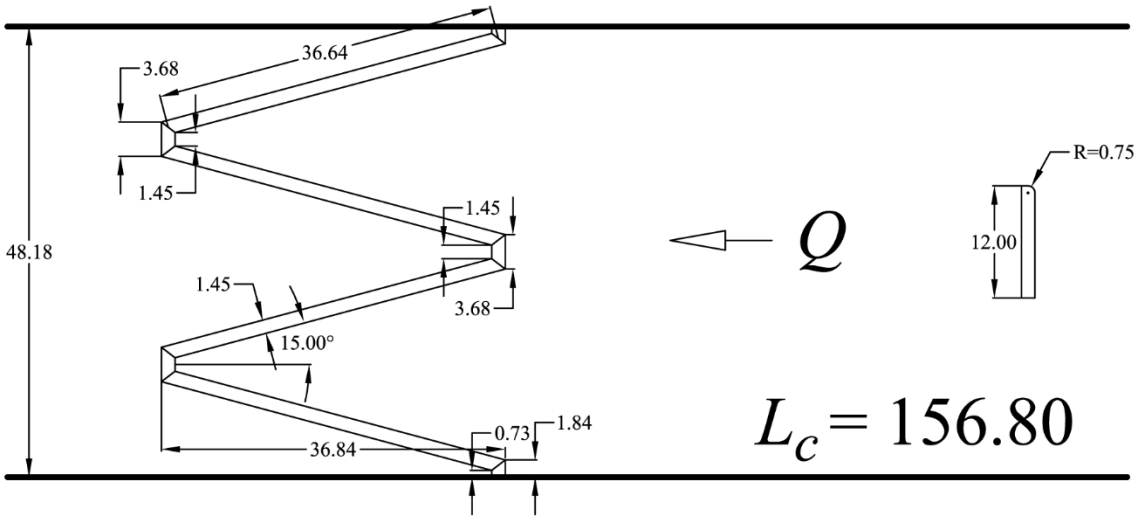

Fig. A-22. α = 15°, *QR*, *A*=1t_w, normal orientation, *P*=12 in, schematic

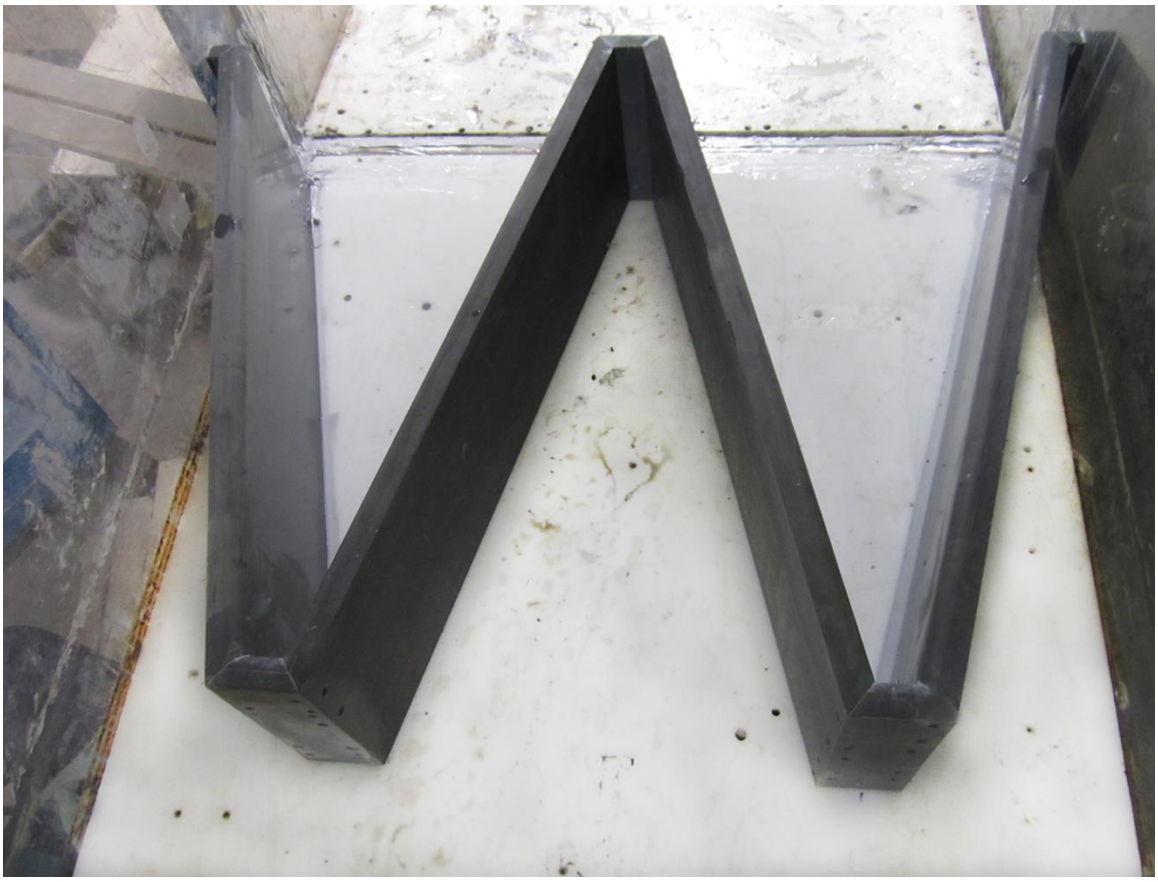

Fig. A-23. α = 15°, *QR*, *A*=1t_w, normal orientation, *P*=12 in, photograph

APPENDIX B

Data

Table B-1. α = 12°, *HR*, $A=1t_w$, inverted orientation, data

Experimental Data for Labyrinth Weir, 2-Cycle, Trapezoidal, Half Round, α =12°, A =1 t_w, Inverted Orientation

	Measured (Model)	Design (AutoCAD)
P (ft)	1	1.000
L_c (in)	192.9	191.7432
t_w (in)	1.450	1.45
W (in)	48.4125	48.1800
N	2	2
g	32.174	
$L_{c\text{-}cycle}$ (in)	96.46875	
w (in)	24.20625	

Leak	
Time (sec)	480
Water level drop (ft)	0.0106
Volume (in^3)	1735.9174
Leak (cfs)	0.0020929

Crest point gage reference (ft)	0.9757083

Run No.	Q (cfs)	Point Gage (ft)	H (ft)	U.S. Vel. (fps)	H_T (ft)	H_T/P	C_d Eq 1
1	2	3	4	5	6	7	8
1	0.70	1.0280	0.052	0.128	0.053	0.053	0.680
2	1.21	1.0490	0.073	0.216	0.074	0.074	0.698
3	1.59	1.0630	0.087	0.282	0.089	0.089	0.702
4	1.87	1.0725	0.097	0.329	0.098	0.098	0.704
5	2.19	1.0830	0.107	0.383	0.110	0.110	0.704
6	2.94	1.1070	0.131	0.505	0.135	0.135	0.688
7	3.51	1.1250	0.149	0.595	0.155	0.155	0.670
8	4.15	1.1455	0.170	0.694	0.177	0.177	0.647
9	4.44	1.1560	0.180	0.738	0.189	0.189	0.630
10	5.61	1.1925	0.217	0.909	0.230	0.230	0.593
11	7.27	1.2410	0.265	1.143	0.286	0.286	0.554
12	7.80	1.2560	0.280	1.213	0.303	0.303	0.543
13	8.34	1.2720	0.296	1.285	0.322	0.322	0.531
14	10.04	1.3210	0.345	1.501	0.380	0.380	0.498
15	10.41	1.3310	0.355	1.547	0.392	0.392	0.492
16	11.62	1.3680	0.392	1.690	0.437	0.437	0.468
17	12.66	1.4005	0.425	1.806	0.476	0.476	0.449
18	13.37	1.4240	0.448	1.882	0.503	0.503	0.435
19	6.48	1.2180	0.242	1.033	0.259	0.259	0.572
20	5.15	1.1770	0.201	0.844	0.212	0.212	0.613
21	5.39	1.1850	0.209	0.878	0.221	0.221	0.602
22	4.83	1.1670	0.191	0.795	0.201	0.201	0.622
23	9.02	1.2920	0.316	1.372	0.346	0.346	0.516
24	14.24	1.4535	0.478	1.971	0.538	0.538	0.419
25	15.73	1.5050	0.529	2.117	0.599	0.599	0.395
26	17.23	1.5560	0.580	2.256	0.659	0.659	0.374
27	19.40	1.6300	0.654	2.445	0.747	0.747	0.349

Table B-2. α = 12°, *HR*, $A=1t_w$, normal orientation, data

Experimental Data for Labyrinth Weir, 2-Cycle, Trapezoidal, Half Round, α =12°, A =1 t_w, Normal Orientation

	Measured (Model)	Design (AutoCAD)
P (ft)	1	1.000
L_c (in)	192.9	191.7432
t_w (in)	1.450	1.45
W (in)	48.4125	48.1800
N	2	2
g	32.174	
$L_{c\text{-}cycle}$ (in)	96.46875	
w (in)	24.20625	

Leak	
Time (sec)	480
Water level drop (ft)	0.005333
Volume (in^3)	873.363
Leak (cfs)	0.001053

Crest point gage reference (ft)	0.97625

Run No.	Q (cfs)	Point Gage (ft)	H (ft)	U.S. Vel. (fps)	H_T (ft)	H_T/P	C_d Eq 1
1	2	3	4	5	6	7	8
1	0.71	1.0300	0.054	0.128	0.054	0.054	0.657
2	1.21	1.0510	0.075	0.217	0.075	0.075	0.681
3	1.60	1.0650	0.089	0.282	0.090	0.090	0.689
4	1.87	1.0740	0.098	0.329	0.099	0.099	0.695
5	2.25	1.0860	0.110	0.391	0.112	0.112	0.697
6	2.73	1.1010	0.125	0.471	0.128	0.128	0.693
7	3.25	1.1160	0.140	0.555	0.145	0.145	0.690
8	3.71	1.1300	0.154	0.628	0.160	0.160	0.677
9	3.97	1.1420	0.166	0.665	0.173	0.173	0.644
10	4.50	1.1520	0.176	0.750	0.184	0.184	0.662
11	5.00	1.1755	0.199	0.820	0.210	0.210	0.607
12	6.16	1.2100	0.234	0.987	0.249	0.249	0.578
13	7.07	1.2365	0.260	1.115	0.280	0.280	0.557
14	7.89	1.2600	0.284	1.225	0.307	0.307	0.540
15	8.34	1.2740	0.298	1.284	0.323	0.323	0.529
16	9.30	1.3010	0.325	1.408	0.356	0.356	0.511
17	10.05	1.3220	0.346	1.503	0.381	0.381	0.498
18	10.50	1.3350	0.359	1.557	0.396	0.396	0.490
19	11.26	1.3570	0.381	1.649	0.423	0.423	0.477
20	11.98	1.3780	0.402	1.733	0.448	0.448	0.465
21	12.84	1.4040	0.428	1.829	0.480	0.480	0.450
22	13.31	1.4190	0.443	1.879	0.498	0.498	0.442
23	14.28	1.4520	0.476	1.980	0.537	0.537	0.423
24	15.73	1.5000	0.524	2.124	0.594	0.594	0.400
25	17.87	1.5750	0.599	2.317	0.682	0.682	0.369
26	20.51	1.6615	0.685	2.545	0.786	0.786	0.343

Table B-3. α = 12°, *HR*, $A=2t_w$, inverted orientation, data

Experimental Data for Labyrinth Weir, 2-Cycle, Trapezoidal, Half Round, α =12°, A =2 t_w, Inverted Orientation

	Measured (Model)	Design (AutoCAD)
P (ft)	1	1.000
L_c (in)	181.0	180.6950
t_w (in)	1.450	1.45
W (in)	48.4125	48.1800
N	2	2
g	32.174	
$L_{c\text{-}cycle}$ (in)	90.5	
w (in)	24.20625	

Leak	
Time (sec)	480
Water level drop (ft)	0.005333
Volume (in^3)	873.363
Leak (cfs)	0.001053

Crest point gage reference (ft)	0.9736667

Run No.	Q (cfs)	Point Gage (ft)	H (ft)	U.S. Vel. (fps)	H_T (ft)	H_T/P	C_d Eq 1
1	2	3	4	5	6	7	8
1	1.11	1.0470	1.047	0.199	0.074	0.074	0.684
2	1.50	1.0630	1.063	0.266	0.090	0.090	0.685
3	1.88	1.0760	1.076	0.329	0.104	0.104	0.693
4	2.51	1.0970	1.097	0.434	0.126	0.126	0.694
5	3.13	1.1200	1.120	0.532	0.151	0.151	0.663
6	3.73	1.1400	1.140	0.624	0.172	0.172	0.645
7	4.18	1.1550	1.155	0.694	0.189	0.189	0.632
8	4.72	1.1735	1.174	0.773	0.209	0.209	0.611
9	6.33	1.2260	1.226	1.002	0.268	0.268	0.565
10	7.53	1.2640	1.264	1.165	0.311	0.311	0.537
11	8.98	1.3100	1.310	1.349	0.365	0.365	0.505
12	10.23	1.3490	1.349	1.502	0.410	0.410	0.482
13	11.87	1.4030	1.403	1.689	0.474	0.474	0.451
14	14.09	1.4780	1.478	1.922	0.562	0.562	0.415
15	16.17	1.5510	1.551	2.120	0.647	0.647	0.385
16	20.43	1.7020	1.702	2.481	0.824	0.824	0.339

Table B-4. α = 12°, *HR*, $A=2t_w$, inverted orientation, data

Experimental Data for Labyrinth Weir, 2-Cycle, Trapezoidal, Half Round, α =12°, A =0 t_w, Inverted Orientation

	Measured (Model)	Design (AutoCAD)
P (ft)	1	1.000
L_c (in)	214.0	214.0016
t_w (in)	1.450	1.45
W (in)	48.4125	48.1800
N	2	2
g	32.174	
$L_{c\text{-}cycle}$ (in)	107	
w (in)	24.20625	

Leak	
Time (sec)	300
Water level drop (ft)	0.01898
Volume (in^3)	3108.14
Leak (cfs)	0.005996

Crest point gage reference (ft)	0.9764333

Run No.	Q (cfs)	Point Gage (ft)	H (ft)	U.S. Vel. (fps)	H_T (ft)	H_T/P	C_d Eq 1
1	2	3	4	5	6	7	8
1	0.76	1.0300	0.054	0.138	0.054	0.054	0.639
2	1.21	1.0470	0.071	0.217	0.071	0.071	0.668
3	1.58	1.0605	0.084	0.281	0.085	0.085	0.667
4	1.88	1.0705	0.094	0.332	0.096	0.096	0.667
5	2.37	1.0850	0.109	0.414	0.111	0.111	0.670
6	2.97	1.1050	0.129	0.512	0.133	0.133	0.646
7	3.54	1.1230	0.147	0.602	0.152	0.152	0.626
8	4.20	1.1430	0.167	0.703	0.174	0.174	0.605
9	5.16	1.1740	0.198	0.848	0.209	0.209	0.568
10	6.68	1.2250	0.249	1.061	0.266	0.266	0.511
11	8.13	1.2590	0.283	1.264	0.307	0.307	0.500
12	9.14	1.2875	0.311	1.396	0.341	0.341	0.481
13	10.29	1.3195	0.343	1.540	0.380	0.380	0.461
14	11.39	1.3485	0.372	1.676	0.416	0.416	0.446
15	12.62	1.3850	0.409	1.817	0.460	0.460	0.424
16	13.76	1.4190	0.443	1.944	0.501	0.501	0.407
17	15.28	1.4700	0.494	2.097	0.562	0.562	0.380
18	17.26	1.5350	0.559	2.287	0.640	0.640	0.354
19	18.55	1.5760	0.600	2.405	0.689	0.689	0.340
20	20.33	1.6320	0.656	2.560	0.757	0.757	0.323

Table B-5. α = 12°, *HR*, A=0$t_{w\text{-}us}$, inverted orientation, data

Experimental Data for Labyrinth Weir, 2-Cycle, Trapezoidal, Half Round, α=12°, A=0 $t_{w\text{-}us}$, Inverted Orientation

	Measured (Model)	Design (AutoCAD)
P (ft)	1	1.000
L_c (in)	202.8	202.8725
t_w (in)	1.450	1.45
W (in)	48.4125	48.1800
N	2	2
g	32.174	
$L_{c\text{-}cycle}$ (in)	101.375	
w (in)	24.20625	

Leak	
Time (sec)	600
Water level drop (ft)	0.01900
Volume (in^3)	3111.55
Leak (cfs)	0.003001

Crest point gage reference (ft)	0.5339176

Run No.	Q (cfs)	Point Gage (ft)	H (ft)	U.S. Vel. (fps)	H_T (ft)	H_T/P	C_d Eq 1
1	2	3	4	5	6	7	8
1	0.73	0.5890	0.055	0.147	0.055	0.055	0.619
2	1.21	0.6070	0.073	0.239	0.074	0.074	0.663
3	1.56	0.6200	0.086	0.307	0.088	0.088	0.668
4	1.88	0.6310	0.097	0.366	0.099	0.099	0.666
5	2.73	0.6560	0.122	0.520	0.126	0.126	0.672
6	3.35	0.6750	0.141	0.629	0.147	0.147	0.655
7	3.87	0.6900	0.156	0.719	0.164	0.164	0.644
8	4.28	0.7015	0.168	0.789	0.177	0.177	0.634
9	4.82	0.7215	0.188	0.876	0.200	0.200	0.599
10	6.83	0.7780	0.244	1.192	0.266	0.266	0.551
11	8.51	0.8220	0.288	1.440	0.320	0.320	0.520
12	10.78	0.8825	0.349	1.751	0.396	0.396	0.478
13	12.42	0.9270	0.393	1.961	0.453	0.453	0.451
14	13.94	0.9710	0.437	2.141	0.508	0.508	0.426
15	7.24	0.7870	0.253	1.256	0.278	0.278	0.548
16	5.28	0.7320	0.198	0.952	0.212	0.212	0.598
17	6.86	0.7780	0.244	1.196	0.266	0.266	0.552
18	12.75	0.9360	0.402	2.001	0.464	0.464	0.446
19	15.20	1.0100	0.476	2.279	0.557	0.557	0.405
20	19.02	1.1270	0.593	2.664	0.703	0.703	0.357
21	22.50	1.2310	0.697	2.975	0.835	0.835	0.327

Table B-6. α = 12°, *HR*, A=1$t_{w\text{-}vw}$, inverted orientation, data

Experimental Data for Labyrinth Weir, 2-Cycle, Trapezoidal, Half Round, α =12°, A =1 $t_{w\text{-}vw}$, Inverted Orientation

	Measured (Model)	Design (AutoCAD)
P (ft)	1	1.000
L_c (in)	178.1	177.6952
t_w (in)	1.450	1.45
W (in)	45.4125	45.1800
N	2	2
g	32.174	
$L_{c\text{-}cycle}$ (in)	89.0625	
w (in)	22.70625	

Leak	
Time (sec)	480
Water level drop (ft)	0.00050
Volume (in^3)	81.88
Leak (cfs)	0.000099

Crest point gage reference (ft)	0.975

Run No.	Q (cfs)	Point Gage (ft)	H (ft)	U.S. Vel. (fps)	H_T (ft)	H_T/P	C_d Eq 1
1	2	3	4	5	6	7	8
1	0.71	1.0320	0.057	0.136	0.057	0.057	0.649
2	1.25	1.0555	0.081	0.236	0.081	0.081	0.676
3	1.59	1.0685	0.094	0.299	0.095	0.095	0.685
4	1.88	1.0790	0.104	0.350	0.106	0.106	0.685
5	2.74	1.1075	0.133	0.501	0.136	0.136	0.686
6	3.36	1.1310	0.156	0.605	0.162	0.162	0.652
7	4.31	1.1630	0.188	0.759	0.197	0.197	0.621
8	5.21	1.1940	0.219	0.899	0.232	0.232	0.589
9	7.19	1.2565	0.282	1.192	0.304	0.304	0.542
10	8.95	1.3140	0.339	1.433	0.371	0.371	0.499
11	10.76	1.3730	0.398	1.662	0.441	0.441	0.463
12	12.37	1.4310	0.456	1.849	0.509	0.509	0.429
13	14.22	1.4970	0.522	2.048	0.587	0.587	0.398
14	16.19	1.5720	0.597	2.240	0.675	0.675	0.368
15	18.23	1.6460	0.671	2.429	0.763	0.763	0.345
16	20.28	1.7230	0.748	2.601	0.853	0.853	0.324
17	1.00	1.0460	0.071	0.191	0.072	0.072	0.653
18	1.89	1.0800	0.105	0.353	0.107	0.107	0.679
19	2.97	1.1160	0.141	0.540	0.146	0.146	0.672
20	9.17	1.3230	0.348	1.459	0.381	0.381	0.490
21	11.62	1.4060	0.431	1.760	0.479	0.479	0.441
22	13.70	1.4820	0.507	1.989	0.569	0.569	0.402
23	5.97	1.2220	0.247	1.012	0.263	0.263	0.557
24	8.13	1.2890	0.314	1.320	0.341	0.341	0.513
25	9.98	1.3495	0.375	1.563	0.413	0.413	0.474
26	15.75	1.5590	0.584	2.194	0.659	0.659	0.371
27	17.51	1.6220	0.647	2.361	0.734	0.734	0.351

Table B-7. α = 12°, *QR*, $A=1t_w$, inverted orientation, data

Experimental Data for Labyrinth Weir, 2-Cycle, Trapezoidal, Quarter Round, α =12°, A =1 t_w, Inverted Orientation

	Measured (Model)	Design (AutoCAD)
P (ft)	1	1.000
L_c (in)	192.2	191.7432
t_w (in)	1.450	1.45
W (in)	48.4125	48.1800
N	2	2
g	32.174	
$L_{c\text{-}cycle}$ (in)	96.078125	
w (in)	24.20625	

Leak	
Time (sec)	480
Water level drop (ft)	0.00533
Volume (in^3)	872.8717
Leak (cfs)	0.0010524

Crest point gage reference (ft)	0.97375

Run No.	Q (cfs)	Point Gage (ft)	H (ft)	U.S. Vel. (fps)	H_T (ft)	H_T/P	C_d Eq 1
1	2	3	4	5	6	7	8
1	0.70	1.0320	0.058	0.127	0.059	0.059	0.580
2	1.12	1.0515	0.078	0.199	0.078	0.078	0.594
3	1.41	1.0645	0.091	0.249	0.092	0.092	0.592
4	1.65	1.0740	0.100	0.290	0.102	0.102	0.596
5	1.85	1.0815	0.108	0.323	0.109	0.109	0.597
6	2.07	1.0900	0.116	0.359	0.118	0.118	0.595
7	2.63	1.1100	0.136	0.450	0.139	0.139	0.590
8	3.13	1.1265	0.153	0.530	0.157	0.157	0.588
9	3.69	1.1445	0.171	0.616	0.177	0.177	0.580
10	4.15	1.1590	0.185	0.687	0.193	0.193	0.573
11	5.12	1.1905	0.217	0.829	0.227	0.227	0.551
12	6.35	1.2290	0.255	1.003	0.271	0.271	0.526
13	7.78	1.2715	0.298	1.198	0.320	0.320	0.502
14	7.17	1.2540	0.280	1.116	0.300	0.300	0.511
15	9.48	1.3205	0.347	1.416	0.378	0.378	0.477
16	10.74	1.3570	0.383	1.570	0.422	0.422	0.458
17	11.98	1.3980	0.424	1.710	0.470	0.470	0.435
18	13.16	1.4375	0.464	1.837	0.516	0.516	0.414
19	14.38	1.4790	0.505	1.960	0.565	0.565	0.395
20	15.84	1.5280	0.554	2.103	0.623	0.623	0.376
21	17.11	1.5705	0.597	2.222	0.673	0.673	0.362
22	18.29	1.6125	0.639	2.323	0.723	0.723	0.348
23	19.39	1.6510	0.677	2.415	0.768	0.768	0.336
24	20.43	1.6870	0.713	2.500	0.810	0.810	0.327
25	14.00	1.4650	0.491	1.925	0.549	0.549	0.402
26	7.98	1.2750	0.301	1.226	0.325	0.325	0.504
27	3.65	1.1430	0.169	0.610	0.175	0.175	0.581

Table B-8. α = 12°, *QR*, $A=2t_w$, inverted orientation, data

Experimental Data for Labyrinth Weir, 2-Cycle, Trapezoidal, Quarter Round, α =12°, A =2 t_w, Inverted Orientation

	Measured (Model)	Design (AutoCAD)
P (ft)	1	1.000
L_c (in)	181.0	180.6950
t_w (in)	1.450	1.45
W (in)	48.4125	48.1800
N	2	2
g	32.174	
$L_{c\text{-}cycle}$ (in)	90.5	
w (in)	24.20625	

Leak	
Time (sec)	480
Water level drop (ft)	0.0035
Volume (in^3)	573.18029
Leak (cfs)	0.000691

Crest point gage reference (ft)	0.9730833

Run No.	Q (cfs)	Point Gage (ft)	H (ft)	U.S. Vel. (fps)	H_T (ft)	H_T/P	C_d Eq 1
1	2	3	4	5	6	7	8
1	0.70	1.0360	0.063	0.126	0.063	0.063	0.545
2	1.21	1.0610	0.088	0.215	0.089	0.089	0.570
3	1.59	1.0765	0.103	0.278	0.105	0.105	0.581
4	1.94	1.0900	0.117	0.336	0.119	0.119	0.588
5	2.72	1.1190	0.146	0.463	0.149	0.149	0.586
6	3.37	1.1420	0.169	0.564	0.174	0.174	0.577
7	3.89	1.1590	0.186	0.643	0.192	0.192	0.571
8	4.33	1.1745	0.201	0.709	0.209	0.209	0.561
9	5.05	1.1990	0.226	0.814	0.236	0.236	0.546
10	6.24	1.2380	0.265	0.981	0.280	0.280	0.523
11	6.96	1.2600	0.287	1.079	0.305	0.305	0.512
12	7.36	1.2730	0.300	1.132	0.320	0.320	0.505
13	8.17	1.2985	0.325	1.236	0.349	0.349	0.491
14	8.92	1.3220	0.349	1.331	0.376	0.376	0.479
15	9.67	1.3460	0.373	1.423	0.404	0.404	0.466
16	10.45	1.3710	0.398	1.514	0.434	0.434	0.454
17	11.44	1.4050	0.432	1.626	0.473	0.473	0.436
18	12.63	1.4450	0.472	1.754	0.520	0.520	0.418
19	13.91	1.4910	0.518	1.884	0.573	0.573	0.398
20	15.31	1.5400	0.567	2.019	0.630	0.630	0.379
21	17.63	1.6210	0.648	2.229	0.725	0.725	0.354
22	19.08	1.6690	0.696	2.355	0.782	0.782	0.342
23	20.44	1.7210	0.748	2.459	0.842	0.842	0.328

Table B-9. α = 12°, *QR*, $A=0t_w$, inverted orientation, data

Experimental Data for Labyrinth Weir, 2-Cycle, Trapezoidal, Quarter Round, α =12°, A =0 t_w, Inverted Orientation

	Measured (Model)	Design (AutoCAD)
P (ft)	1.01	1.000
L_c (in)	214.1	214.0016
t_w (in)	1.450	1.45
W (in)	48.4125	48.1800
N	2	2
g	32.174	
$L_{c\text{-}cycle}$ (in)	107.0625	
w (in)	24.20625	

Leak	
Time (sec)	510
Water level drop (ft)	0.02275
Volume (in^3)	3725.6719
Leak (cfs)	0.0042276

Crest point gage reference (ft)	0.9716667

Run No.	Q (cfs)	Point Gage (ft)	H (ft)	U.S. Vel. (fps)	H_T (ft)	H_T/P	C_d Eq 1
1	2	3	4	5	6	7	8
1	0.70	1.0290	0.057	0.127	0.058	0.057	0.534
2	1.22	1.0530	0.081	0.216	0.082	0.081	0.545
3	1.56	1.0660	0.094	0.273	0.095	0.095	0.554
4	1.89	1.0780	0.106	0.327	0.108	0.107	0.557
5	2.35	1.0940	0.122	0.404	0.125	0.124	0.559
6	2.98	1.1150	0.143	0.504	0.147	0.146	0.552
7	3.54	1.1330	0.161	0.591	0.167	0.165	0.544
8	4.18	1.1540	0.182	0.688	0.190	0.188	0.530
9	5.23	1.1870	0.215	0.843	0.226	0.224	0.509
10	6.81	1.2350	0.263	1.065	0.281	0.278	0.479
11	8.19	1.2745	0.303	1.249	0.327	0.324	0.459
12	9.27	1.3010	0.329	1.391	0.359	0.356	0.451
13	10.32	1.3310	0.359	1.520	0.395	0.391	0.435
14	11.42	1.3625	0.391	1.652	0.433	0.429	0.420
15	12.62	1.3990	0.427	1.788	0.477	0.472	0.401
16	13.58	1.4290	0.457	1.891	0.513	0.508	0.387
17	15.41	1.4880	0.516	2.077	0.583	0.578	0.362
18	17.45	1.5545	0.583	2.271	0.663	0.656	0.339
19	18.74	1.5980	0.626	2.384	0.715	0.708	0.325
20	20.44	1.6550	0.683	2.526	0.782	0.775	0.309

Table B-10. α = 12°, *QR*, $A=1t_w$, normal orientation, data

Experimental Data for Labyrinth Weir, 2-Cycle, Trapezoidal, Quarter Round, α =12°, A =1 t_w, Normal Orientation

	Measured (Model)	Design (AutoCAD)
P (ft)	1.5	1.500
L_c (in)	191.9	191.7432
t_w (in)	1.450	1.45
W (in)	48.4125	48.1800
N	2	2
g	32.174	
$L_{c\text{-}cycle}$ (in)	95.9375	
w (in)	24.20625	

Leak	
Time (sec)	480
Water level drop (ft)	0.00442
Volume (in^3)	723.3
Leak (cfs)	0.00087

Crest point gage reference (ft)	1.0480

Run No.	Q (cfs)	Point Gage (ft)	H (ft)	U.S. Vel. (fps)	H_T (ft)	H_T/P	C_d Eq 1
1	2	3	4	5	6	7	8
1	1.05	1.1230	0.076	0.149	0.076	0.051	0.589
2	1.40	1.1370	0.090	0.196	0.090	0.060	0.605
3	1.73	1.1500	0.103	0.241	0.103	0.069	0.608
4	2.00	1.1590	0.112	0.277	0.113	0.075	0.617
5	2.71	1.1830	0.136	0.371	0.138	0.092	0.620
6	3.37	1.2040	0.157	0.455	0.160	0.107	0.617
7	3.78	1.2160	0.169	0.507	0.173	0.115	0.616
8	5.70	1.2720	0.225	0.743	0.233	0.155	0.592
9	5.69	1.2730	0.226	0.741	0.234	0.156	0.587
10	7.84	1.3325	0.285	0.990	0.300	0.200	0.557
11	9.31	1.3730	0.326	1.152	0.346	0.231	0.534
12	10.58	1.4100	0.363	1.286	0.388	0.259	0.512
13	11.89	1.4470	0.400	1.419	0.431	0.287	0.492
14	12.92	1.4760	0.429	1.521	0.465	0.310	0.477
15	13.92	1.5070	0.460	1.615	0.500	0.333	0.460
16	15.16	1.5415	0.494	1.730	0.541	0.360	0.446
17	16.31	1.5760	0.529	1.833	0.581	0.387	0.431
18	13.93	1.5030	0.456	1.620	0.496	0.331	0.466
19	11.19	1.4250	0.378	1.350	0.406	0.271	0.506
20	7.82	1.3300	0.283	0.990	0.298	0.199	0.563
21	4.52	1.2380	0.191	0.599	0.196	0.131	0.608
22	0.78	1.1100	0.062	0.112	0.062	0.041	0.589
23	1.28	1.1320	0.084	0.180	0.085	0.056	0.608
24	1.90	1.1560	0.108	0.264	0.109	0.073	0.616
25	2.51	1.1770	0.129	0.344	0.131	0.087	0.619
26	3.16	1.1980	0.150	0.428	0.153	0.102	0.618
27	3.69	1.2140	0.166	0.496	0.170	0.113	0.616
28	7.28	1.3160	0.268	0.928	0.281	0.188	0.571
29	8.79	1.3590	0.311	1.096	0.330	0.220	0.543
30	10.45	1.4050	0.357	1.273	0.382	0.255	0.517
31	11.48	1.4350	0.387	1.378	0.417	0.278	0.499
32	12.59	1.4670	0.419	1.489	0.453	0.302	0.482
33	13.60	1.4960	0.448	1.586	0.487	0.325	0.468
34	14.67	1.5260	0.478	1.687	0.522	0.348	0.455
35	15.65	1.5520	0.504	1.778	0.553	0.369	0.445
36	16.76	1.5850	0.537	1.877	0.592	0.395	0.431
37	18.07	1.6220	0.574	1.990	0.636	0.424	0.417
38	19.22	1.6500	0.602	2.090	0.670	0.447	0.410
39	20.81	1.6890	0.641	2.225	0.718	0.479	0.400
40	22.19	1.7220	0.674	2.339	0.759	0.506	0.392
41	14.65	1.5240	0.476	1.686	0.520	0.347	0.457
42	11.49	1.4340	0.386	1.380	0.416	0.277	0.501
43	10.40	1.4030	0.355	1.269	0.380	0.253	0.519
44	8.76	1.3570	0.309	1.093	0.328	0.218	0.546
45	1.09	1.1240	0.076	0.153	0.076	0.051	0.601
46	3.14	1.1970	0.149	0.426	0.152	0.101	0.621
47	4.32	1.2320	0.184	0.575	0.189	0.126	0.613
48	6.47	1.2940	0.246	0.834	0.257	0.171	0.581
49	5.18	1.2570	0.209	0.681	0.216	0.144	0.603
50	7.50	1.3225	0.275	0.952	0.289	0.192	0.565

Table B-11. α = 15°, *QR*, $A=1t_w$, normal orientation, P=1.5 (ft), data

Experimental Data for Labyrinth Weir, 2-Cycle, Trapezoidal, Quarter Round, α=15°, A=1 t_w, Normal Orientation

	Measured (Model)	Design (AutoCAD)
P (ft)	1.5	1.500
L_c (in)	156.8	156.7988
t_w (in)	1.450	1.45
W (in)	48.4125	48.1800
N	2	2
g	32.174	
$L_{c\text{-}cycle}$ (in)	78.4	
w (in)	24.20625	

Leak	
Time (sec)	480
Water level drop (ft)	0.00350
Volume (in^3)	573.2
Leak (cfs)	0.00069

Crest point gage reference (ft)	1.0445

Run No.	Q (cfs)	Point Gage (ft)	H (ft)	U.S. Vel. (fps)	H_T (ft)	H_T/P	C_d Eq 1
1	2	3	4	5	6	7	8
1	0.94	1.1240	0.080	0.133	0.080	0.053	0.600
2	1.41	1.1470	0.103	0.197	0.103	0.069	0.610
3	2.75	1.2020	0.158	0.372	0.160	0.106	0.618
4	3.70	1.2370	0.193	0.490	0.196	0.131	0.609
5	5.19	1.2870	0.243	0.671	0.249	0.166	0.597
6	6.40	1.3250	0.281	0.810	0.291	0.194	0.584
7	6.67	1.3335	0.289	0.841	0.300	0.200	0.581
8	6.68	1.3340	0.290	0.842	0.301	0.200	0.580
9	7.26	1.3530	0.309	0.906	0.321	0.214	0.570
10	7.32	1.3550	0.311	0.913	0.323	0.216	0.569
11	9.17	1.4140	0.370	1.111	0.389	0.259	0.542
12	10.57	1.4590	0.415	1.253	0.439	0.293	0.520
13	11.73	1.4965	0.452	1.366	0.481	0.321	0.503
14	12.44	1.5195	0.475	1.432	0.507	0.338	0.493
15	13.06	1.5390	0.495	1.490	0.529	0.353	0.486
16	13.75	1.5620	0.518	1.553	0.555	0.370	0.476
17	15.63	1.6190	0.575	1.720	0.620	0.414	0.458
18	17.40	1.6740	0.630	1.870	0.684	0.456	0.440
19	18.32	1.7050	0.661	1.943	0.719	0.479	0.430
20	19.74	1.7470	0.703	2.056	0.768	0.512	0.420
21	21.77	1.8100	0.766	2.209	0.841	0.561	0.404

Table B-12. α = 15°, *QR*, $A=1t_w$, normal orientation, P=1.25 (ft), data

Experimental Data for Labyrinth Weir, 2-Cycle, Trapezoidal, Quarter Round, α=15°, A=1 t_w, Normal Orientation

	Measured (Model)	Design (AutoCAD)
P (ft)	1.25	1.250
L_c (in)	157.0	156.7988
t_w (in)	1.450	1.45
W (in)	48.4125	48.1800
N	2	2
g	32.174	
$L_{c\text{-}cycle}$ (in)	78.5	
w (in)	24.20625	

Leak	
Time (sec)	480
Water level drop (ft)	0.00125
Volume (in^3)	204.7
Leak (cfs)	0.00025

Crest point gage reference (ft)	1.0445

Run No.	Q (cfs)	Point Gage (ft)	H (ft)	U.S. Vel. (fps)	H_T (ft)	H_T/P	C_d Eq 1
1	2	3	4	5	6	7	8
1	1.22	0.8910	0.093	0.198	0.094	0.075	0.606
2	1.60	0.9085	0.111	0.257	0.112	0.089	0.612
3	1.40	0.8995	0.102	0.227	0.102	0.082	0.611
4	1.85	0.9190	0.121	0.296	0.122	0.098	0.617
5	2.27	0.9365	0.139	0.359	0.141	0.112	0.616
6	2.91	0.9605	0.163	0.454	0.166	0.133	0.617
7	3.54	0.9830	0.185	0.544	0.190	0.152	0.613
8	3.94	0.9970	0.199	0.600	0.205	0.164	0.608
9	3.54	0.9830	0.185	0.544	0.190	0.152	0.612
10	6.34	1.0760	0.278	0.921	0.291	0.233	0.576
11	5.13	1.0370	0.239	0.763	0.248	0.198	0.593
12	7.79	1.1210	0.323	1.103	0.342	0.274	0.557
13	6.47	1.0800	0.282	0.938	0.296	0.237	0.575
14	6.92	1.0940	0.296	0.996	0.311	0.249	0.569
15	9.01	1.1590	0.361	1.248	0.385	0.308	0.538
16	10.23	1.1950	0.397	1.390	0.427	0.342	0.524
17	9.69	1.1790	0.381	1.328	0.408	0.327	0.530
18	11.56	1.2355	0.438	1.537	0.474	0.379	0.506
19	12.63	1.2680	0.470	1.650	0.512	0.410	0.492
20	13.71	1.3010	0.503	1.760	0.551	0.441	0.479
21	16.47	1.3840	0.586	2.028	0.650	0.520	0.449
22	17.83	1.4385	0.641	2.138	0.712	0.569	0.425
23	21.76	1.5590	0.761	2.464	0.855	0.684	0.393
24	10.42	1.2005	0.403	1.412	0.434	0.347	0.522
25	14.03	1.3100	0.512	1.793	0.562	0.450	0.476
26	15.79	1.3640	0.566	1.964	0.626	0.501	0.456

Table B-13. α = 15°, *QR*, $A=1t_w$, normal orientation, P=1.0 (ft), data

Experimental Data for Labyrinth Weir, 2-Cycle, Trapezoidal, Quarter Round, α =15°, A =1 t_w, Normal Orientation

	Measured (Model)	Design (AutoCAD)
P (ft)	1	1.000
L_c (in)	157.1	156.7988
t_w (in)	1.450	1.45
W (in)	48.4125	48.1800
N	2	2
g	32.174	
$L_{c\text{-}cycle}$ (in)	78.5625	
w (in)	24.20625	

Leak	
Time (sec)	480
Water level drop (ft)	0.00175
Volume (in^3)	286.6
Leak (cfs)	0.00035

Crest point gage reference (ft)	0.5456667

Run No.	Q (cfs)	Point Gage (ft)	H (ft)	U.S. Vel. (fps)	H_T (ft)	H_T/P	C_d Eq 1
1	2	3	4	5	6	7	8
1	3.46	0.7290	0.183	0.631	0.190	0.190	0.599
2	4.52	0.7650	0.219	0.802	0.229	0.229	0.587
3	8.69	0.8975	0.352	1.409	0.383	0.383	0.524
4	6.31	0.8230	0.277	1.075	0.295	0.295	0.561
5	3.36	0.7255	0.180	0.615	0.186	0.186	0.600
6	4.29	0.7580	0.212	0.766	0.221	0.221	0.588
7	5.19	0.7890	0.243	0.907	0.256	0.256	0.572
8	6.22	0.8210	0.275	1.062	0.293	0.293	0.561
9	7.41	0.8580	0.312	1.233	0.336	0.336	0.543
10	8.37	0.8870	0.341	1.366	0.370	0.370	0.530
11	9.01	0.9070	0.361	1.452	0.394	0.394	0.520
12	10.38	0.9510	0.405	1.626	0.446	0.446	0.497
13	11.60	0.9900	0.444	1.774	0.493	0.493	0.478
14	12.68	1.0280	0.482	1.894	0.538	0.538	0.459
15	13.83	1.0660	0.520	2.019	0.584	0.584	0.443
16	15.42	1.1210	0.575	2.180	0.649	0.649	0.421
17	16.19	1.1480	0.602	2.255	0.681	0.681	0.411

Table B-14. α = 15°, *QR*, A=1t_w, normal orientation, N=6, data

Experimental Data for Labyrinth Weir, 6-Cycle, Trapezoidal, Quarter Round, α=15°, A=1 t_w, Normal Orientation

	Measured (Model)	Design (AutoCAD)
P (ft)	0.98	1.000
L_c (in)	98.5	98.0895
t_w (in)	1.450	1.45
W (in)	48.4125	48.1800
N	6	6
g	32.174	
$L_{c\text{-}cycle}$ (in)	16.42	
w (in)	8.07	

Leak	
Time (sec)	600
Water level drop (ft)	0.0005
Volume (in^3)	982.5948
Leak (cfs)	7.898E-05

Crest point gage reference (ft)	0.5301806

Run No.	Q (cfs)	Point Gage (ft)	H (ft)	U.S. Vel. (fps)	H_T (ft)	H_T/P	C_d Eq 1
1	2	3	4	5	6	7	8
1	0.75	0.6350	0.105	0.149	0.105	0.108	0.504
2	1.08	0.6640	0.134	0.207	0.134	0.138	0.497
3	1.43	0.6940	0.164	0.269	0.165	0.169	0.487
4	1.91	0.7310	0.201	0.350	0.203	0.208	0.477
5	2.48	0.7600	0.230	0.444	0.233	0.238	0.503
6	2.92	0.7890	0.259	0.512	0.263	0.269	0.493
7	3.53	0.8310	0.301	0.602	0.306	0.314	0.475
8	3.88	0.8530	0.323	0.651	0.329	0.337	0.467
9	0.57	0.6150	0.085	0.113	0.085	0.087	0.521
10	0.76	0.6360	0.106	0.149	0.106	0.109	0.500
11	5.18	0.9350	0.405	0.824	0.415	0.425	0.441
12	8.46	1.1150	0.585	1.207	0.607	0.622	0.407
13	11.18	1.2520	0.722	1.477	0.756	0.774	0.388
14	13.74	1.3680	0.838	1.711	0.883	0.905	0.377
15	19.54	1.6070	1.077	2.171	1.150	1.178	0.361
16	8.41	1.1110	0.581	1.202	0.603	0.618	0.409
18	0.99	0.6550	0.125	0.191	0.125	0.128	0.506
19	1.37	0.6910	0.161	0.259	0.162	0.166	0.480
20	1.73	0.7190	0.189	0.319	0.190	0.195	0.474
21	1.94	0.7340	0.204	0.354	0.206	0.211	0.473
22	2.39	0.7550	0.225	0.429	0.228	0.233	0.501
23	2.86	0.7865	0.256	0.503	0.260	0.267	0.491
24	3.24	0.8130	0.283	0.560	0.288	0.295	0.479
25	3.58	0.8350	0.305	0.609	0.311	0.318	0.471
26	3.91	0.8560	0.326	0.655	0.332	0.340	0.464
27	4.21	0.8750	0.345	0.696	0.352	0.361	0.459

APPENDIX C

VBA Code Used to Calculate

Discharge and Uncertainty

```
Option Explicit
'for use with 4-ft rectangular flume with transmitters in UWRL (9-15-2007)
'calibration of o-plates 2/2/2010
Function flowt4(Size, dH)
Dim beta, A, Dorifice, Dpipe, pi, C, g As Double
pi = 3.14159265359
g = 32.174
If (Size = 8) Then
   C = 0.6205 ' previously was 0.616 '0.6033
   Dorifice = 5.5839 '5.719
   Dpipe = 7.932 '7.625
   beta = Dorifice / Dpipe
   A = Dorifice ^ 2 * pi * 0.25 / 144
Else
If (Size = 20) Then
   C = 0.6282  'previously was 0.611
   Dorifice = 14.625
   Dpipe = 19.5
   beta = Dorifice / Dpipe
   beta = Dorifice / Dpipe
   A = Dorifice ^ 2 * pi * 0.25 / 144
Else
End If
End If

flowt4 = C * A * (2 * g * dH) ^ 0.5 / (1 - beta ^ 4) ^ 0.5

End Function

'4-ft Flume Calculation
'To determine uncertainty in single sample measurement, from Kline and McClintock
1953
Function SSUCd4ft(Size, mA, deltaH, Q, Ptgage, Ht, P, Lc, W, Yplatform, Yramp, Yref,
g)
Dim beta, Aorifice, Dorifice, Dpipe, pi, C As Double
Dim wQ, wLc, wHt, wC, wW, wPtgage, wH, wP, wYplatform, wYramp, wYref, wmA,
H
Dim dQ, dH, dP, dYplatform, dYramp
pi = 3.14159265359
Lc = Lc / 12 'convert from inches to feet
```

```
W = W / 12 'convert from inches to feet

'Calculate Q in 4-ft flume
If (Size = 8) Then
   C = 0.6205 ' previously was 0.616 '0.6033
   Dorifice = 5.5839 '5.719
   Dpipe = 7.932 '7.625
   beta = Dorifice / Dpipe
   Aorifice = Dorifice ^ 2 * pi * 0.25 / 144
Else
If (Size = 20) Then
   C = 0.6282  'previously was 0.611
   Dorifice = 14.625
   Dpipe = 19.5
   beta = Dorifice / Dpipe
   beta = Dorifice / Dpipe
   Aorifice = Dorifice ^ 2 * pi * 0.25 / 144
Else
End If
End If

Q = C * Aorifice * (2 * g * deltaH) ^ 0.5 / (1 - beta ^ 4) ^ 0.5
H = Ptgage - Yref
Ht = H + Q ^ 2 / (2 * g * W ^ 2 * (H + P + Yplatform - Yramp) ^ 2)

'Assign values from instrumentation
'wQtank = 0.0015
wQ = 0.0025 * Q
wLc = (1 / 32) / (2 * 12) '+- 1/64 of inch
wW = (1 / 16) / 2 '+- error, can read smaller but have to average diff flume widths
wPtgage = 0.001 / 2 '+-error in feet
wYref = 0.001 / 2 '+-error in feet
wmA = 0.01 / 2 '+-error in mA
wYramp = (1 / 32) / (2 * 12) '+- 1/64 of inch
wYplatform = (1 / 32) / (2 * 12) '+- 1/64 of inch

'Calculate uncertainties
wH = (((wPtgage / H) ^ 2 + (wYref * (-1) / H) ^ 2) ^ (1 / 2)) * H
  'Calc wHt by taking derivatives
   dH = 1 - (Q ^ 2) / (g * W ^ 2 * (H + P + Yplatform - Yramp) ^ 3)
```

```
    dQ = Q / (g * W ^ 2 * (H + P + Yplatform - Yramp) ^ 2)
    dP = -Q ^ 2 / (g * W ^ 2 * (H + P + Yplatform - Yramp) ^ 3)
    dYplatform = Q ^ 2 / (g * W ^ 2 * (H + P + Yplatform - Yramp) ^ 3)
    dYramp = Q ^ 2 / (g * W ^ 2 * (H + P + Yplatform - Yramp) ^ 3)
wHt = (((wH * dH / Ht) ^ 2 + (wQ * dQ / Ht) ^ 2 + (wP * dP / Ht) ^ 2 + (wYplatform *
dYplatform / Ht) ^ 2 + (wYramp * dYramp / Ht) ^ 2) ^ (1 / 2)) * Ht

'%Uncertainty of single Cd value from labyrinth in 4-ft flume
SSUCd4ft = ((wQ / Q) ^ 2 + (-wLc / Lc) ^ 2 + (-27 / 8 * wHt / Ht) ^ 2) ^ (1 / 2)


End Function
```